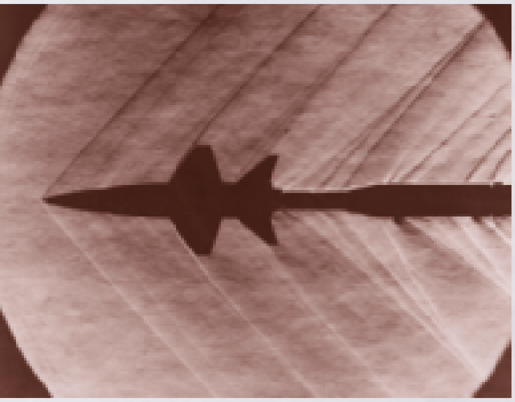

11 Compressible Flow

CHAPTER OPENING PHOTO: Supersonic flow past a scale model of the X-15 experimental aircraft. An object moving through a fluid at supersonic speed (Mach number greater than one) creates shock waves (a discontinuity in flow conditions shown by the light and dark lines), which would be heard as a sonic boom as the object passes overhead. (Photograph courtesy of NASA)

Learning Objectives

After completing this chapter, you should be able to:

- distinguish between incompressible and compressible flows, and know when the approximations associated with assuming fluid incompressibility are acceptable.
- understand some important features of different categories of compressible flows of ideal gases.
- explain speed of sound and Mach number and their practical significance.
- solve useful problems involving isentropic and nonisentropic flows including flows across normal shock waves.
- appreciate the compelling similarities between compressible flows of gases and open-channel flows of liquids.
- move on to understanding more advanced concepts about compressible flows.

Most first courses in fluid mechanics concentrate on constant density (incompressible) flows. In earlier chapters of this book, we mainly considered incompressible flow behavior. In a few instances, variable density (compressible) flow effects were covered briefly. The notion of an incompressible fluid is convenient because when constant density and constant (including zero) viscosity are assumed, problem solutions are greatly simplified. Also, fluid incompressibility allows us to build on the Bernoulli equation as was done, for example, in Chapter 5. Preceding examples should have convinced us that nearly incompressible flows are common in everyday experiences.

Any study of fluid mechanics would, however, be incomplete without a brief introduction to compressible flow behavior. Fluid compressibility is a very important consideration in numerous engineering applications of fluid mechanics. For example, the measurement of high-speed flow velocities requires compressible flow theory. The flows in gas turbine engine components are generally compressible. Many aircraft fly fast enough to involve compressible flow.

The variation of fluid density for compressible flows requires attention to density and other fluid property relationships. The fluid equation of state, often unimportant for incompressible flows, is vital in the analysis of compressible flows. Also, temperature variations for compressible flows are usually significant, and thus the energy equation is important. Curious phenomena can occur with compressible flows. For example, with compressible flows we can have fluid acceleration because of friction, fluid deceleration in a converging duct, fluid temperature decrease with heating, and the formation of abrupt discontinuities in flows across which fluid properties change appreciably.

For simplicity, in this introductory study of compressibility effects we mainly consider the steady, one-dimensional, constant (including zero) viscosity, compressible flow of an ideal gas. We limit our study to compressibility due to high-speed flow. In this chapter, one-dimensional flow refers to flow involving uniform distributions of fluid properties over any flow cross-sectional area. Both frictionless ($\mu = 0$) and frictional ($\mu \neq 0$) compressible flows are considered. If the change in volume associated with a change of pressure is considered a measure of compressibility, our experience suggests that gases and vapors are much more compressible than liquids. We focus our attention on the compressible flow of a gas because such flows occur often. We limit our discussion to ideal gases, since the equation of state for an ideal gas is uncomplicated, yet representative of actual gases at pressures and temperatures of engineering interest, and because the flow trends associated with an ideal gas are generally applicable to other compressible fluids.

An excellent film about compressible flow is available (see Ref. 1). This resource is a useful supplement to the material covered in this chapter.

11.1 Ideal Gas Relationships

V11.1 Lighter flame

Before we can proceed to develop ***compressible flow*** equations, we need to become more familiar with the fluid we will work with, the ideal gas. Specifically, we must learn how to evaluate ideal gas property changes. The equation of state for an ***ideal gas*** is

$$\rho = \frac{p}{RT} \tag{11.1}$$

We have already discussed fluid pressure, p, density, ρ, and temperature, T, in earlier chapters. The gas constant, R, represents a constant for each distinct ideal gas or mixture of ideal gases, where

$$R = \frac{\lambda}{M_{\text{gas}}} \tag{11.2}$$

With this notation, λ is the universal gas constant and M_{gas} is the molecular weight of the ideal gas or gas mixture. Listed in Table 1.4 are values of the gas constants of some commonly used gases. Knowing the pressure and temperature of a gas, we can estimate its density. Nonideal gas state equations are beyond the scope of this text, and those interested in this topic are directed to texts on engineering thermodynamics, for example, Ref. 2. Note that the trends of ideal gas flows are generally good indicators of what nonideal gas flow behavior is like.

We consider ideal gas flows only.

For an ideal gas, ***internal energy***, $\check{u}$, is part of the stored energy of the gas as explained in Section 5.3 and is considered to be a function of temperature only (Ref. 2). Thus, the ideal gas specific heat at constant volume, c_v, can be expressed as

$$c_v = \left(\frac{\partial \check{u}}{\partial T}\right)_v = \frac{d\check{u}}{dT} \tag{11.3}$$

where the subscript v on the partial derivative refers to differentiation at constant specific volume, $v = 1/\rho$. From Eq. 11.3 we conclude that for a particular ideal gas, c_v is a function of temperature only. Equation 11.3 can be rearranged to yield

$$d\check{u} = c_v \, dT$$

Thus,

$$\check{u}_2 - \check{u}_1 = \int_{T_1}^{T_2} c_v \, dT \tag{11.4}$$

Equation 11.4 is useful because it allows us to evaluate the change in internal energy, $\check{u}_2 - \check{u}_1$, associated with ideal gas flow from section (1) to section (2) in a flow. For simplicity, we can assume that c_v is constant for a particular ideal gas and obtain from Eq. 11.4

$$\boxed{\check{u}_2 - \check{u}_1 = c_v(T_2 - T_1)} \tag{11.5}$$

Actually, c_v for a particular gas varies with temperature (see Ref. 2). However, for moderate changes in temperature, the constant c_v assumption is reasonable.

The fluid property ***enthalpy***, $\check{h}$, is defined as

$$\check{h} = \check{u} + \frac{p}{\rho} \tag{11.6}$$

It combines internal energy, $\check{u}$, and pressure energy, p/ρ, and is useful when dealing with the energy equation (Eq. 5.69). For an ideal gas, we have already stated that

$$\check{u} = \check{u}(T)$$

From the equation of state (Eq. 11.1)

$$\frac{p}{\rho} = RT$$

Thus, it follows that

$$\check{h} = \check{h}(T)$$

Since for an ideal gas, enthalpy is a function of temperature only, the ideal gas specific heat at constant pressure, c_p, can be expressed as

$$c_p = \left(\frac{\partial \check{h}}{\partial T}\right)_p = \frac{d\check{h}}{dT} \tag{11.7}$$

where the subscript p on the partial derivative refers to differentiation at constant pressure, and c_p is a function of temperature only. The rearrangement of Eq. 11.7 leads to

$$d\check{h} = c_p \, dT$$

and

$$\check{h}_2 - \check{h}_1 = \int_{T_1}^{T_2} c_p \, dT \tag{11.8}$$

Equation 11.8 is useful because it allows us to evaluate the change in enthalpy, $\check{h}_2 - \check{h}_1$, associated with ideal gas flow from section (1) to section (2) in a flow. For simplicity, we can assume that c_p is constant for a specific ideal gas and obtain from Eq. 11.8

$$\boxed{\check{h}_2 - \check{h}_1 = c_p(T_2 - T_1)} \tag{11.9}$$

As is true for c_v, the value of c_p for a given gas varies with temperature. Nevertheless, for moderate changes in temperature, the constant c_p assumption is reasonable.

For moderate temperature changes, specific heat values can be considered constant.

From Eqs. 11.5 and 11.9 we see that changes in internal energy and enthalpy are related to changes in temperature by values of c_v and c_p. We turn our attention now to developing useful relationships for determining c_v and c_p. Combining Eqs. 11.6 and 11.1 we get

$$\check{h} = \check{u} + RT \tag{11.10}$$

Differentiating Eq. 11.10 leads to

$$d\check{h} = d\check{u} + R\,dT$$

or

$$\frac{d\check{h}}{dT} = \frac{d\check{u}}{dT} + R \tag{11.11}$$

From Eqs. 11.3, 11.7, and 11.11 we conclude that

$$\boxed{c_p - c_v = R} \tag{11.12}$$

Equation 11.12 indicates that the difference between c_p and c_v is constant for each ideal gas regardless of temperature. Also $c_p > c_v$. If the ***specific heat ratio,*** k, is defined as

$$k = \frac{c_p}{c_v} \tag{11.13}$$

then combining Eqs. 11.12 and 11.13 leads to

$$\boxed{c_p = \frac{Rk}{k-1}} \tag{11.14}$$

and

$$\boxed{c_v = \frac{R}{k-1}} \tag{11.15}$$

The gas constant is related to the specific heat values.

Actually, c_p, c_v, and k are all somewhat temperature dependent for any ideal gas. We will assume constant values for these variables in this book. Values of k and R for some commonly used gases at nominal temperatures are listed in Table 1.4. These tabulated values can be used with Eqs. 11.13 and 11.14 to determine the values of c_p and c_v. Example 11.1 demonstrates how internal energy and enthalpy changes can be calculated for a flowing ideal gas having constant c_p and c_v.

EXAMPLE 11.1 Internal Energy, Enthalpy, and Density for an Ideal Gas

GIVEN Air flows steadily between two sections in a long, straight portion of 10 cm diameter pipe as is indicated in Fig. E11.1. The uniformly distributed temperature and pressure at each section are $T_1 = 300$ k, $p_1 = 690$ kPa, and $T_2 = 252$ k, $p_2 = 127$ kPa.

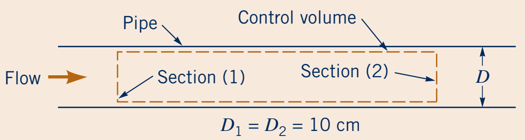

■ **Figure E11.1**

FIND Calculate the **(a)** change in internal energy between sections (1) and (2), **(b)** change in enthalpy between sections (1) and (2), and **(c)** change in density between sections (1) and (2).

SOLUTION

(a) Assuming air behaves as an ideal gas, we can use Eq. 11.5 to evaluate the change in internal energy between sections (1) and (2). Thus

$$\check{u}_2 - \check{u}_1 = c_v(T_2 - T_1) \tag{1}$$

From Eq. 11.15 we have

$$c_v = \frac{R}{k-1} \tag{2}$$

and from Table 1.4, $R = 286.9$ and $k = 1.4$. Throughout this book, we use the nominal values of k for common gases listed in Table 1.4 and consider these values as being representative.

From Eq. 2 we obtain

$$c_v = \frac{286.9}{(1.4-1)}\ \text{J/kg}\cdot\text{K}$$
$$= 717\ \text{J/kg}\cdot\text{K} \tag{3}$$

Combining Eqs. 1 and 3 yields

$$\begin{aligned}\check{u}_2 - \check{u}_1 = c_v(T_2 - T_1) &= 717 \text{ J/kg} \cdot \text{K} \\ &\times (252 \text{ K} - 300 \text{ K}) \\ &= -34{,}416 \text{ J/kg}\end{aligned} \qquad \textbf{(Ans)}$$

(b) For enthalpy change we use Eq. 11.9. Thus

$$\check{h}_2 - \check{h}_1 = c_p(T_2 - T_1) \qquad \textbf{(4)}$$

where since $k = c_p/c_v$ we obtain

$$\begin{aligned}c_p = kc_v &= (1.4)\, 717 \text{ J/kg} \cdot \text{K} \\ &= 1004 \text{ J/kg} \cdot \text{K}\end{aligned} \qquad \textbf{(5)}$$

From Eqs. 4 and 5 we obtain

$$\begin{aligned}\check{h}_2 - \check{h}_1 = c_p(T_2 - T_1) &= 1004 \text{ J/kg} \cdot \text{K} \\ &\times (252 \text{ K} - 300 \text{ K}) \\ &= -48{,}192 \text{ J/kg} \cdot \text{K}\end{aligned} \qquad \textbf{(Ans)}$$

(c) For density change we use the ideal gas equation of state (Eq. 11.1) to get

$$\rho_2 - \rho_1 = \frac{p_2}{RT_2} - \frac{p_1}{RT_1} = \frac{1}{R}\left(\frac{p_2}{T_2} - \frac{p_1}{T_1}\right) \qquad \textbf{(6)}$$

Using the pressures and temperatures given in the problem statement we calculate from Eq. 6

$$\begin{aligned}\rho_2 - \rho_1 &= \frac{1}{286.9 \text{ J/kg} \cdot \text{K}} \\ &\times \left[\frac{127 \times 10^3 \text{ Pa}}{252 \text{ K}} - \frac{690 \times 10^3 \text{ Pa}}{300 \text{ K}}\right]\end{aligned}$$

or

$$\rho_2 - \rho_1 = -6.26 \text{ kg/m}^3 \qquad \textbf{(Ans)}$$

COMMENT This is a significant change in density when compared with the upstream density

$$\begin{aligned}\rho_1 = \frac{p_1}{RT_1} &= \frac{690 \times 10^3 \text{ Pa}}{(286.9 \text{ J/kg} \cdot \text{K})(300 \text{ K})} \\ &= 8.02 \text{ kg/m}^3\end{aligned}$$

Compressibility effects are important for this flow.

Changes in entropy are important because they are related to loss of available energy.

For compressible flows, changes in the thermodynamic property ***entropy***, s, are important. For any pure substance including ideal gases, the "first $T\,ds$ equation" is (see Ref. 2)

$$T\,ds = d\check{u} + pd\left(\frac{1}{\rho}\right) \qquad \textbf{(11.16)}$$

where T is absolute temperature, s is entropy, $\check{u}$ is internal energy, p is absolute pressure, and ρ is density. Differentiating Eq. 11.6 leads to

$$d\check{h} = d\check{u} + pd\left(\frac{1}{\rho}\right) + \left(\frac{1}{\rho}\right)dp \qquad \textbf{(11.17)}$$

By combining Eqs. 11.16 and 11.17, we obtain

$$T\,ds = d\check{h} - \left(\frac{1}{\rho}\right)dp \qquad \textbf{(11.18)}$$

Equation 11.18 is often referred to as the "second $T\,ds$ equation." For an ideal gas, Eqs. 11.1, 11.3, and 11.16 can be combined to yield

$$ds = c_v\frac{dT}{T} + \frac{R}{1/\rho}\,d\left(\frac{1}{\rho}\right) \qquad \textbf{(11.19)}$$

and Eqs. 11.1, 11.7, and 11.18 can be combined to yield

$$ds = c_p\frac{dT}{T} - R\frac{dp}{p} \qquad \textbf{(11.20)}$$

If c_p and c_v are assumed to be constant for a given gas, Eqs. 11.19 and 11.20 can be integrated to get

Changes in entropy are related to changes in temperature, pressure, and density.

$$s_2 - s_1 = c_v \ln \frac{T_2}{T_1} + R \ln \frac{\rho_1}{\rho_2} \tag{11.21}$$

and

$$s_2 - s_1 = c_p \ln \frac{T_2}{T_1} - R \ln \frac{p_2}{p_1} \tag{11.22}$$

Equations 11.21 and 11.22 allow us to calculate the change of entropy of an ideal gas flowing from one section to another with constant specific heat values (c_p and c_v).

EXAMPLE 11.2 Entropy for an Ideal Gas

GIVEN Consider the airflow of Example 11.1.

FIND Calculate the change in entropy, $s_2 - s_1$, between sections (1) and (2).

SOLUTION

Assuming that the flowing air in Fig. E11.1 behaves as an ideal gas, we can calculate the entropy change between sections by using either Eq. 11.21 or Eq. 11.22. We use both to demonstrate that the same result is obtained either way.

From Eq. 11.21,

$$s_2 - s_1 = c_v \ln \frac{T_2}{T_1} + R \ln \frac{\rho_1}{\rho_2} \tag{1}$$

To evaluate $s_2 - s_1$ from Eq. 1 we need the density ratio, ρ_1/ρ_2, which can be obtained from the ideal gas equation of state (Eq. 11.1) as

$$\frac{\rho_1}{\rho_2} = \left(\frac{p_1}{T_1}\right)\left(\frac{T_2}{p_2}\right) \tag{2}$$

and thus from Eqs. 1 and 2,

$$s_2 - s_1 = c_v \ln \frac{T_2}{T_1} + R \ln \left[\left(\frac{p_1}{T_1}\right)\left(\frac{T_2}{p_2}\right)\right] \tag{3}$$

By substituting values already identified in the Example 11.1 problem statement and solution into Eq. 3 with

$$\left(\frac{p_1}{T_1}\right)\left(\frac{T_2}{p_2}\right) = \left(\frac{690 \times 10^3 \text{ Pa}}{300 \text{ K}}\right)\left(\frac{252 \text{ K}}{127 \times 10^3 \text{ Pa}}\right) = 4.56$$

we get

$$s_2 - s_1 = (717 \text{ J/kg}) \ln \left(\frac{252 \text{ K}}{300 \text{ K}}\right) + (286.9 \text{ J/kg} \cdot \text{K}) \ln 4.56$$

or

$$s_2 - s_1 = 310 \text{ J/kg} \cdot \text{K} \qquad \textbf{(Ans)}$$

From Eq. 11.22,

$$s_2 - s_1 = c_p \ln \frac{T_2}{T_1} - R \ln \frac{p_2}{p_1} \tag{4}$$

By substituting known values into Eq. 4 we obtain

$$s_2 - s_1 = (1004 \text{ J/kg} \cdot \text{K}) \ln \left(\frac{252 \text{ K}}{300 \text{ K}}\right) - (286.9 \text{ J/kg} \cdot \text{K}) \ln \left(\frac{127 \times 10^3 \text{ Pa}}{690 \times 10^3 \text{ Pa}}\right)$$

or

$$s_2 - s_1 = 310 \text{ J/kg} \cdot \text{K} \qquad \textbf{(Ans)}$$

COMMENT As anticipated, both Eqs. 11.21 and 11.22 yield the same result for the entropy change, $s_2 - s_1$.

Note that since the ideal gas equation of state was used in the derivation of the entropy difference equations, both the pressures and temperatures used must be absolute.

If internal energy, enthalpy, and entropy changes for ideal gas flow with variable specific heats are desired, Eqs. 11.4, 11.8, and 11.19 or 11.20 must be used as explained in Ref. 2. Detailed tables (see, for example, Ref. 3) are available for variable specific heat calculations.

The second law of thermodynamics requires that the ***adiabatic*** and frictionless flow of any fluid results in $ds = 0$ or $s_2 - s_1 = 0$. Constant entropy flow is called ***isentropic*** flow. For the isentropic flow of an ideal gas with constant c_p and c_v, we get from Eqs. 11.21 and 11.22

$$c_v \ln \frac{T_2}{T_1} + R \ln \frac{\rho_1}{\rho_2} = c_p \ln \frac{T_2}{T_1} - R \ln \frac{p_2}{p_1} = 0 \tag{11.23}$$

By combining Eq. 11.23 with Eqs. 11.14 and 11.15 we obtain

$$\left(\frac{T_2}{T_1}\right)^{k/(k-1)} = \left(\frac{\rho_2}{\rho_1}\right)^k = \left(\frac{p_2}{p_1}\right) \tag{11.24}$$

which is a useful relationship between temperature, density, and pressure for the isentropic flow of an ideal gas. From Eq. 11.24 we can conclude that

$$\boxed{\frac{p}{\rho^k} = \text{constant}} \tag{11.25}$$

for an ideal gas with constant c_p and c_v flowing isentropically, a result already used without proof earlier in Chapters 1, 3, and 5.

Fluids in the News

Hilsch tube (Ranque vortex tube) Years ago (around 1930) a French physics student (George Ranque) discovered that appreciably warmer and colder portions of *rapidly swirling airflow* could be separated in a simple apparatus consisting of a tube open at both ends into which was introduced, somewhere in between the two openings, swirling air at *high pressure.* Warmer air near the outer portion of the swirling air flowed out one open end of the tube through a simple valve and colder air near the inner portion of the swirling air flowed out the opposite end of the tube. Rudolph Hilsch, a German physicist, improved on this discovery (ca. 1947). Hot air temperatures of 127 °C and cold air temperatures of −46 °C have been claimed in an optimized version of this apparatus. Thus far the inefficiency of the process has prevented it from being widely adopted. (See Problem 11.4LL.)

11.2 Mach Number and Speed of Sound

Mach number is the ratio of local flow and sound speeds.

The ***Mach number***, Ma, was introduced in Chapters 1 and 7 as a dimensionless measure of compressibility in a fluid flow. In this and subsequent sections, we develop some useful relationships involving the Mach number. The Mach number is defined as the ratio of the value of the local flow velocity, V, to the local ***speed of sound***, c. In other words,

$$\text{Ma} = \frac{V}{c}$$

What we perceive as sound generally consists of weak pressure pulses that move through air with a Mach number of one. When our eardrums respond to a succession of moving pressure pulses, we hear sounds.

To better understand the notion of speed of sound, we analyze the one-dimensional fluid mechanics of an infinitesimally thin, weak pressure pulse moving at the speed of sound through a fluid at rest (see Fig. 11.1*a*). Ahead of the pressure pulse, the fluid velocity is zero, and the fluid pressure and density are p and ρ. Behind the pressure pulse, the fluid velocity has changed by an amount δV, and the pressure and density of the fluid have also changed by amounts δp and $\delta\rho$. We select an infinitesimally thin control volume that moves with the pressure pulse as is sketched

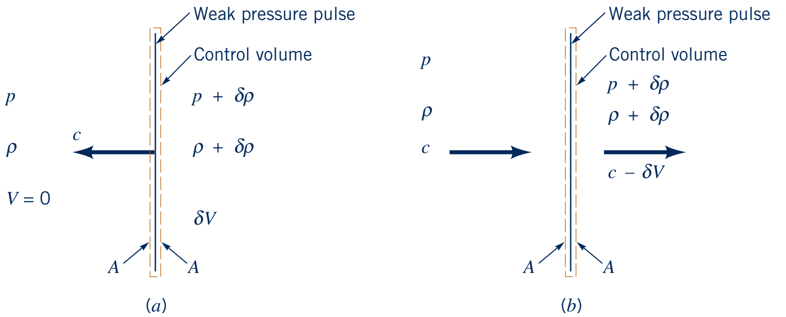

■ **Figure 11.1** (*a*) **Weak pressure pulse moving through a fluid at rest. (*b*) The flow relative to a control volume containing a weak pressure pulse.**

in Fig. 11.1*a*. The speed of the weak pressure pulse is considered constant and in one direction only; thus, our control volume is inertial.

For an observer moving with this control volume (Fig. 11.1*b*), it appears as if fluid is entering the control volume through surface area A with speed c at pressure p and density ρ and leaving the control volume through surface area A with speed $c - \delta V$, pressure $p + \delta p$, and density $\rho + \delta\rho$. When the continuity equation (Eq. 5.16) is applied to the flow through this control volume, the result is

$$\rho A c = (\rho + \delta\rho)A(c - \delta V) \tag{11.26}$$

The changes in fluid properties across a sound wave are very small compared to their local values.

or

$$\rho c = \rho c - \rho\,\delta V + c\,\delta\rho - (\delta\rho)(\delta V) \tag{11.27}$$

Since $(\delta\rho)(\delta V)$ is much smaller than the other terms in Eq. 11.27, we drop it from further consideration and keep

$$\rho\,\delta V = c\,\delta\rho \tag{11.28}$$

The linear momentum equation (Eq. 5.29) can also be applied to the flow through the control volume of Fig. 11.1*b*. The result is

$$-c\rho c A + (c - \delta V)(\rho + \delta\rho)(c - \delta V)A = pA - (p + \delta p)A \tag{11.29}$$

Note that any frictional forces are considered as being negligibly small. We again neglect higher order terms [such as $(\delta V)^2$ compared to $c\,\delta V$, for example] and combine Eqs. 11.26 and 11.29 to get

$$-c\rho c A + (c - \delta V)\rho A c = -\delta p A$$

or

$$\rho\delta V = \frac{\delta p}{c} \tag{11.30}$$

From Eqs. 11.28 (continuity) and 11.30 (linear momentum) we obtain

$$c^2 = \frac{\delta p}{\delta\rho}$$

or

$$c = \sqrt{\frac{\delta p}{\delta\rho}} \tag{11.31}$$

This expression for the speed of sound results from application of the conservation of mass and conservation of linear momentum principles to the flow through the control volume of Fig. 11.1*b*. These principles were similarly used in Section 10.2.1 to obtain an expression for the speed of surface waves traveling on the surface of fluid in a channel.

The conservation of energy principle can also be applied to the flow through the control volume of Fig. 11.1*b*. If the energy equation (Eq. 5.103) is used for the flow through this control volume, the result is

$$\frac{\delta p}{\rho} + \delta\left(\frac{V^2}{2}\right) + g\,\delta z = \delta(\text{loss}) \tag{11.32}$$

For gas flow we can consider $g\,\delta z$ as being negligibly small in comparison to the other terms in the equation. Also, if we assume that the flow is frictionless, then $\delta(\text{loss}) = 0$ and Eq. 11.32 becomes

$$\frac{\delta p}{\rho} + \frac{(c - \delta V)^2}{2} - \frac{c^2}{2} = 0$$

or, neglecting $(\delta V)^2$ compared to $c\,\delta V$, we obtain

$$\rho\,\delta V = \frac{\delta p}{c} \tag{11.33}$$

By combining Eqs. 11.28 (continuity) and 11.33 (energy) we again find that

$$c = \sqrt{\frac{\delta p}{\delta \rho}}$$

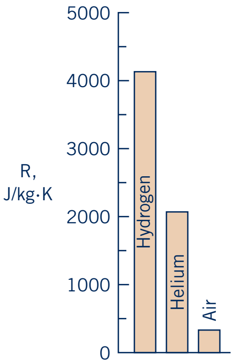

which is identical to Eq. 11.31. Thus, the conservation of linear momentum and the conservation of energy principles lead to the same result. If we further assume that the frictionless flow through the control volume of Fig. 11.1*b* is adiabatic (no heat transfer), then the flow is isentropic. In the limit, as δp becomes vanishingly small ($\delta p \rightarrow \partial p \rightarrow 0$)

$$c = \sqrt{\left(\frac{\partial p}{\partial \rho}\right)_s} \qquad \textbf{(11.34)}$$

where the subscript s is used to designate that the partial differentiation occurs at constant entropy.

Equation 11.34 suggests to us that we can calculate the speed of sound by determining the partial derivative of pressure with respect to density at constant entropy. For the isentropic flow of an ideal gas (with constant c_p and c_v), we learned earlier (Eq. 11.25) that

$$p = (\text{constant})(\rho^k)$$

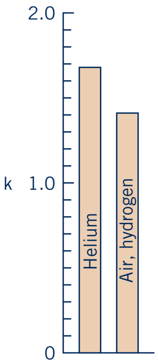

and thus

$$\left(\frac{\partial p}{\partial \rho}\right)_s = (\text{constant})\, k\rho^{k-1} = \frac{p}{\rho^k}\, k\rho^{k-1} = \frac{p}{\rho}\, k = RTk \qquad \textbf{(11.35)}$$

Thus, for an ideal gas

$$c = \sqrt{RTk} \qquad \textbf{(11.36)}$$

From Eq. 11.36 and the charts in the margin we conclude that for a given temperature, the speed of sound, c, in hydrogen and in helium, is higher than in air.

More generally, the bulk modulus of elasticity, E_v, of any fluid including liquids is defined as (see Section 1.7.1)

Speed of sound is larger in fluids that are more difficult to compress.

$$E_v = \frac{dp}{d\rho/\rho} = \rho\left(\frac{\partial p}{\partial \rho}\right)_s \qquad \textbf{(11.37)}$$

Thus, in general, from Eqs. 11.34 and 11.37,

$$c = \sqrt{\frac{E_v}{\rho}} \qquad \textbf{(11.38)}$$

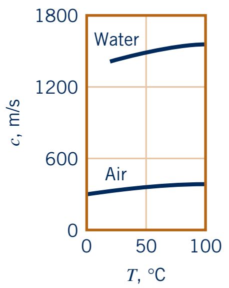

Values of the speed of sound are tabulated in Tables B.1 and B.2 for water and in Tables B.3 and B.4 for air. From experience we know that air is more easily compressed than water. Note from the values of c in Tables B.1 through B.4 and the graph in the margin that the speed of sound in air is much less than it is in water. From Eq. 11.37, we can conclude that if a fluid is truly incompressible, its bulk modulus would be infinitely large, as would be the speed of sound in that fluid. Thus, an incompressible flow must be considered an idealized approximation of reality.

Fluids in the News

Sonification The normal human ear is capable of detecting even very subtle sound patterns produced by *sound waves*. Most of us can distinguish the bark of a dog from the meow of a cat or the roar of a lion, or identify a person's voice on the telephone before they identify who is calling. The number of "things" we can identify from subtle sound patterns is enormous. Combine this ability with the power of computers to transform the information from sensor transducers into variations in pitch, rhythm, and volume and you have *sonification*, the representation of data in the form of sound. With this emerging technology, pathologists may soon learn to "hear" abnormalities in tissue samples, engineers may "hear" flaws in gas turbine engine blades being inspected, and scientists may "hear" a desired attribute in a newly invented material. Perhaps the concept of hearing the trends in data sets may become as commonplace as seeing them. Analysts may listen to the stock market and make decisions. Of course, none of this can happen in a vacuum.

Example 11.3 Speed of Sound

GIVEN Consider the data in Table B.2.

FIND Verify the speed of sound for air at 0 °C.

Solution

In Table B.2, we find the speed of sound of air at 0 °C given as 331.4 m/s. Assuming that air behaves as an ideal gas, we can calculate the speed of sound from Eq. 11.36 as

$$c = \sqrt{RTk} \tag{1}$$

The value of the gas constant is obtained from Table 1.4 as

$$R = 286.9 \text{ J/(kg} \cdot \text{K)}$$

and the specific heat ratio is listed in Table B.2 as

$$k = 1.401$$

By substituting values of R, k, and T into Eq. 1 we obtain

$$c = \sqrt{[(286.9) \text{ J/(kg} \cdot \text{K)}](273.15 \text{ K})(1.401)}$$
$$= 331.4 \text{ (J/kg)}^{1/2}$$

Thus, since $1 \text{ J/kg} = 1 \text{ N} \cdot \text{m/kg} = 1 \text{ (kg} \cdot \text{m/s}^2) \cdot \text{m/kg} = 1 \text{ (m/s)}^2$, we obtain

$$c = 331.4 \text{ m/s} \qquad \textbf{(Ans)}$$

COMMENT The value of the speed of sound calculated with Eq. 11.36 agrees very well with the value of c listed in Table B.2. The ideal gas approximation does not compromise this result significantly.

11.3 Categories of Compressible Flow

Compressibility effects are more important at higher Mach numbers.

In Section 3.8.1, we learned that the effects of compressibility become more significant as the Mach number increases. For example, the error associated with using $\rho V^2/2$ in calculating the ***stagnation pressure*** of an ideal gas increases at larger Mach numbers. From Fig. 3.24 we can conclude that incompressible flows can only occur at low Mach numbers.

Experience has also demonstrated that compressibility can have a large influence on other important flow variables. For example, in Fig. 11.2 the variation of drag coefficient with Reynolds

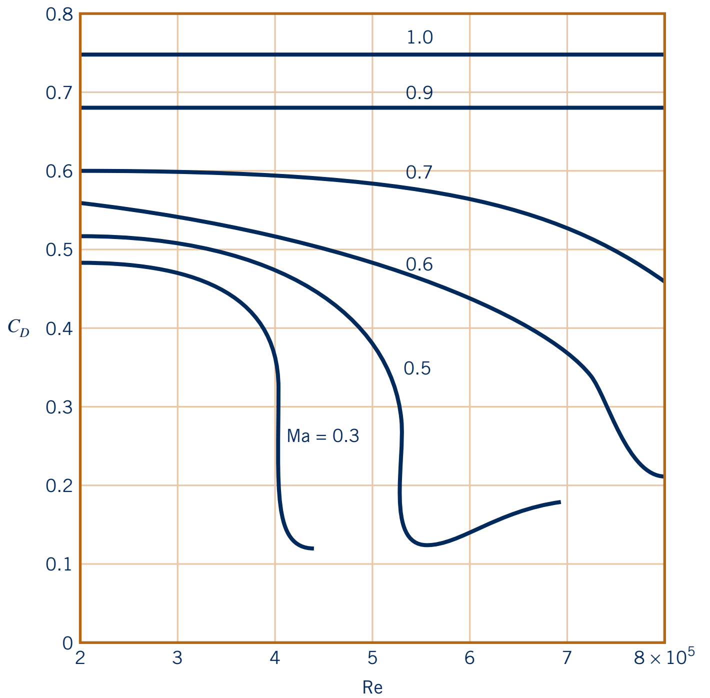

■ **Figure 11.2 The variation of the drag coefficient of a sphere with Reynolds number and Mach number. (Adapted from Fig. 1.8 in Ref. 1 of Chapter 9.)**

V11.2 Waves on a water surface

The wave pattern from a moving source is not symmetrical.

number and Mach number is shown for airflow over a sphere. Compressibility effects can be of considerable importance.

To further illustrate some curious features of compressible flow, a simplified example is considered. Imagine the emission of weak pressure pulses from a point source. These pressure waves are spherical and expand radially outward from the point source at the speed of sound, c. If a pressure wave is emitted at different times, t_{wave}, we can determine where several waves will be at a common instant of time, t, by using the relationship

$$r = (t - t_{\text{wave}})c$$

where r is the radius of the sphere-shaped wave emitted at time $= t_{\text{wave}}$. For a stationary point source, the symmetrical wave pattern shown in Fig. 11.3*a* is involved.

When the point source moves to the left with a constant velocity, V, the wave pattern is no longer symmetrical. In Figs. 11.3*b*, 11.3*c*, and 11.3*d* are illustrated the wave patterns at $t = 3$ s for different values of V. Also shown with a "+" are the positions of the moving point source at values of time, t, equal to 0 s, 1 s, 2 s, and 3 s. Knowing where the point source has been at different instances is important because it indicates to us where the different waves originated.

From the pressure wave patterns of Fig. 11.3, we can draw some useful conclusions. Before doing this we should recognize that if instead of moving the point source to the left, we held the point source stationary and moved the fluid to the right with velocity V, the resulting pressure wave patterns would be identical to those indicated in Fig. 11.3.

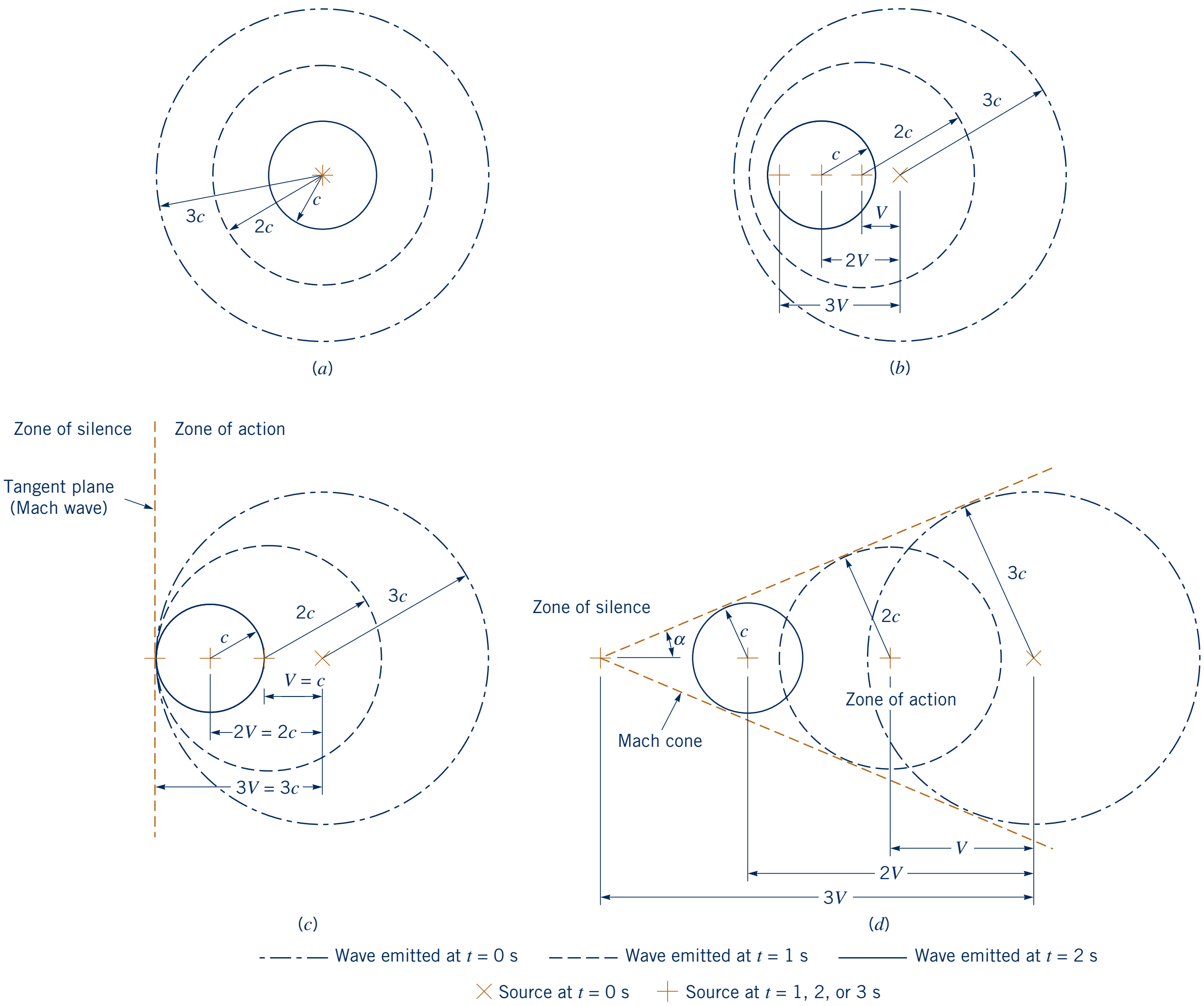

Figure 11.3 (*a*) **Pressure waves at $t = 3$ s, $V = 0$; (*b*) pressure waves at $t = 3$ s, $V < c$; (*c*) pressure waves at $t = 3$ s, $V = c$; (*d*) pressure waves at $t = 3$ s, $V > c$.**

When the point source and the fluid are stationary, the pressure wave pattern is symmetrical (Fig. 11.3*a*) and an observer anywhere in the pressure field would hear the same sound frequency from the point source. When the velocity of the point source (or the fluid) is very small in comparison with the speed of sound, the pressure wave pattern will still be nearly symmetrical. The speed of sound in an incompressible fluid is infinitely large. Thus, the stationary point source and stationary fluid situation are representative of incompressible flows. For truly incompressible flows, the communication of pressure information throughout the flow field is unrestricted and instantaneous ($c = \infty$).

Fluids in the News

Pistol shrimp confound blast detectors Authorities are on the trail of fishermen in Southeast Asia and along Africa's east coast who illegally blast coral reefs to rubble to increase their catch. Researchers at Hong Kong University of Science and Technology have developed a method of using underwater microphones (hydrophones) to pick up the noise from such blasts. One complicating factor in the development of such a system is the noise produced by the claw-clicking pistol shrimp that live on the reefs. The third right appendage of the 5 cm long pistol shrimp is adapted into a huge claw with a moveable finger that can be snapped shut with so much force that the resulting *sound waves* kill or stun nearby prey. When near the hydrophones, the shrimp can generate short-range shock waves that are bigger than the signal from a distant blast. By recognizing the differences between the signatures of the sound from an explosion and that of the pistol shrimp "blast," the scientists can differentiate between the two and pinpoint the location of the illegal blasts.

V11.3 Jet noise

When the point source moves in fluid at rest (or when fluid moves past a stationary point source), the pressure wave patterns vary in asymmetry, with the extent of asymmetry depending on the ratio of the point source (or fluid) velocity and the speed of sound. When $V/c < 1$, the wave pattern is similar to the one shown in Fig. 11.3*b*. This flow is considered ***subsonic*** and compressible. A stationary observer will hear a different sound frequency coming from the point source depending on where the observer is relative to the source because the wave pattern is asymmetrical. We call this phenomenon the Doppler effect. Pressure information can still travel unrestricted throughout the flow field, but not symmetrically or instantaneously.

When $V/c = 1$, pressure waves are not present ahead of the moving point source. The flow is ***sonic.*** If you were positioned to the left of the moving point source, you would not hear the point source until it was coincident with your location. For flow moving past a stationary point source at the speed of sound ($V/c = 1$), the pressure waves are all tangent to a plane that is perpendicular to the flow and that passes through the point source. The concentration of pressure waves in this tangent plane suggests the formation of a significant pressure variation across the plane. This plane is often called a ***Mach wave***. Note that communication of pressure information is restricted to the region of flow downstream of the Mach wave. The region of flow upstream of the Mach wave is called the *zone of silence,* and the region of flow downstream of the tangent plane is called the *zone of action.*

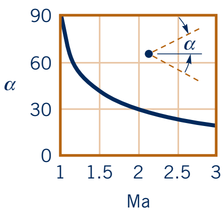

When $V > c$, the flow is ***supersonic,*** and the pressure wave pattern resembles the one depicted in Fig. 11.3*d*. A cone (***Mach cone***) that is tangent to the pressure waves can be constructed to represent the Mach wave that separates the zone of silence from the zone of action in this case. The communication of pressure information is restricted to the zone of action. From the sketch of Fig. 11.3*d*, we can see that the angle of this cone, α, is given by

$$\sin \alpha = \frac{c}{V} = \frac{1}{\text{Ma}} \qquad \textbf{(11.39)}$$

V11.4 Speed boat

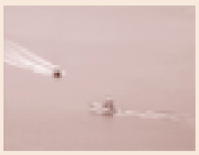

This relationship between Mach number, Ma, and Mach cone angle, α, shown by the figure in the margin, is valid for $V/c > 1$ only. The concentration of pressure waves at the surface of the Mach cone suggests a significant pressure, and thus density, variation across the cone surface. (See the photograph at the beginning of this chapter.) An abrupt density change can be visualized in a flow field by using special optics. Examples of flow visualization methods include the schlieren, shadowgraph, and interferometer techniques (see Ref. 4). A schlieren photo of a flow for which $V > c$ is shown in Fig. 11.4. The airflow through the row of compressor blade airfoils is as shown with the arrow. The flow enters supersonically ($\text{Ma}_1 = 1.14$) and

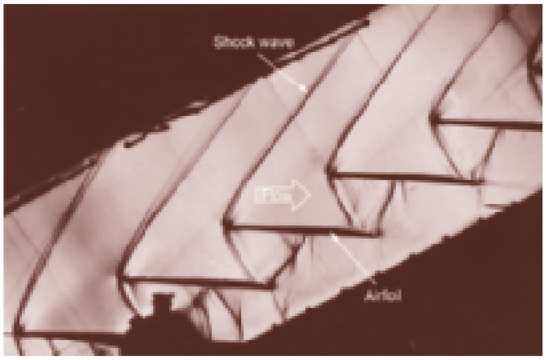

■ **Figure 11.4** **The Schlieren visualization of flow (supersonic to subsonic) through a row of compressor airfoils. (Photograph provided by Dr. Hans Starken, Germany.)**

V11.5 Compressible flow visualization

leaves subsonically ($Ma_2 = 0.86$). The center two airfoils have pressure tap hoses connected to them. Regions of significant changes in fluid density appear in the supersonic portion of the flow. Also, the region of separated flow on each airfoil is visible.

This discussion about pressure wave patterns suggests the following categories of fluid flow:

1. Incompressible flow: $Ma \leq 0.3$. Unrestricted, nearly symmetrical and instantaneous pressure communication.
2. Compressible subsonic flow: $0.3 < Ma < 1.0$. Unrestricted but noticeably asymmetrical pressure communication.
3. Compressible supersonic flow: $Ma \geq 1.0$. Formation of Mach wave; pressure communication restricted to zone of action.

In addition to the above-mentioned categories of flows, two other regimes are commonly referred to: namely, ***transonic flows*** ($0.9 \leq Ma \leq 1.2$) and ***hypersonic flows*** ($Ma > 5$). Modern aircraft are mainly powered by gas turbine engines that involve transonic flows. When a space shuttle reenters the Earth's atmosphere, the flow is hypersonic. Future aircraft may be expected to operate from subsonic to hypersonic flow conditions.

Fluids in the News

Supersonic and compressible flows in gas turbines Modern gas turbine engines commonly involve compressor and turbine blades that are moving so fast that the fluid flows over the blades are locally *supersonic*. Density varies considerably in these flows so they are also considered to be *compressible*. *Shock waves* can form when these supersonic flows are sufficiently decelerated. Shocks formed at blade leading edges or on blade surfaces can interact with other blades and shocks and seriously affect blade aerodynamic and structural performance. It is possible to have supersonic flows past blades near the outer diameter of a rotor with *subsonic flows* near the inner diameter of the same rotor. These rotors are considered to be *transonic* in their operation. Very large aero gas turbines can involve thrust levels exceeding 445 kN. Two of these engines are sufficient to carry over 350 passengers halfway around the world at high subsonic speed. (See Problem 11.5LL.)

EXAMPLE 11.4 Mach Cone

GIVEN An aircraft cruising at 1000 m elevation, z, above you moves past in a flyby. It is moving with a Mach number equal to 1.5 and the ambient temperature is 20 °C.

FIND How many seconds after the plane passes overhead do you expect to wait before you hear the aircraft?

SOLUTION

Since the aircraft is moving supersonically ($Ma > 1$), we can imagine a Mach cone originating from the forward tip of the craft as is illustrated in Fig. E11.4*a*. A photograph of this phenomenon is shown in Fig. E11.4*b*. When the surface of the cone reaches the

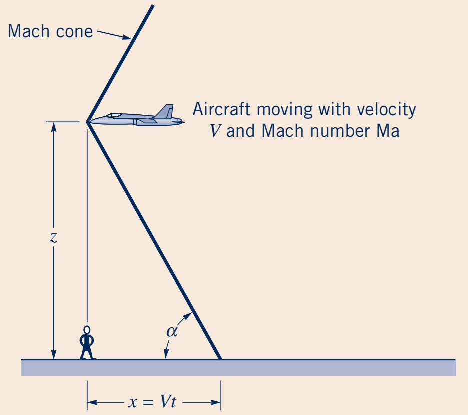

■ **Figure E11.4*a***

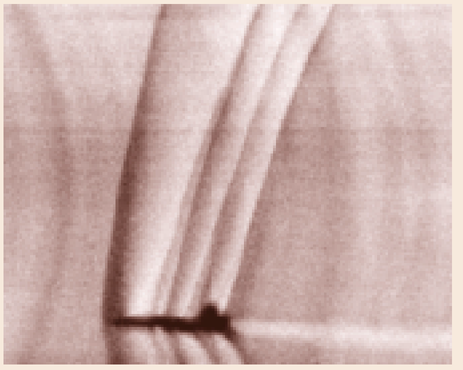

■ **Figure E11.4*b*** **NASA Schlieren photograph of shock waves from a T-38 aircraft at Mach 1.1, 3962 m.**

observer, the "sound" of the aircraft is perceived. The angle α in Fig. E11.4 is related to the elevation of the plane, z, and the ground distance, x, by

$$\alpha = \tan^{-1}\frac{z}{x} = \tan^{-1}\frac{1000}{Vt} \tag{1}$$

Also, assuming negligible change of Mach number with elevation, we can use Eq. 11.39 to relate Mach number to the angle α. Thus,

$$\text{Ma} = \frac{1}{\sin\alpha} \tag{2}$$

Combining Eqs. 1 and 2 we obtain

$$\text{Ma} = \frac{1}{\sin\left[\tan^{-1}(1000/Vt)\right]} \tag{3}$$

The speed of the aircraft can be related to the Mach number with

$$V = (\text{Ma})c \tag{4}$$

where c is the speed of sound. From Table B.2, $c = 343.3$ m/s. Using Ma $= 1.5$, we get from Eqs. 3 and 4

$$1.5 = \frac{1}{\sin\left\{\tan^{-1}\left[\dfrac{1000\text{ m}}{(1.5)(343.3\text{ m/s})t}\right]\right\}}$$

or

$$t = 2.17\text{ s} \qquad \textbf{(Ans)}$$

COMMENT By repeating the calculations for various values of Mach number, Ma, the results shown in Fig. E11.4*c* are obtained. Note that for subsonic flight (Ma < 1) there is no delay since the sound travels faster than the aircraft. You can hear a subsonic aircraft approaching.

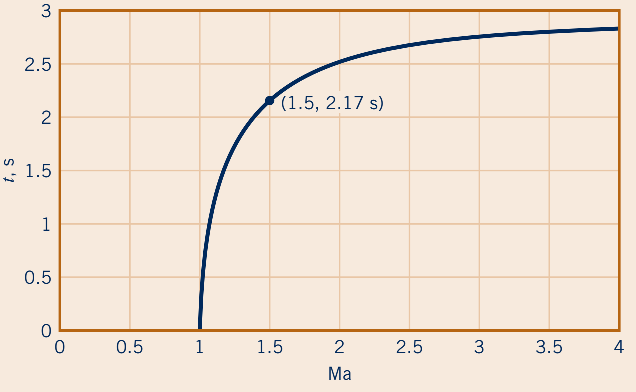

■ **Figure E11.4*c***

11.4 Isentropic Flow of an Ideal Gas

In this section, we consider in further detail the steady, one-dimensional, isentropic flow of an ideal gas with constant specific heat values (c_p and c_v). Because the flow is steady throughout, shaft work cannot be involved. Also, as explained earlier, the one-dimensionality of flows we discuss in this chapter implies velocity and fluid property changes in the streamwise direction only. We consider flows through finite control volumes with uniformly distributed velocities and fluid properties at each section of flow. Much of what we develop can also apply to the flow of a fluid particle along its pathline.

An important class of isentropic flow involves no heat transfer and zero friction.

Isentropic flow involves constant entropy and was discussed earlier in Section 11.1, where we learned that adiabatic and frictionless (reversible) flow is one form of isentropic flow. Some ideal gas relationships for isentropic flows were developed in Section 11.1. An isentropic flow is not achievable with actual fluids because of friction. Nonetheless, the study of isentropic flow trends is useful because it helps us to gain an understanding of actual compressible flow phenomena including choked flow, shock waves, acceleration from subsonic to supersonic flow, and deceleration from supersonic to subsonic flow.

11.4.1 Effect of Variations in Flow Cross-Sectional Area

When fluid flows steadily through a conduit that has a flow cross-sectional area that varies with axial distance, the conservation of mass (continuity) equation

$$\dot{m} = \rho A V = \text{constant} \tag{11.40}$$

can be used to relate the flow rates at different sections. For incompressible flow, the fluid density remains constant and the flow velocity from section to section varies inversely with cross-sectional area. However, when the flow is compressible, density, cross-sectional area, and flow velocity can all vary from section to section. We proceed to determine how fluid density and flow velocity change with axial location in a variable area duct when the fluid is an ideal gas and the flow through the duct is steady and isentropic.

In Chapter 3, Newton's second law was applied to the inviscid (frictionless) and steady flow of a fluid particle. For the streamwise direction, the result (Eq. 3.5) for either compressible or incompressible flows is

$$dp + \tfrac{1}{2}\rho\, d(V^2) + \gamma\, dz = 0 \tag{11.41}$$

The frictionless flow from section to section through a finite control volume is also governed by Eq. 11.41, if the flow is one-dimensional, because every particle of fluid involved will have the same experience. For ideal gas flow, the potential energy difference term, $\gamma\, dz$, can be dropped because of its small size in comparison to the other terms, namely, dp and $d(V^2)$. Thus, an appropriate equation of motion in the streamwise direction for the steady, one-dimensional, and isentropic (adiabatic and frictionless) flow of an ideal gas is obtained from Eq. 11.41 as

$$\frac{dp}{\rho V^2} = -\frac{dV}{V} \tag{11.42}$$

If we form the logarithm of both sides of the continuity equation (Eq. 11.40), the result is

$$\ln \rho + \ln A + \ln V = \text{constant} \tag{11.43}$$

Density, cross-sectional area, and velocity may all vary for a compressible flow.

Differentiating Eq. 11.43 we get

$$\frac{d\rho}{\rho} + \frac{dA}{A} + \frac{dV}{V} = 0$$

or

$$-\frac{dV}{V} = \frac{d\rho}{\rho} + \frac{dA}{A} \tag{11.44}$$

Now we combine Eqs. 11.42 and 11.44 to obtain

$$\frac{dp}{\rho V^2}\left(1 - \frac{V^2}{dp/d\rho}\right) = \frac{dA}{A} \tag{11.45}$$

Since the flow being considered is isentropic, the speed of sound is related to variations of pressure with density by Eq. 11.34, repeated here for convenience as

$$c = \sqrt{\left(\frac{\partial p}{\partial \rho}\right)_s}$$

Equation 11.34, combined with the definition of Mach number

$$\text{Ma} = \frac{V}{c} \tag{11.46}$$

and Eq. 11.45 yields

$$\frac{dp}{\rho V^2}(1 - \text{Ma}^2) = \frac{dA}{A} \tag{11.47}$$

Equations 11.42 and 11.47 merge to form

$$\frac{dV}{V} = -\frac{dA}{A}\frac{1}{(1 - \mathrm{Ma}^2)} \tag{11.48}$$

We can use Eq. 11.48 to conclude that when the flow is subsonic ($\mathrm{Ma} < 1$), velocity and section area changes are in opposite directions. In other words, the area increase associated with subsonic flow through a diverging duct like the one shown in Fig. 11.5*a* is accompanied by a velocity decrease. Subsonic flow through a converging duct (see Fig. 11.5*b*) involves an increase of velocity. These trends are consistent with incompressible flow behavior, which we described earlier in this book, for instance, in Chapters 3 and 8.

A converging duct will decelerate a supersonic flow and accelerate a subsonic flow.

Equation 11.48 also serves to show us that when the flow is supersonic ($\mathrm{Ma} > 1$), velocity and area changes are in the same direction. A diverging duct (Fig. 11.5*a*) will accelerate a supersonic flow. A converging duct (Fig. 11.5*b*) will decelerate a supersonic flow. These trends are the opposite of what happens for incompressible and subsonic compressible flows.

To better understand why subsonic and supersonic duct flows are so different, we combine Eqs. 11.44 and 11.48 to form

$$\frac{d\rho}{\rho} = \frac{dA}{A}\frac{\mathrm{Ma}^2}{(1 - \mathrm{Ma}^2)} \tag{11.49}$$

Using Eq. 11.49, we can conclude that for subsonic flows ($\mathrm{Ma} < 1$), density and area changes are in the same direction, whereas for supersonic flows ($\mathrm{Ma} > 1$), density and area changes are in opposite directions. Since ρAV must remain constant (Eq. 11.40), when the duct diverges and the flow is subsonic, density and area both increase and thus flow velocity must decrease. However, for supersonic flow through a diverging duct, when the area increases, the density decreases enough so that the flow velocity has to increase to keep ρAV constant.

By rearranging Eq. 11.48, we can obtain

$$\frac{dA}{dV} = -\frac{A}{V}(1 - \mathrm{Ma}^2) \tag{11.50}$$

Equation 11.50 gives us some insight into what happens when $\mathrm{Ma} = 1$. For $\mathrm{Ma} = 1$, Eq. 11.50 requires that $dA/dV = 0$. This result suggests that the area associated with $\mathrm{Ma} = 1$ is either a minimum or a maximum amount.

A ***converging–diverging duct*** (Fig. 11.6*a* and margin photograph) involves a minimum area. If the flow entering such a duct were subsonic, Eq. 11.48 discloses that the fluid velocity would increase in the converging portion of the duct, and achievement of a sonic condition ($\mathrm{Ma} = 1$) at the minimum area location appears possible. If the flow entering the converging–diverging duct is supersonic, Eq. 11.48 states that the fluid velocity would decrease in the converging portion of the duct and the sonic condition at the minimum area is possible.

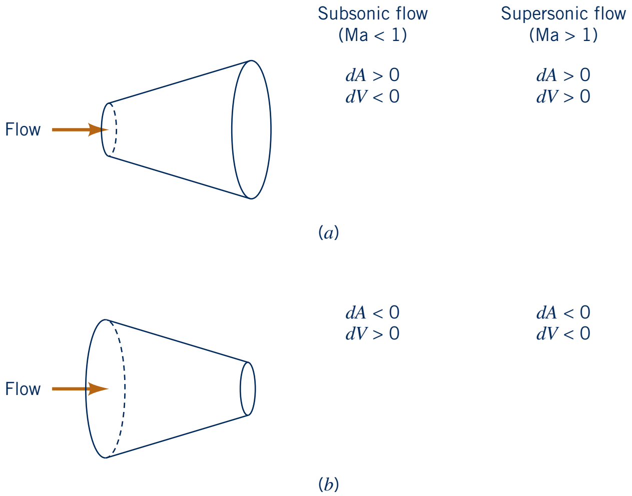

■ **Figure 11.5** ***(a)* A diverging duct. *(b)* A converging duct.**

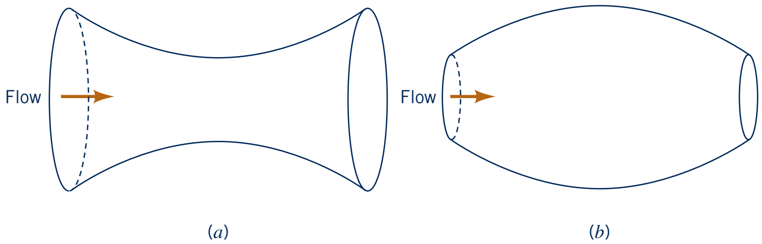

■ **Figure 11.6** ***(a)* A converging–diverging duct. *(b)* A diverging–converging duct.**

A diverging–converging duct (Fig. 11.6*b*), on the other hand, would involve a maximum area. If the flow entering this duct were subsonic, the fluid velocity would decrease in the diverging portion of the duct and the sonic condition could not be attained at the maximum area location. For supersonic flow in the diverging portion of the duct, the fluid velocity would increase and thus Ma = 1 at the maximum area is again impossible.

A converging–diverging duct is required to accelerate a flow from subsonic to supersonic flow conditions.

For the steady isentropic flow of an ideal gas, we conclude that the sonic condition (Ma = 1) can be attained in a converging–diverging duct at the minimum area location. This minimum area location is often called the ***throat*** of the converging–diverging duct. Furthermore, to achieve supersonic flow from a subsonic state in a duct, a converging–diverging area variation is necessary. For this reason, we often refer to such a duct as a *converging–diverging nozzle*. Note that a converging–diverging duct can also decelerate a supersonic flow to subsonic conditions. Thus, a converging–diverging duct can be a nozzle or a diffuser depending on whether the flow in the converging portion of the duct is subsonic or supersonic. A supersonic wind tunnel test section is generally preceded by a converging–diverging nozzle and followed by a converging–diverging diffuser (see Ref. 1). Further details about steady, isentropic, ideal gas flow through a converging–diverging duct are discussed in the next section.

11.4.2 Converging–Diverging Duct Flow

In the preceding section, we discussed the variation of density and velocity of the steady isentropic flow of an ideal gas through a variable area duct. We proceed now to develop equations that help us determine how other important flow properties vary in these flows.

It is convenient to use the stagnation state of the fluid as a reference state for compressible flow calculations. The stagnation state is associated with zero flow velocity and an entropy value that corresponds to the entropy of the flowing fluid. The subscript 0 is used to designate the stagnation state. Thus, stagnation temperature and pressure are T_0 and p_0. For example, if the fluid flowing through the converging–diverging duct of Fig. 11.6*a* were drawn isentropically from the atmosphere, the atmospheric pressure and temperature would represent the stagnation state of the flowing fluid. The stagnation state can also be achieved by isentropically decelerating a flow to zero velocity. This can be accomplished with a diverging duct for subsonic flows or a converging–diverging duct for supersonic flows. Also, as discussed earlier in Chapter 3, an approximately isentropic deceleration can be accomplished with a Pitot-static tube (see Fig. 3.6). It is thus possible to measure, with only a small amount of uncertainty, values of stagnation pressure, p_0, and stagnation temperature, T_0, of a flowing fluid.

In Section 11.1, we demonstrated that for the isentropic flow of an ideal gas (see Eq. 11.25)

$$\frac{p}{\rho^k} = \text{constant} = \frac{p_0}{\rho_0^k}$$

The streamwise equation of motion for steady and frictionless flow (Eq. 11.41) can be expressed for an ideal gas as

$$\frac{dp}{\rho} + d\left(\frac{V^2}{2}\right) = 0 \qquad \textbf{(11.51)}$$

since the potential energy term, $\gamma\, dz$, can be considered as being negligibly small in comparison with the other terms involved.

By incorporating Eq. 11.25 into Eq. 11.51 we obtain

$$\frac{p_0^{1/k}}{\rho_0}\frac{dp}{(p)^{1/k}} + d\left(\frac{V^2}{2}\right) = 0 \tag{11.52}$$

Consider the steady, one-dimensional, isentropic flow of an ideal gas with constant c_p and c_v through the converging–diverging nozzle of Fig. 11.6*a*. Equation 11.52 is valid for this flow and can be integrated between the common stagnation state of the flowing fluid to the state of the gas at any location in the converging–diverging duct to give

$$\frac{k}{k-1}\left(\frac{p_0}{\rho_0} - \frac{p}{\rho}\right) - \frac{V^2}{2} = 0 \tag{11.53}$$

By using the ideal gas equation of state (Eq. 11.1) with Eq. 11.53, we obtain

$$\frac{kR}{k-1}(T_0 - T) - \frac{V^2}{2} = 0 \tag{11.54}$$

It is of interest to note that combining Eqs. 11.14 and 11.54 leads to

$$c_p(T_0 - T) - \frac{V^2}{2} = 0$$

For isentropic flows the temperature, pressure, and density ratios are functions of the Mach number.

which, when merged with Eq. 11.9, results in

$$\check{h}_0 - \left(\check{h} + \frac{V^2}{2}\right) = 0 \tag{11.55}$$

where $\check{h}_0$ is the stagnation enthalpy. If the steady-flow energy equation (Eq. 5.69) is applied to the flow situation we are presently considering, the resulting equation will be identical to Eq. 11.55. Further, we conclude that the stagnation enthalpy is constant. The conservation of momentum and energy principles lead to the same equation (Eq. 11.55) for steady isentropic flows.

The definition of Mach number (Eq. 11.46) and the speed of sound relationship for ideal gases (Eq. 11.36) can be combined with Eq. 11.54 to yield

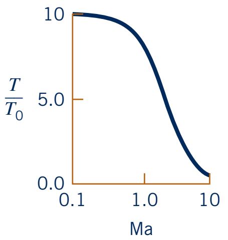

$$\boxed{\frac{T}{T_0} = \frac{1}{1 + [(k-1)/2]\text{Ma}^2}} \tag{11.56}$$

which is graphed in the margin for air. With Eq. 11.56 we can calculate the temperature of an ideal gas anywhere in the converging–diverging duct of Fig. 11.6*a* if the flow is steady, one-dimensional, and isentropic, provided we know the value of the local Mach number and the stagnation temperature.

We can also develop an equation for pressure variation. Since $p/\rho = RT$, then

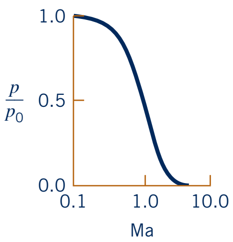

$$\left(\frac{p}{p_0}\right)\left(\frac{\rho_0}{\rho}\right) = \frac{T}{T_0} \tag{11.57}$$

From Eqs. 11.57 and 11.25 we obtain

$$\left(\frac{p}{p_0}\right) = \left(\frac{T}{T_0}\right)^{k/(k-1)} \tag{11.58}$$

Combining Eqs. 11.58 and 11.56 leads to

$$\boxed{\frac{p}{p_0} = \left\{\frac{1}{1 + [(k-1)/2]\text{Ma}^2}\right\}^{k/(k-1)}} \tag{11.59}$$

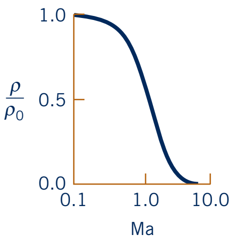

For density variation we consolidate Eqs. 11.56, 11.57, and 11.59 to get

$$\boxed{\frac{\rho}{\rho_0} = \left\{\frac{1}{1 + [(k-1)/2]\text{Ma}^2}\right\}^{1/(k-1)}} \tag{11.60}$$

These relationships are graphed in the margin for air.

A very useful means of keeping track of the states of an isentropic flow of an ideal gas involves a ***temperature–entropy (T–s) diagram,*** as is shown in Fig. 11.7. Experience has shown (see, for example, Refs. 2 and 3) that lines of constant pressure are generally as are sketched in Fig. 11.7. An isentropic flow is confined to a vertical line on a $T-s$ diagram. The vertical line in Fig. 11.7 is representative of flow between the stagnation state and any state within the converging–diverging nozzle. Equation 11.56 shows that fluid temperature decreases with an increase in Mach number. Thus, the lower temperature levels on a $T-s$ diagram correspond to higher Mach numbers. Equation 11.59 suggests that fluid pressure also decreases with an increase in Mach number. Thus, lower fluid temperatures and pressures are associated with higher Mach numbers in our isentropic converging–diverging duct example.

One way to produce flow through a converging–diverging duct like the one in Fig. 11.6*a* is to connect the downstream end of the duct to a vacuum pump. When the pressure at the downstream end of the duct (the back pressure) is decreased slightly, air will flow from the atmosphere through the duct and vacuum pump. Neglecting friction and heat transfer and considering the air to act as an ideal gas, Eqs. 11.56, 11.59, and 11.60 and a $T-s$ diagram can be used to describe steady flow through the converging–diverging duct.

If the pressure in the duct is only slightly less than atmospheric pressure, we predict with Eq. 11.59 that the Mach number levels in the duct will be low. Thus, with Eq. 11.60 we conclude that the variation of fluid density in the duct is also small. The continuity equation (Eq. 11.40) leads us to state that there is a small amount of fluid flow acceleration in the converging portion of the duct followed by flow deceleration in the diverging portion of the duct. We considered this type of flow when we discussed the Venturi meter in Section 3.6.3. The $T-s$ diagram for this flow is sketched in Fig. 11.8.

We next consider what happens when the back pressure is lowered further. Since the flow starts from rest upstream of the converging portion of the duct of Fig. 11.6*a*, Eqs. 11.48 and 11.50 reveal to us that flow up to the nozzle throat can be accelerated to a maximum allowable Mach number of 1 at the throat. Thus, when the duct back pressure is lowered sufficiently, the Mach number at the throat of the duct will be 1. Any further decrease of the back pressure will not affect the flow in the converging portion of the duct because, as is discussed in Section 11.3, information about pressure cannot move upstream when $\text{Ma} = 1$. When $\text{Ma} = 1$ at the throat of the converging–diverging duct, we have a condition called ***choked flow.*** Some useful equations for choked flow are developed below.

Choked flow occurs when the Mach number is 1.0 at the minimum cross-sectional area.

We have already used the stagnation state for which $\text{Ma} = 0$ as a reference condition. It will prove helpful to us to use the state associated with $\text{Ma} = 1$ and the same entropy level as the flowing fluid as another reference condition we shall call the ***critical state,*** denoted $(\ )^*$.

The ratio of pressure at the converging–diverging duct throat for choked flow, p^*, to stagnation pressure, p_0, is referred to as the ***critical pressure ratio.*** By substituting $\text{Ma} = 1$ into Eq. 11.59 we obtain

$$\frac{p^*}{p_0} = \left(\frac{2}{k+1}\right)^{k/(k-1)} \tag{11.61}$$

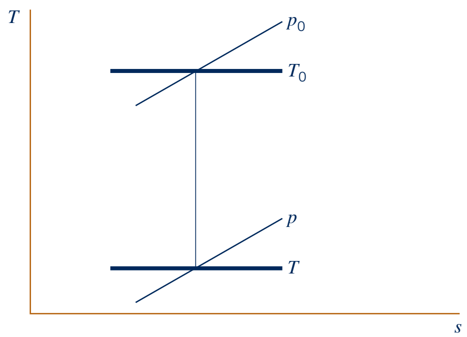

Figure 11.7 **The ($T-s$) diagram relating stagnation and static states.**

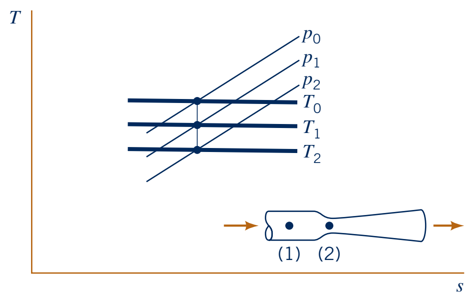

Figure 11.8 **The $T-s$ diagram for Venturi meter flow.**

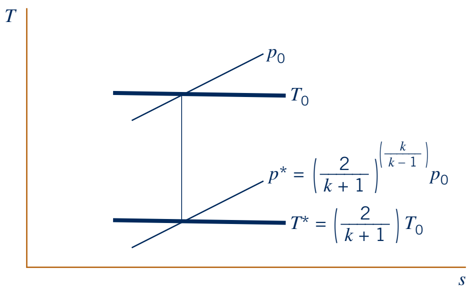

■ **Figure 11.9** **The relationship between the stagnation and critical states.**

For $k = 1.4$, the nominal value of k for air, Eq. 11.61 yields

$$\left(\frac{p^*}{p_0}\right)_{k=1.4} = 0.528 \qquad \textbf{(11.62)}$$

Because the stagnation pressure for our converging–diverging duct example is the atmospheric pressure, p_{atm}, the throat pressure for choked air flow is, from Eq. 11.62

$$p^*_{k=1.4} = 0.528 p_{atm}$$

We can get a relationship for the critical temperature ratio, T^*/T_0, by substituting Ma = 1 into Eq. 11.56. Thus,

$$\frac{T^*}{T_0} = \frac{2}{k+1} \qquad \textbf{(11.63)}$$

or for $k = 1.4$

$$\left(\frac{T^*}{T_0}\right)_{k=1.4} = 0.833 \qquad \textbf{(11.64)}$$

For the duct of Fig. 11.6*a*, Eq. 11.64 yields

$$T^*_{k=1.4} = 0.833 T_{atm}$$

The stagnation and critical states are at the same entropy level.

The stagnation and critical pressures and temperatures are shown on the $T-s$ diagram of Fig. 11.9.

When we combine the ideal gas equation of state (Eq. 11.1) with Eqs. 11.61 and 11.63, for Ma = 1 we get

$$\frac{\rho^*}{\rho_0} = \left(\frac{p^*}{T^*}\right)\left(\frac{T_0}{p_0}\right) = \left(\frac{2}{k+1}\right)^{k/(k-1)}\left(\frac{k+1}{2}\right) = \left(\frac{2}{k+1}\right)^{1/(k-1)} \qquad \textbf{(11.65)}$$

For air ($k = 1.4$), Eq. 11.65 leads to

$$\left(\frac{\rho^*}{\rho_0}\right)_{k=1.4} = 0.634 \qquad \textbf{(11.66)}$$

and we see that when the converging–diverging duct flow is choked, the density of the air at the duct throat is 63.4% of the density of atmospheric air.

EXAMPLE 11.5 Isentropic Flow in a Converging Duct

GIVEN A converging duct passes air steadily from standard atmospheric conditions to a receiver pipe as illustrated in Fig. E11.5*a*. The throat (minimum) flow cross-sectional area of the converging duct is 1×10^{-4} m^2. The receiver pressure is (**a**) 80 kPa (abs), (**b**) 40 kPa (abs).

FIND Determine the mass flowrate through the duct and sketch temperature–entropy diagrams for situations (**a**) and (**b**).

Solution

To determine the mass flowrate through the converging duct, we use Eq. 11.40. Thus,

$$\dot{m} = \rho A V = \text{constant}$$

or in terms of the given throat area, A_{th},

$$\dot{m} = \rho_{\text{th}} A_{\text{th}} V_{\text{th}} \qquad (1)$$

We assume that the flow through the converging duct is isentropic and that the air behaves as an ideal gas with constant c_p and c_v. Then, from Eq. 11.60

$$\frac{\rho_{\text{th}}}{\rho_0} = \left\{\frac{1}{1 + [(k-1)/2]\text{Ma}_{\text{th}}^2}\right\}^{1/(k-1)} \qquad (2)$$

The stagnation density, ρ_0, for the standard atmosphere is 1.23 kg/m^3, and the specific heat ratio is 1.4. To determine the throat Mach number, Ma_{th}, we can use Eq. 11.59,

$$\frac{p_{\text{th}}}{p_0} = \left\{\frac{1}{1 + [(k-1)/2]\text{Ma}_{\text{th}}^2}\right\}^{k/(k-1)} \qquad (3)$$

The critical pressure, p^*, is obtained from Eq. 11.62 as

$$\begin{aligned} p^* &= 0.528 p_0 = 0.528 p_{\text{atm}} \\ &= (0.528)[101 \text{ kPa(abs)}] = 53.3 \text{ kPa(abs)} \end{aligned}$$

If the receiver pressure, p_{re}, is greater than or equal to p^*, then $p_{\text{th}} = p_{\text{re}}$. If $p_{\text{re}} < p^*$, then $p_{\text{th}} = p^*$ and the flow is choked. With p_{th}, p_0, and k known, Ma_{th} can be obtained from Eq. 3, and ρ_{th} can be determined from Eq. 2.

The flow velocity at the throat can be obtained from Eqs. 11.36 and 11.46 as

$$V_{\text{th}} = \text{Ma}_{\text{th}} c_{\text{th}} = \text{Ma}_{\text{th}} \sqrt{R T_{\text{th}} k} \qquad (4)$$

The value of temperature at the throat, T_{th}, can be calculated from Eq. 11.56,

$$\frac{T_{\text{th}}}{T_0} = \frac{1}{1 + [(k-1)/2]\text{Ma}_{\text{th}}^2} \qquad (5)$$

Since the flow through the converging duct is assumed to be isentropic, the stagnation temperature is considered constant at the standard atmosphere value of $T_0 = 15 \text{ K} + 273 \text{ K} = 288 \text{ K}$. Note that absolute pressures and temperatures are used.

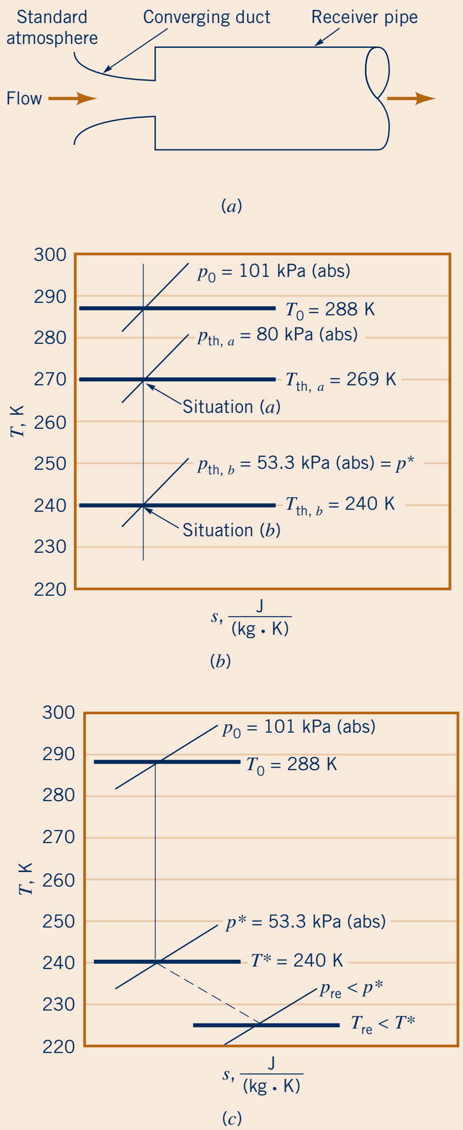

■ **Figure E11.5**

(a) For $p_{\text{re}} = 80 \text{ kPa(abs)} > 53.3 \text{ kPa(abs)} = p^*$, we have $p_{\text{th}} = 80$ kPa(abs). Then from Eq. 3

$$\frac{80 \text{ kPa(abs)}}{101 \text{ kPa(abs)}} = \left\{\frac{1}{1 + [(1.4-1)/2]\text{Ma}_{\text{th}}^2}\right\}^{1.4/(1.4-1)}$$

or

$$\text{Ma}_{\text{th}} = 0.587$$

From Eq. 2

$$\frac{\rho_{\text{th}}}{1.23 \text{ kg/m}^3} = \left\{\frac{1}{1 + [(1.4-1)/2](0.587)^2}\right\}^{1/(1.4-1)}$$

or

$$\rho_{\text{th}} = 1.04 \text{ kg/m}^3$$

From Eq. 5

$$\frac{T_{\text{th}}}{288 \text{ K}} = \frac{1}{1 + [(1.4-1)/2](0.587)^2}$$

or

$$T_{\text{th}} = 269 \text{ K}$$

Substituting $\text{Ma}_{\text{th}} = 0.587$ and $T_{\text{th}} = 269$ K into Eq. 4 we obtain

$$\begin{aligned} V_{\text{th}} &= 0.587 \sqrt{[286.9 \text{ J/(kg} \cdot \text{K)}](269 \text{ K})(1.4)} \\ &= 193 \text{ (J/kg)}^{1/2} \end{aligned}$$

Thus, since $1 \text{ J/kg} = 1 \text{ N} \cdot \text{m/kg} = 1 \text{ (kg} \cdot \text{m/s}^2) \cdot \text{m/kg} = (\text{m/s})^2$, we obtain

$$V_{\text{th}} = 193 \text{ m/s}$$

Finally from Eq. 1 we have

$$\dot{m} = (1.04 \text{ kg/m}^3)(1 \times 10^{-4} \text{ m}^2)(193 \text{ m/s})$$
$$= 0.0201 \text{ kg/s} \qquad \textbf{(Ans)}$$

(b) For $p_{re} = 40$ kPa(abs) < 53.3 kPa(abs) $= p^*$, we have $p_{th} = p^* = 53.3$ kPa(abs) and $\text{Ma}_{th} = 1$. The converging duct is choked. From Eq. 2 (see also Eq. 11.66)

$$\frac{\rho_{th}}{1.23 \text{ kg/m}^3} = \left\{\frac{1}{1 + [(1.4 - 1)/2](1)^2}\right\}^{1/(1.4-1)}$$

or

$$\rho_{th} = 0.780 \text{ kg/m}^3$$

From Eq. 5 (see also Eq. 11.64),

$$\frac{T_{th}}{288 \text{ K}} = \frac{1}{1 + [(1.4 - 1)/2](1)^2}$$

or

$$T_{th} = 240 \text{ K}$$

From Eq. 4,

$$V_{th} = (1)\sqrt{[286.9 \text{ J/(kg} \cdot \text{K)}](240 \text{ K})(1.4)}$$
$$= 310 \text{ (J/kg)}^{1/2} = 310 \text{ m/s}$$

since $1 \text{ J/kg} = 1 \text{ N} \cdot \text{m/kg} = 1 (\text{kg} \cdot \text{m/s}^2) \cdot \text{m/kg} = (\text{m/s})^2$. Finally from Eq. 1

$$\dot{m} = (0.780 \text{ kg/m}^3)(1 \times 10^{-4} \text{ m}^2)(310 \text{ m/s})$$
$$= 0.0242 \text{ kg/s} \qquad \textbf{(Ans)}$$

From the values of throat temperature and throat pressure calculated above for flow situations (a) and (b), we can construct the temperature–entropy diagram shown in Fig. E11.5*b*.

COMMENT Note that the flow from standard atmosphere to the receiver for receiver pressure, p_{re}, greater than or equal to the critical pressure, p^*, is isentropic. When the receiver pressure is less than the critical pressure as in situation (b) above, what is the flow like downstream from the exit of the converging duct? Experience suggests that this flow, when $p_{re} < p^*$, is three-dimensional and nonisentropic and involves a drop in pressure from p_{th} to p_{re}, a drop in temperature, and an increase of entropy as are indicated in Fig. E11.5*c*.

Isentropic flow Eqs. 11.56, 11.59, and 11.60 have been used to construct Fig. D.1 in Appendix D for air ($k = 1.4$). Examples 11.6 and 11.7 illustrate how these graphs of T/T_0, p/p_0, and ρ/ρ_0 as a function of Mach number, Ma, can be used to solve compressible flow problems.

EXAMPLE 11.6 Use of Compressible Flow Graphs in Solving Problems

GIVEN Consider the flow described in Example 11.5.

FIND Solve Example 11.5 using Fig. D.1 of Appendix D.

SOLUTION

We still need the density and velocity of the air at the converging duct throat to solve for mass flowrate from

$$\dot{m} = \rho_{th} A_{th} V_{th} \qquad \textbf{(1)}$$

(a) Since the receiver pressure, $p_{re} = 80$ kPa(abs), is greater than the critical pressure, $p^* = 53.3$ kPa(abs), the throat pressure, p_{th}, is equal to the receiver pressure. Thus

$$\frac{p_{th}}{p_0} = \frac{80 \text{ kPa(abs)}}{101 \text{ kPa(abs)}} = 0.792$$

From Fig. D.1, for $p/p_0 = 0.79$, we get from the graph

$$\text{Ma}_{th} = 0.59$$

$$\frac{T_{th}}{T_0} = 0.94 \qquad \textbf{(2)}$$

$$\frac{\rho_{th}}{\rho_0} = 0.85 \qquad \textbf{(3)}$$

Thus, from Eqs. 2 and 3

$$T_{th} = (0.94)(288 \text{ K}) = 271 \text{ K}$$

and

$$\rho_{th} = (0.85)(1.23 \text{ kg/m}^3) = 1.04 \text{ kg/m}^3$$

Furthermore, using Eqs. 11.36 and 11.46 we get

$$V_{th} = \text{Ma}_{th}\sqrt{RT_{th}k}$$
$$= (0.59)\sqrt{[286.9 \text{ J/(kg} \cdot \text{K)}](269 \text{ K})(1.4)}$$
$$= 194 \text{ (J/kg)}^{1/2} = 194 \text{ m/s}$$

since $1 \text{ J/kg} = 1 \text{ N} \cdot \text{m/kg} = 1 (\text{kg} \cdot \text{m/s}^2) \cdot \text{m/kg} = (\text{m/s})^2$. Finally, from Eq. 1

$$\dot{m} = (1.04 \text{ kg/m}^3)(1 \times 10^{-4} \text{ m}^2)(194 \text{ m/s})$$
$$= 0.0202 \text{ kg/s} \qquad \textbf{(Ans)}$$

(b) For $p_{re} = 40$ kPa(abs) < 53.3 kPa(abs) $= p^*$, the throat pressure is equal to 53.3 kPa(abs) and the duct is choked with $\text{Ma}_{th} = 1$. From Fig. D.1, for Ma = 1 we get

$$\frac{T_{th}}{T_0} = 0.83 \quad \textbf{(4)}$$

and

$$\frac{\rho_{th}}{\rho_0} = 0.64 \quad \textbf{(5)}$$

From Eqs. 4 and 5 we obtain

$$T_{th} = (0.83)(288 \text{ K}) = 240 \text{ K}$$

and

$$\rho_{th} = (0.64)(1.23 \text{ kg/m}^3) = 0.79 \text{ kg/m}^3$$

Also, from Eqs. 11.36 and 11.46 we conclude that

$$\begin{aligned} V_{th} &= \text{Ma}_{th}\sqrt{RT_{th}k} \\ &= (1)\sqrt{[286.9 \text{ J/(kg}\cdot\text{K)}](240 \text{ K})(1.4)} \\ &= 310 \text{ (J/kg)}^{1/2} = 310 \text{ m/s} \end{aligned}$$

Then, from Eq. 1

$$\begin{aligned} \dot{m} &= (0.79 \text{ kg/m}^3)(1 \times 10^{-4} \text{ m}^2)(310 \text{ m/s}) \\ &= 0.024 \text{ kg/s} \end{aligned} \quad \textbf{(Ans)}$$

COMMENT The values from Fig. D.1 resulted in answers for mass flowrate that are close (within the accuracy of reading data from the figures) to those using the ideal gas equations (see Example 11.5).

The temperature–entropy diagrams remain the same as those provided in the solution of Example 11.5.

Example 11.7 Static to Stagnation Pressure Ratio

GIVEN The static pressure to stagnation pressure ratio at a point in a flow stream is measured with a Pitot-static tube (see Fig. 3.6) as being equal to 0.82. The stagnation temperature of the fluid is 20 °C.

FIND Determine the flow velocity if the fluid is **(a)** air, **(b)** helium.

Solution

We consider both air and helium, flowing as described above, to act as ideal gases with constant specific heats. Then, we can use any of the ideal gas relationships developed in this chapter. To determine the flow velocity, we can combine Eqs. 11.36 and 11.46 to obtain

$$V = \text{Ma}\sqrt{RTk} \quad \textbf{(1)}$$

By knowing the value of static to stagnation pressure ratio, p/p_0, and the specific heat ratio we can obtain the corresponding Mach number from Eq. 11.59, or for air, from Fig. D.1. Figure D.1 cannot be used for helium, since k for helium is 1.66 and Fig. D.1 is for $k = 1.4$ only. With Mach number, specific heat ratio, and stagnation temperature known, the value of static temperature can be subsequently ascertained from Eq. 11.56 (or Fig. D.1 for air).

(a) For air, $p/p_0 = 0.82$; thus from Fig. D.1,

$$\text{Ma} = 0.54 \quad \textbf{(2)}$$

and

$$\frac{T}{T_0} = 0.94 \quad \textbf{(3)}$$

Then, from Eq. 3

$$T = (0.94)[20 \text{ K} + 274 \text{ K}] = 294 \text{ K} \quad \textbf{(4)}$$

and using Eqs. 1, 2, and 4 we get

$$\begin{aligned} V &= (0.54)\sqrt{(286.9 \text{ J/kg}\cdot\text{K})(294 \text{ K})(1.4)} \\ &= 186 \text{ m/s} \end{aligned} \quad \textbf{(Ans)}$$

(b) For helium, $p/p_0 = 0.82$ and $k = 1.66$. By substituting these values into Eq. 11.59 we get

$$0.82 = \left\{\frac{1}{1 + [(1.66 - 1)/2]\,\text{Ma}^2}\right\}^{1.66/(1.66-1)}$$

or

$$\text{Ma} = 0.499$$

From Eq. 11.56 we obtain

$$\frac{T}{T_0} = \frac{1}{1 + [(k-1)/2]\text{Ma}^2}$$

Thus,

$$\begin{aligned} T &= \left\{\frac{1}{1 + [(1.66 - 1)/2](0.499)^2}\right\}[(20 + 274) \text{ K}] \\ &= 272 \text{ K} \end{aligned}$$

From Eq. 1 we obtain

$$\begin{aligned} V &= (0.499)\sqrt{[286.9 \text{ J/kg}\cdot\text{K}](272 \text{ K})(1.66)} \\ &= 180 \text{ m/s} \end{aligned}$$

COMMENT Note that the isentropic flow equations and Fig. D.1 for $k = 1.4$ were used presently to describe fluid particle isentropic flow along a pathline in a stagnation process. Even though these equations and graph were developed for one-dimensional duct flows, they can be used for frictionless, adiabatic pathline flows also.

Furthermore, while the Mach numbers calculated above are of similar size for the air and helium flows, the flow speed is much larger for helium than for air because the speed of sound in helium is much larger than it is in air.

Also included in Fig. D.1 is a graph of the ratio of local area, A, to critical area, A^*, for different values of local Mach number. The importance of this area ratio is clarified below.

For choked flow through the converging–diverging duct of Fig. 11.6*a*, the conservation of mass equation (Eq. 11.40) yields

$$\rho A V = \rho^* A^* V^*$$

or

$$\frac{A}{A^*} = \left(\frac{\rho^*}{\rho}\right)\left(\frac{V^*}{V}\right) \tag{11.67}$$

From Eqs. 11.36 and 11.46, we obtain

$$V^* = \sqrt{RT^*k} \tag{11.68}$$

and

$$V = \text{Ma}\sqrt{RTk} \tag{11.69}$$

By combining Eqs. 11.67, 11.68, and 11.69 we get

$$\frac{A}{A^*} = \frac{1}{\text{Ma}}\left(\frac{\rho^*}{\rho_0}\right)\left(\frac{\rho_0}{\rho}\right)\sqrt{\frac{(T^*/T_0)}{(T/T_0)}} \tag{11.70}$$

The incorporation of Eqs. 11.56, 11.60, 11.63, 11.65, and 11.70 results in

$$\frac{A}{A^*} = \frac{1}{\text{Ma}}\left\{\frac{1 + [(k-1)/2]\text{Ma}^2}{1 + [(k-1)/2]}\right\}^{(k+1)/[2(k-1)]} \tag{11.71}$$

The ratio of flow area to the critical area is a useful concept for isentropic duct flow.

Equation 11.71 was used to generate the values of A/A^* for air ($k = 1.4$) in Fig. D.1. These values of A/A^* are graphed as a function of Mach number in Fig. 11.10. As is demonstrated in the following examples, whether or not the critical area, A^*, is physically present in the flow, the area ratio, A/A^*, is still a useful concept for the isentropic flow of an ideal gas through a converging–diverging duct.

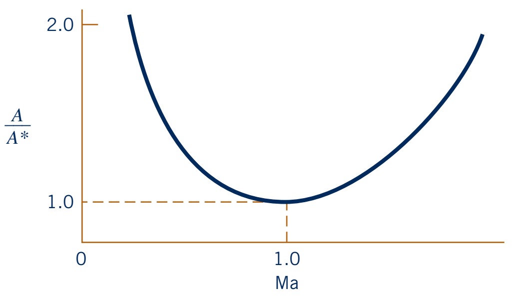

■ **Figure 11.10 The variation of area ratio with Mach number for isentropic flow of an ideal gas (k = 1.4, linear coordinate scales).**

EXAMPLE 11.8 Isentropic Choked Flow in a Converging–Diverging Duct with Subsonic Entry

GIVEN Air enters subsonically from standard atmosphere and flows isentropically through a choked converging–diverging duct having a circular cross-sectional area, A, that varies with axial distance from the throat, x, according to the formula

$$A = 0.1 + x^2$$

where A is in square meters and x is in meters. The duct extends from $x = -0.5$ m to $x = +0.5$ m.

FIND For this flow situation, sketch the side view of the duct and graph the variation of Mach number, static temperature to stagnation temperature ratio, T/T_0, and static pressure to stagnation pressure ratio, p/p_0, through the duct from $x = -0.5$ m to $x = +0.5$ m. Also show the possible fluid states at $x = -0.5$ m, 0 m, and $+0.5$ m using temperature–entropy coordinates.

SOLUTION

The side view of the converging–diverging duct is a graph of radius r from the duct axis as a function of axial distance. For a circular flow cross section we have

$$A = \pi r^2 \tag{1}$$

where

$$A = 0.1 + x^2 \tag{2}$$

Thus, combining Eqs. 1 and 2, we have

$$r = \left(\frac{0.1 + x^2}{\pi}\right)^{1/2} \tag{3}$$

and a graph of radius as a function of axial distance can be easily constructed (see Fig. E11.8*a*).

Since the converging–diverging duct in this example is choked, the throat area is also the critical area, A^*. From Eq. 2 we see that

$$A^* = 0.1 \text{ m}^2 \tag{4}$$

For any axial location, from Eqs. 2 and 4 we get

$$\frac{A}{A^*} = \frac{0.1 + x^2}{0.1} \tag{5}$$

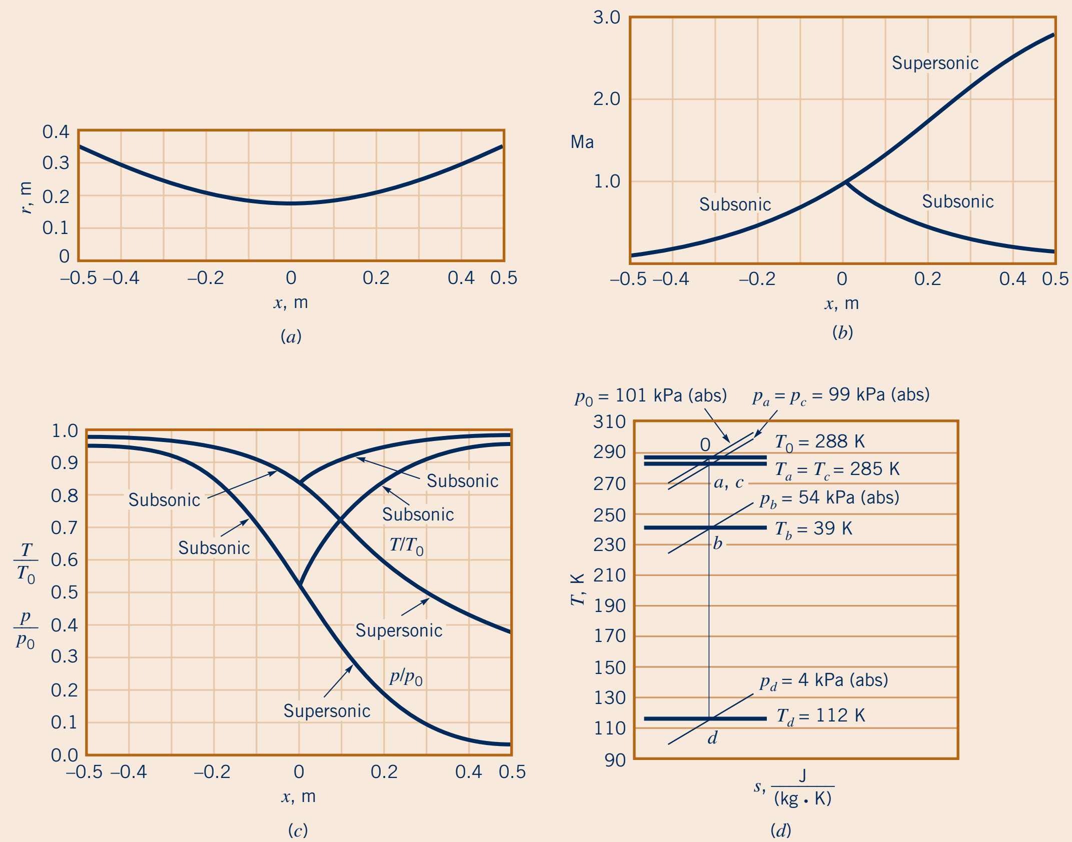

■ **Figure E11.8**

Values of A/A^* from Eq. 5 can be used in Eq. 11.71 to calculate corresponding values of Mach number, Ma. For air with $k = 1.4$, we could enter Fig. D.1 with values of A/A^* and read off values of the Mach number. With values of Mach number ascertained, we could use Eqs. 11.56 and 11.59 to calculate related values of T/T_0 and p/p_0. For air with $k = 1.4$, Fig. D.1 could be entered with A/A^* or Ma to get values of T/T_0 and p/p_0. To solve this example, we elect to use values from Fig. D.1.

The following table was constructed by using Eqs. 3 and 5 and Fig. D.1.

With the air entering the choked converging–diverging duct subsonically, only one isentropic solution exists for the converging portion of the duct. This solution involves an accelerating flow that becomes sonic ($\text{Ma} = 1$) at the throat of the passage. Two isentropic flow solutions are possible for the diverging portion of the duct—one subsonic, the other supersonic. If the pressure ratio, p/p_0, is set at 0.98 at $x = +0.5$ m (the outlet), the subsonic flow will occur. Alternatively, if p/p_0 is set at 0.04 at $x = +0.5$ m, the supersonic flow field will exist. These conditions are illustrated in Fig. E11.8. An unchoked subsonic flow through the converging–diverging duct of this example is discussed in Example 11.10. Choked flows involving flows other than the two isentropic flows in the diverging portion of the duct of this example are discussed after Example 11.10.

x (m)	From Eq. 3, r (m)	From Eq. 5, A/A^*	From Fig. D.1 Ma	T/T_0	p/p_0	State
Subsonic Solution						
−0.5	0.334	3.5	0.17	0.99	0.98	*a*
−0.4	0.288	2.6	0.23	0.99	0.97	
−0.3	0.246	1.9	0.32	0.98	0.93	
−0.2	0.211	1.4	0.47	0.96	0.86	
−0.1	0.187	1.1	0.69	0.91	0.73	
0	0.178	1	1.00	0.83	0.53	*b*
+0.1	0.187	1.1	0.69	0.91	0.73	
+0.2	0.211	1.4	0.47	0.96	0.86	
+0.3	0.246	1.9	0.32	0.98	0.93	
+0.4	0.288	2.6	0.23	0.99	0.97	
+0.5	0.344	3.5	0.17	0.99	0.98	*c*
Supersonic Solution						
+0.1	0.187	1.1	1.37	0.73	0.33	
+0.2	0.211	1.4	1.76	0.62	0.18	
+0.3	0.246	1.9	2.14	0.52	0.10	
+0.4	0.288	2.6	2.48	0.45	0.06	
+0.5	0.334	3.5	2.80	0.39	0.04	*d*

COMMENT Note that if the diverging portion of this duct is extended, larger values of A/A^* and Ma are achieved. From Fig. D1, note that further increases of A/A^* result in smaller changes of Ma after A/A^* values of about 10. The ratio of p/p_0 becomes vanishingly small, suggesting a practical limit to the expansion.

EXAMPLE 11.9 Isentropic Choked Flow in a Converging–Diverging Duct with Supersonic Entry

GIVEN Air enters supersonically with T_0 and p_0 equal to standard atmosphere values and flows isentropically through the choked converging–diverging duct described in Example 11.8.

FIND Graph the variation of Mach number, Ma, static temperature to stagnation temperature ratio, T/T_0, and static pressure to stagnation pressure ratio, p/p_0, through the duct from $x = -0.5$ m to $x = +0.5$ m. Also show the possible fluid states at $x = -0.5$ m, 0 m, and $+0.5$ m by using temperature–entropy coordinates.

SOLUTION

With the air entering the converging–diverging duct of Example 11.8 supersonically instead of subsonically, a unique isentropic flow solution is obtained for the converging portion of the duct. Now, however, the flow decelerates to the sonic condition at the throat. The two solutions obtained previously in Example 11.8 for the diverging portion are still valid. Since the area variation in the duct is symmetrical with respect to the duct throat, we can use the supersonic flow values obtained from Example 11.8 for the supersonic flow in the converging portion of the duct. The supersonic flow solution for the converging passage is summarized in the following table. The solution values for the entire duct are graphed in Fig. E11.9.

x (m)	A/A^*	From Fig. D.1 Ma	T/T_0	p/p_0	State
−0.5	3.5	2.8	0.39	0.04	*e*
−0.4	2.6	2.5	0.45	0.06	
−0.3	1.9	2.1	0.52	0.10	
−0.2	1.4	1.8	0.62	0.18	
−0.1	1.1	1.4	0.73	0.33	
0	1	1.0	0.83	0.53	*b*

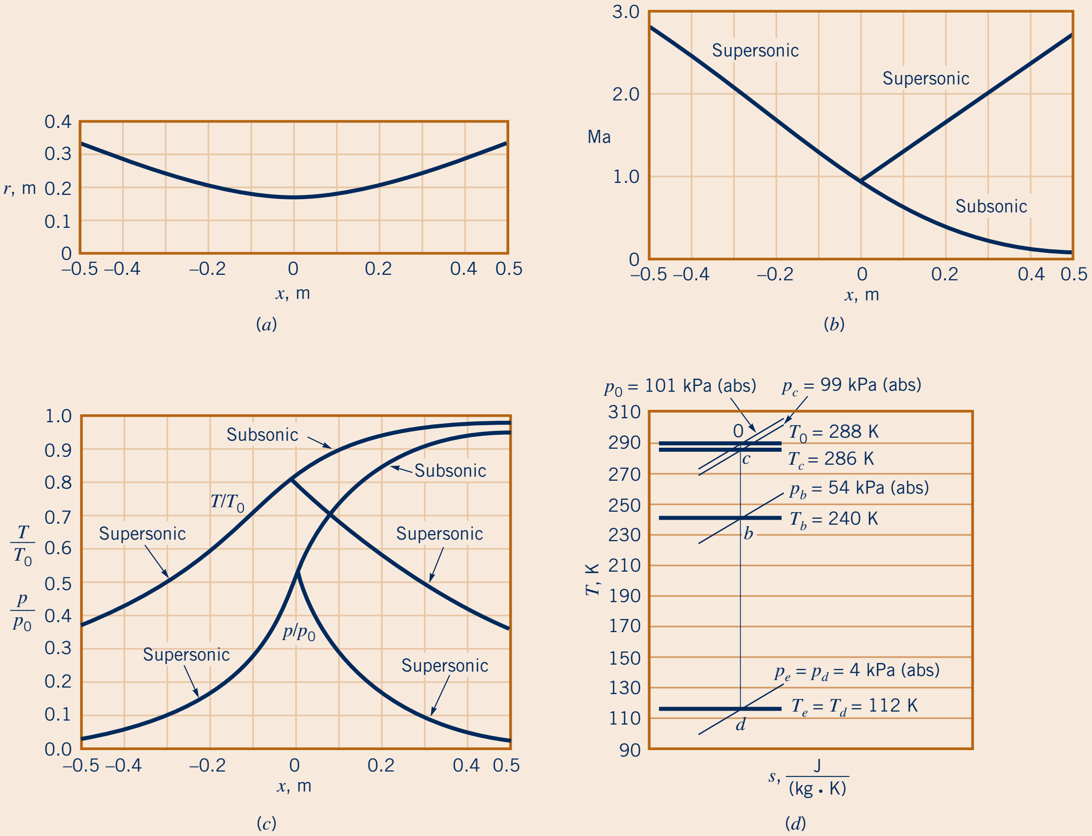

Figure E11.9

EXAMPLE 11.10 Isentropic Unchoked Flow in a Converging–Diverging Duct

GIVEN Air flows subsonically and isentropically through the converging–diverging duct of Example 11.8.

FIND Graph the variation of Mach number, Ma, static temperature to stagnation temperature ratio, T/T_0, and the static pressure to stagnation pressure ratio, p/p_0, through the duct from $x = -0.5$ m to $x = +0.5$ m for Ma $= 0.48$ at $x = 0$ m. Show the corresponding temperature–entropy diagram.

SOLUTION

Since for this example, Ma $= 0.48$ at $x = 0$ m, the isentropic flow through the converging–diverging duct will be entirely subsonic and not choked. For air ($k = 1.4$) flowing isentropically through the duct, we can use Fig. D.1 for flow field quantities. Entering Fig. D.1 with Ma $= 0.48$ we read off $p/p_0 = 0.85$, $T/T_0 = 0.96$, and $A/A^* = 1.4$. Even though the duct flow is not choked in this example and A^* does not therefore exist physically, it still represents a valid reference. For a given isentropic flow, p_0, T_0, and A^* are constants. Since A at $x = 0$ m is equal to 0.10 m^2 (from Eq. 2 of Example 11.8), A^* for this example is

$$A^* = \frac{A}{(A/A^*)} = \frac{0.10 \text{ m}^2}{1.4} = 0.07 \text{ m}^2 \qquad \textbf{(1)}$$

With known values of duct area at different axial locations, we can calculate corresponding area ratios, A/A^*, knowing $A^* = 0.07$ m^2. Having values of the area ratio, we can use Fig. D.1 and obtain related values of Ma, T/T_0, and p/p_0. The following table summarizes flow quantities obtained in this manner. The results are graphed in Fig. E11.10.

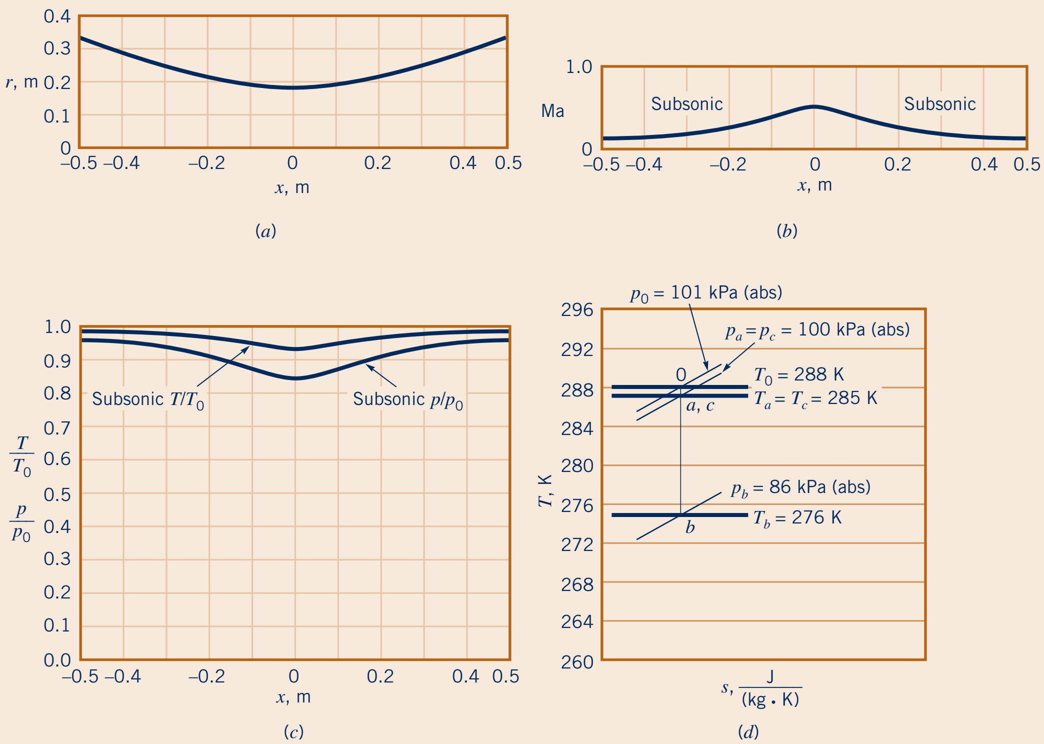

■ **Figure E11.10**

A more precise solution for the flow of this example could have been obtained with isentropic flow equations by following the steps outlined below.

1. Use Eq. 11.59 to get p/p_0 at $x = 0$ knowing k and Ma = 0.48.
2. From Eq. 11.71, obtain value of A/A^* at $x = 0$ knowing k and Ma.
3. Determine A^* knowing A and A/A^* at $x = 0$.
4. Determine A/A^* at different axial locations, x.
5. Use Eq. 11.71 and A/A^* from step 4 above to get values of Mach numbers at different axial locations.
6. Use Eqs. 11.56 and 11.59 and Ma from step 5 above to obtain T/T_0 and p/p_0 at different axial locations, x.

COMMENT There are an infinite number of subsonic, isentropic flow solutions for the converging–diverging duct considered in this example (one for any given Ma < 1 at $x = 0$).

	Calculated,	From Fig. D.1			
x (m)	A/A^*	Ma	T/T_0	p/p_0	State
−0.5	5.0	0.12	0.99	0.99	*a*
−0.4	3.7	0.16	0.99	0.98	
−0.3	2.7	0.23	0.99	0.96	
−0.2	2.0	0.31	0.98	0.94	
−0.1	1.6	0.40	0.97	0.89	
0	1.4	0.48	0.96	0.85	*b*
+0.1	1.6	0.40	0.97	0.89	
+0.2	2.0	0.31	0.98	0.94	
+0.3	2.7	0.23	0.99	0.96	
+0.4	3.7	0.16	0.99	0.98	
+0.5	5.0	0.12	0.99	0.99	*c*

Fluids in the News

Liquid knife A supersonic stream of liquid nitrogen is capable of cutting through engineering materials like steel and concrete. Originally developed at the Idaho National Engineering Laboratory for cutting open barrels of waste products, this technology is now more widely available. The fast-moving nitrogen enters the cracks and crevices of the material being cut, then expands rapidly and breaks up the solid material it has penetrated. After doing its work, the nitrogen gas simply becomes part of the atmosphere, which is mostly nitrogen already. This technology is also useful for stripping coatings even from delicate surfaces.

A variety of flow situations can occur for flow in a converging–diverging duct.

V11.6 Rocket engine start-up

The isentropic flow behavior for the converging–diverging duct discussed in Examples 11.8, 11.9, and 11.10 is summarized in the area ratio–Mach number graphs sketched in Fig. 11.11. The points a, b, and c represent states at axial distance $x = -0.5$ m, 0 m, and $+0.5$ m. In Fig. 11.11a, the isentropic flow through the converging–diverging duct is subsonic without choking at the throat. This situation was discussed in Example 11.10. Figure 11.11b represents subsonic to subsonic choked flow (Example 11.8), and Fig. 11.11c is for subsonic to supersonic choked flow (also Example 11.8). The states in Fig. 11.11d are related to the supersonic to supersonic choked flow of Example 11.9; the states in Fig. 11.11e are for the supersonic to subsonic choked flow of Example 11.9. Not covered by an example but also possible are the isentropic flow states a, b, and c shown in Fig. 11.11f for supersonic to supersonic flow without choking. These six categories generally represent the possible kinds of isentropic, ideal gas flow through a converging–diverging duct.

For a given stagnation state (i.e., T_0 and p_0 fixed), ideal gas (k = constant), and converging–diverging duct geometry, an infinite number of isentropic subsonic to subsonic (not choked) and supersonic to supersonic (not choked) flow solutions exist. In contrast, the isentropic subsonic to supersonic (choked), subsonic to subsonic (choked), supersonic to subsonic (choked), and supersonic to supersonic (choked) flow solutions are each unique. The above-mentioned isentropic

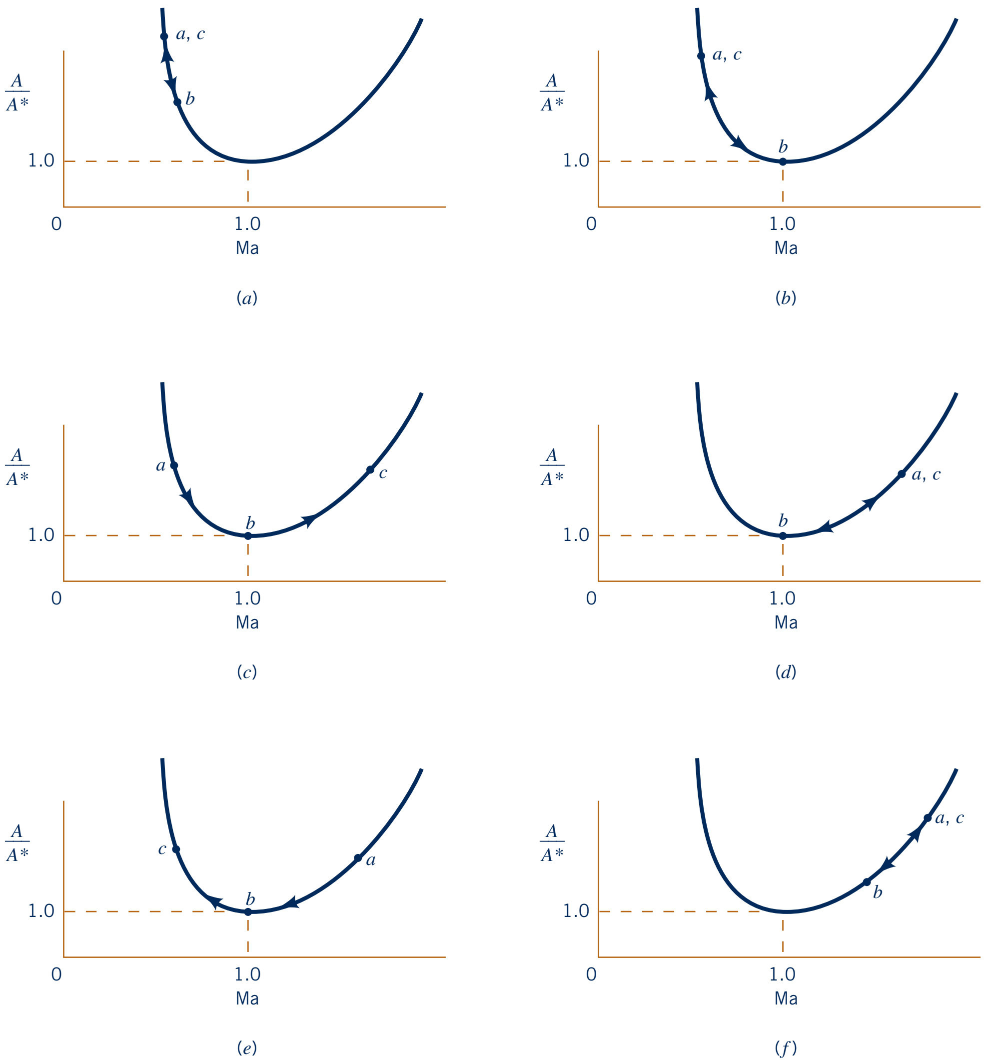

■ **Figure 11.11** **(*a*) Subsonic to subsonic isentropic flow (not choked). (*b*) Subsonic to subsonic isentropic flow (choked). (*c*) Subsonic to supersonic isentropic flow (choked). (*d*) Supersonic to supersonic isentropic flow (choked). (*e*) Supersonic to subsonic isentropic flow (choked). (*f*) Supersonic to supersonic isentropic flow (not choked).**

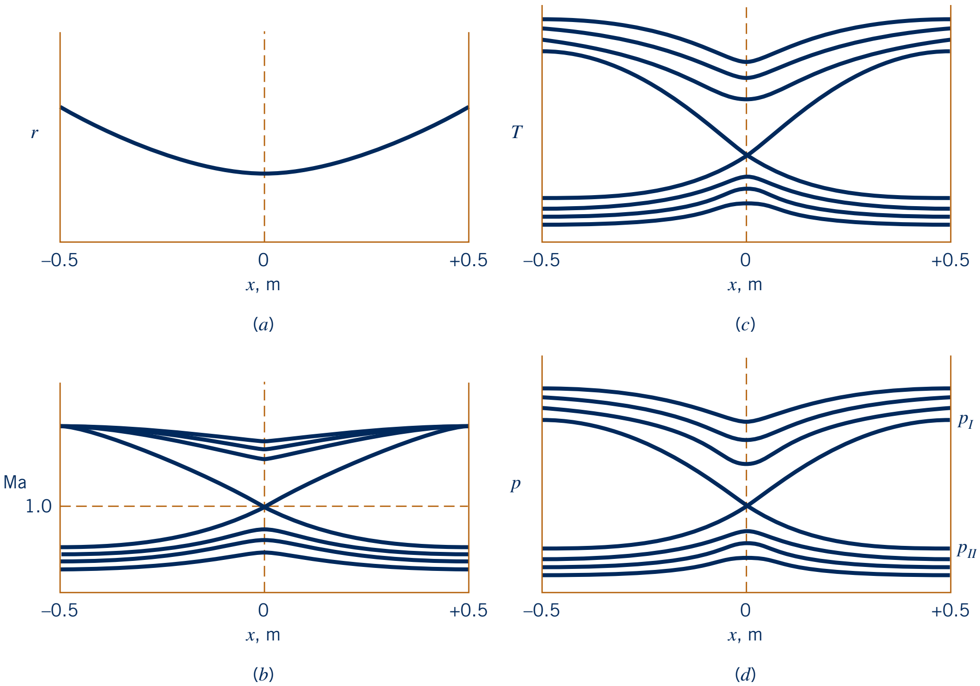

■ **Figure 11.12** **(*a*) The variation of duct radius with axial distance. (*b*) The variation of Mach number with axial distance. (*c*) The variation of temperature with axial distance. (*d*) The variation of pressure with axial distance.**

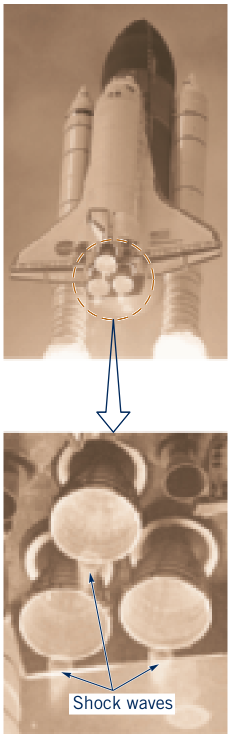

Photographs courtesy of NASA.

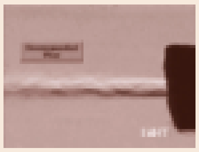

V11.7 Supersonic nozzle flow

flow solutions are represented in Fig. 11.12. When the pressure at $x = +0.5$ (exit) is greater than or equal to p_{I} indicated in Fig. 11.12*d*, an isentropic flow is possible. When the pressure at $x = +0.5$ is equal to or less than p_{II}, isentropic flows in the duct are possible. However, when the exit pressure is less than p_{I} and greater than p_{III} as indicated in Fig. 11.13, isentropic flows are no longer possible in the duct. Determination of the value of p_{III} is discussed in Example 11.19.

Some possible nonisentropic choked flows through our converging–diverging duct are represented in Fig. 11.13. Each abrupt pressure rise shown within and at the exit of the flow passage occurs across a very thin discontinuity in the flow called a ***normal shock wave***. Except for flow across the normal shock wave, the flow is isentropic. The nonisentropic flow equations that describe the changes in fluid properties that take place across a normal shock wave are developed in Section 11.5.3. The less abrupt pressure rise or drop that occurs after the flow leaves the duct is nonisentropic and attributable to three-dimensional ***oblique shock waves*** or **expansion waves** (see margin photograph). If the pressure rises downstream of the duct exit, the flow is considered ***overexpanded***. If the pressure drops downstream of the duct exit, the flow is called ***underexpanded***. Further details about over- and underexpanded flows and oblique shock waves are beyond the scope of this text. Interested readers are referred to

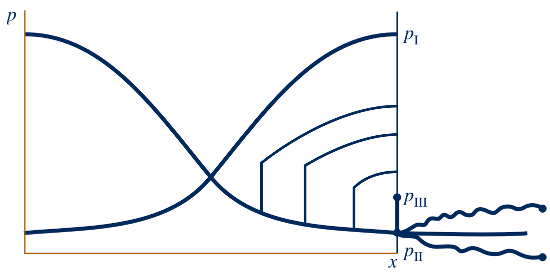

■ **Figure 11.13** **Shock formation in converging–diverging duct flows.**

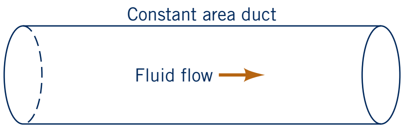

■ **Figure 11.14** **Constant area duct flow.**

texts on compressible flows and gas dynamics (for example, Refs. 4, 5, and 6) for additional material on this subject.

Fluids in the News

Rocket nozzles To develop the massive thrust needed for Space Shuttle liftoff, the gas leaving the rocket *nozzles* must be moving *supersonically*. For this to happen, the nozzle flow path must first *converge*, then *diverge*. Entering the nozzle at very high pressure and temperature, the gas accelerates in the converging portion of the nozzle until the flow *chokes* at the nozzle *throat*. Downstream of the throat, the gas further accelerates in the diverging portion of the nozzle (area ratio of 77.5 to 1), finally exiting into the atmosphere supersonically. At launch, the static pressure of the gas flowing from the nozzle exit is less than atmospheric and so the flow is *overexpanded*. At higher elevations where the atmospheric pressure is much less than at launch level, the static pressure of the gas flowing from the nozzle exit is greater than atmospheric and so now the flow is *underexpanded*. The result is expansion or divergence of the exhaust gas as it exits into the atmosphere. (See Problem 11.46.)

11.4.3 Constant Area Duct Flow

For steady, one-dimensional, isentropic flow of an ideal gas through a constant area duct (see Fig. 11.14), Eq. 11.50 suggests that $dV = 0$ or that flow velocity remains constant. With the energy equation (Eq. 5.69) we can conclude that since flow velocity is constant, the fluid enthalpy and thus temperature are also constant for this flow. This information and Eqs. 11.36 and 11.46 indicate that the Mach number is constant for this flow also. This being the case, Eqs. 11.59 and 11.60 tell us that fluid pressure and density also remain unchanged. Thus, we see that a steady, one-dimensional, isentropic flow of an ideal gas does not involve varying velocity or fluid properties unless the flow cross-sectional area changes.

In Section 11.5 we discuss nonisentropic, steady, one-dimensional flows of an ideal gas through a constant area duct and also a normal shock wave. We learn that friction and/or heat transfer can also accelerate or decelerate a fluid.

11.5 Nonisentropic Flow of an Ideal Gas

Fanno flow involves wall friction with no heat transfer and constant cross-sectional area.

Actual fluid flows are generally nonisentropic. An important example of ***nonisentropic flow*** involves adiabatic (no heat transfer) flow with friction. Flows with heat transfer (diabatic flows) are generally nonisentropic also. In this section we consider the adiabatic flow of an ideal gas through a constant area duct with friction. This kind of flow is often referred to as ***Fanno flow***. We also analyze the diabatic flow of an ideal gas through a constant area duct without friction (***Rayleigh flow***). The concepts associated with Fanno and Rayleigh flows lead to further discussion of normal shock waves.

11.5.1 Adiabatic Constant Area Duct Flow with Friction (Fanno Flow)

Consider the steady, one-dimensional, and adiabatic flow of an ideal gas through the constant area duct shown in Fig. 11.15. This is Fanno flow. For the control volume indicated, the energy equation (Eq. 5.69) leads to

$$\dot{m}\left[\check{h}_2 - \check{h}_1 + \frac{V_2^2 - V_1^2}{2} + \cancelto{0\,(\text{negligibly small for gas flow})}{g(z_2 - z_1)}\right] = \cancelto{0\,(\text{flow is adiabatic})}{\dot{Q}_{\substack{\text{net}\\\text{in.}}}} + \cancelto{0\,(\text{flow is steady throughout})}{\dot{W}_{\substack{\text{shaft}\\\text{net in}}}}$$

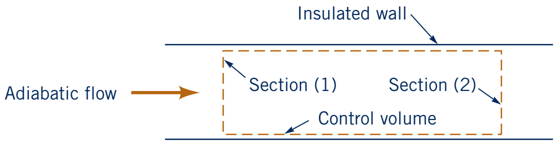

■ **Figure 11.15** **Adiabatic constant area flow.**

or

$$\check{h} + \frac{V^2}{2} = \check{h}_0 = \text{constant} \tag{11.72}$$

where h_0 is the stagnation enthalpy. For an ideal gas we gather from Eq. 11.9 that

$$\check{h} - \check{h}_0 = c_p(T - T_0) \tag{11.73}$$

so that by combining Eqs. 11.72 and 11.73 we get

$$T + \frac{V^2}{2c_p} = T_0 = \text{constant}$$

or

$$T + \frac{(\rho V)^2}{2c_p\rho^2} = T_0 = \text{constant} \tag{11.74}$$

By substituting the ideal gas equation of state (Eq. 11.1) into Eq. 11.74, we obtain

$$T + \frac{(\rho V)^2 T^2}{2c_p(p^2/R^2)} = T_0 = \text{constant} \tag{11.75}$$

From the continuity equation (Eq. 11.40) we can conclude that the density–velocity product, ρV, is constant for a given Fanno flow since the area, A, is constant. Also, for a particular Fanno flow, the stagnation temperature, T_0, is fixed. Thus, Eq. 11.75 allows us to calculate values of fluid temperature corresponding to values of fluid pressure in the Fanno flow. We postpone our discussion of how pressure is determined until later.

As with earlier discussions in this chapter, it is helpful to describe Fanno flow with a temperature–entropy diagram. From the second $T\,ds$ relationship, an expression for entropy variation was already derived (Eq. 11.22). If the temperature, T_1, pressure, p_1, and entropy, s_1, at the entrance of the Fanno flow duct are considered as reference values, then Eq. 11.22 yields

$$s - s_1 = c_p \ln \frac{T}{T_1} - R \ln \frac{p}{p_1} \tag{11.76}$$

Entropy increases in Fanno flows because of wall friction.

Equations 11.75 and 11.76 taken together result in a curve with T–s coordinates as is illustrated in Fig. 11.16. This curve involves a given gas (c_p and R) with fixed values of stagnation temperature, density–velocity product, and inlet temperature, pressure, and entropy. Curves like the one sketched in Fig. 11.16 are called Fanno lines.

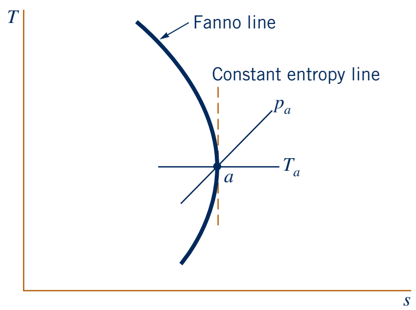

■ **Figure 11.16** **The T–s diagram for Fanno flow.**

EXAMPLE 11.11 Compressible Flow with Friction (Fanno Flow)

GIVEN Air ($k = 1.4$) enters [section (1)] an insulated, constant cross-sectional area duct with the following properties:

$$T_0 = 288 \text{ K}$$
$$T_1 = 286 \text{ K}$$
$$p_1 = 99 \text{ kPa}$$

FIND For Fanno flow, determine corresponding values of fluid temperature and entropy change for various values of downstream pressures and plot the related Fanno line.

SOLUTION

To plot the Fanno line we can use Eq. 11.75

$$T + \frac{(\rho V)^2 T^2}{2c_p p^2/R^2} = T_0 = \text{constant} \quad \textbf{(1)}$$

and Eq. 11.76

$$s - s_1 = c_p \ln \frac{T}{T_1} - R \ln \frac{p}{p_1} \quad \textbf{(2)}$$

to construct a table of values of temperature and entropy change corresponding to different levels of pressure in the Fanno flow.

We need values of the ideal gas constant and the specific heat at constant pressure to use in Eqs. 1 and 2. From Table 1.4 we read for air

$$R = 286.9 \text{ J/kg} \cdot \text{K} = 1004 \text{ J/kg} \cdot \text{K}$$

From Eq. 11.14 we obtain

$$c_p = \frac{Rk}{k-1} \quad \textbf{(3)}$$

or

$$c_p = \frac{(286.9 \text{ J/kg} \cdot \text{K})(1.4)}{1.4 - 1} = 1004 \text{ J/kg} \cdot \text{K}$$

From Eqs. 11.1 and 11.69 we obtain

$$\rho V = \frac{p}{RT} \text{Ma}\sqrt{RTk}$$

and ρV is constant for this flow

$$\rho V = \rho_1 V_1 = \frac{p_1}{RT_1} \text{Ma}_1 \sqrt{RT_1 k} \quad \textbf{(4)}$$

But

$$\frac{T_1}{T_0} = \frac{286 \text{ K}}{288 \text{ K}} = 0.993$$

and from Eq. 11.56, $\text{Ma}_1 = \{(T_0/T_1 - 1)/[(k-1)/2]\}^{1/2}$, or

$$\text{Ma}_1 = \sqrt{\left(\frac{1}{0.993} - 1\right)/0.2} = 0.2$$

Thus, with

$$\sqrt{RT_1 k} = \sqrt{(1.4)(286.9 \text{ J/kg} \cdot \text{K})(286 \text{ K})} = 339 \text{ m/s}$$

Eq. 4 becomes

$$\rho V = \frac{(99 \times 10^3 \text{ Pa})0.2(339 \text{ m/s})}{(286.9 \text{ J/kg} \cdot \text{K})(286 \text{ K})}$$

or

$$\rho V = 81.8 \text{ kg/m}^2\text{s}$$

For $p = 48$ kPa we have from Eq. 1

$$T + \frac{(81.8 \text{ kg/m}^2\text{s})^2 T^2}{2(1004 \text{ J/kg} \cdot \text{K}) \dfrac{(48 \times 10^3 \text{ Pa})^2}{(286.9 \text{ J/kg} \cdot \text{K})}} = 288 \text{ K}$$

or

$$0.12 \times 10^{-3} \,[(\text{kg} \cdot \text{m/s}^2)/\text{N} \cdot \text{K}]\, T^2 + T - 288 \text{ K} = 0$$

Thus,

$$0.12 \times 10^{-3} T^2 + T - 288 = 0$$

Hence,

$$T = 278.7 \text{ K} \quad \textbf{(Ans)}$$

where T is in K.

From Eq. 2, we obtain

$$s - s_1 = (1004 \text{ J/kg} \cdot \text{K}) \ln \left(\frac{278.7 \text{ K}}{286 \text{ K}}\right) - (286.9 \text{ J/kg} \cdot \text{K}) \ln \left(\frac{48 \times 10^3 \text{ Pa}}{99 \times 10^3 \text{ Pa}}\right)$$

or

$$s - s_1 = 181.7 \text{ J/kg} \cdot \text{K} \quad \textbf{(Ans)}$$

Proceeding as outlined above, we construct the table of values shown below and graphed as the Fanno line in Fig. E11.11.

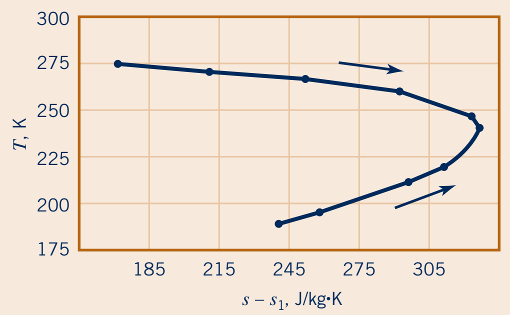

Figure E11.11

The maximum entropy difference occurs at a pressure of 18 kPa and a temperature of 239.4 K.

p (kPa)	T (K)	$s - s_1$ [J/kg . K]
48	278.7	181.7
41	275.6	215.7
34	270.6	251.0
28	264.0	282.0
21	249.3	307.0
18	239.4	310.5
14	220.0	297.8
12	206.8	279.9
10	190.0	247.0
9.6	185.6	235.3

COMMENT Note that for Fanno flow the entropy must increase in the direction of flow. Hence, as discussed in the material that follows this example, this flow can proceed either from subsonic conditions upstream to a sonic condition (Ma = 1) downstream or from supersonic conditions upstream to a sonic condition downstream. The arrows in Fig. 11.11 indicate in which direction a Fanno flow can proceed.

We can learn more about Fanno lines by further analyzing the equations that describe the physics involved. For example, the second $T\,ds$ equation (Eq. 11.18) is

$$T\,ds = d\check{h} - \frac{dp}{\rho} \tag{11.18}$$

For an ideal gas

$$d\check{h} = c_p\,dT \tag{11.7}$$

and

$$\rho = \frac{p}{RT} \tag{11.1}$$

or

$$\frac{dp}{p} = \frac{d\rho}{\rho} + \frac{dT}{T} \tag{11.77}$$

Fanno flow properties can be obtained from the second T ds *equation combined with the continuity and energy equations.*

Thus, consolidating Eqs. 11.1, 11.7, 11.18, and 11.77 we obtain

$$T\,ds = c_p\,dT - RT\left(\frac{d\rho}{\rho} + \frac{dT}{T}\right) \tag{11.78}$$

Also, from the continuity equation (Eq. 11.40), we get for Fanno flow $\rho V =$ constant, or

$$\frac{d\rho}{\rho} = -\frac{dV}{V} \tag{11.79}$$

Substituting Eq. 11.79 into Eq. 11.78 yields

$$T\,ds = c_p\,dT - RT\left(-\frac{dV}{V} + \frac{dT}{T}\right)$$

or

$$\frac{ds}{dT} = \frac{c_p}{T} - R\left(-\frac{1}{V}\frac{dV}{dT} + \frac{1}{T}\right) \tag{11.80}$$

By differentiating the energy equation (11.74) obtained earlier, we obtain

$$\frac{dV}{dT} = -\frac{c_p}{V} \tag{11.81}$$

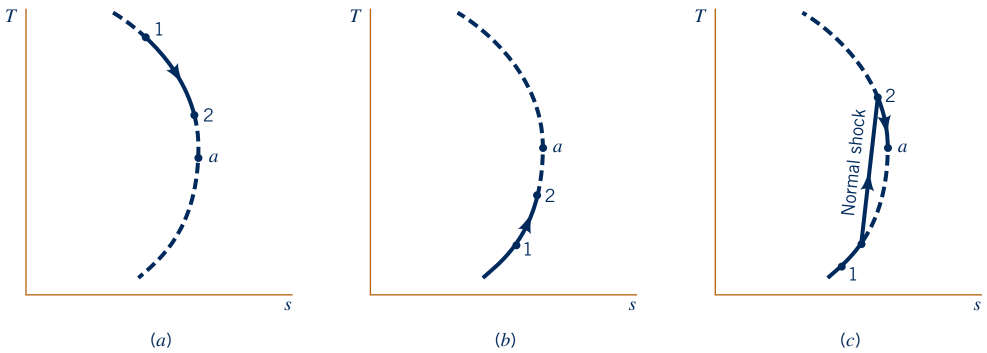

■ **Figure 11.17** ***(a)* Subsonic Fanno flow. *(b)* Supersonic Fanno flow. *(c)* Normal shock occurrence in Fanno flow.**

which, when substituted into Eq. 11.80, results in

$$\frac{ds}{dT} = \frac{c_p}{T} - R\left(\frac{c_p}{V^2} + \frac{1}{T}\right) \qquad \textbf{(11.82)}$$

The Fanno line in Fig. 11.16 goes through a state (labeled state a) for which $ds/dT = 0$. At this state, we can conclude from Eqs. 11.14 and 11.82 that

$$V_a = \sqrt{RT_a k} \qquad \textbf{(11.83)}$$

However, by comparing Eqs. 11.83 and 11.36 we see that the Mach number at state a is 1. Since the stagnation temperature is the same for all points on the Fanno line [see energy equation (Eq. 11.74)], the temperature at point a is the critical temperature, T^*, for the entire Fanno line. Thus, Fanno flow corresponding to the portion of the Fanno line above the critical temperature must be subsonic, and Fanno flow on the line below T^* must be supersonic.

The second law of thermodynamics states that, based on all past experience, entropy can only remain constant or increase for adiabatic flows. For Fanno flow to be consistent with the second law of thermodynamics, flow can only proceed along the Fanno line toward state a, the critical state. The critical state may or may not be reached by the flow. If it is, the Fanno flow is *choked*. Some examples of Fanno flow behavior are summarized in Fig. 11.17. A case involving subsonic Fanno flow that is accelerated by friction to a higher Mach number without choking is illustrated in Fig. 11.17*a*. A supersonic flow that is decelerated by friction to a lower Mach number without choking is illustrated in Fig. 11.17*b*. In Fig. 11.17*c*, an abrupt change from supersonic to subsonic flow in the Fanno duct is represented. This sudden deceleration occurs across a standing *normal shock wave* that is described in more detail in Section 11.5.3.

Friction accelerates a subsonic Fanno flow.

The qualitative aspects of Fanno flow that we have already discussed are summarized in Table 11.1 and Fig. 11.18. To quantify Fanno flow behavior we need to combine a relationship that represents the linear momentum law with the set of equations already derived in this chapter.

■ **Table 11.1**
Summary of Fanno Flow Behavior

	Flow	
Parameter	**Subsonic Flow**	**Supersonic Flow**
Stagnation temperature	Constant	Constant
Ma	Increases (maximum is 1)	Decreases (minimum is 1)
Friction	Accelerates flow	Decelerates flow
Pressure	Decreases	Increases
Temperature	Decreases	Increases

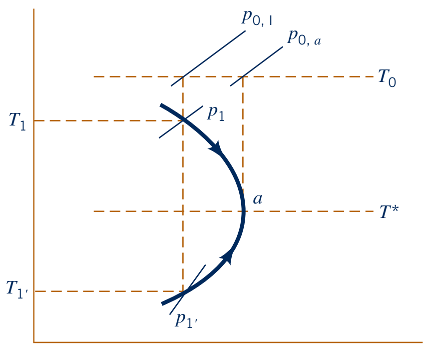

■ **Figure 11.18** **Fanno flow.**

If the linear momentum equation (Eq. 5.22) is applied to the Fanno flow through the control volume sketched in Fig. 11.19*a*, the result is

$$p_1A_1 - p_2A_2 - R_x = \dot{m}(V_2 - V_1)$$

where R_x is the frictional force exerted by the inner pipe wall on the fluid. Since $A_1 = A_2 = A$ and $\dot{m} = \rho AV =$ constant (i.e. $\rho V = \rho_1 V_1 = \rho_2 V_2$), we obtain

$$p_1 - p_2 - \frac{R_x}{A} = \rho V(V_2 - V_1) \tag{11.84}$$

The differential form of Eq. 11.84, which is valid for Fanno flow through the semi-infinitesimal control volume shown in Fig. 11.19*b*, is

$$-dp - \frac{\tau_w \pi D\, dx}{A} = \rho V\, dV \tag{11.85}$$

The wall shear stress, τ_w, is related to the wall friction factor, f, by Eq. 8.20 as

Friction forces in Fanno flow are given in terms of the friction factor.

$$f = \frac{8\tau_w}{\rho V^2} \tag{11.86}$$

By substituting Eq. 11.86 and $A = \pi D^2/4$ into Eq. 11.85, we obtain

$$-dp - f\rho \frac{V^2}{2}\frac{dx}{D} = \rho V\, dV \tag{11.87}$$

or

$$\frac{dp}{p} + \frac{f}{p}\frac{\rho V^2}{2}\frac{dx}{D} + \frac{\rho}{p}\frac{d(V^2)}{2} = 0 \tag{11.88}$$

Combining the ideal gas equation of state (Eq. 11.1), the ideal gas speed-of-sound equation (Eq. 11.36), and the Mach number definition (Eq. 11.46) with Eq. 11.88 leads to

$$\frac{dp}{p} + \frac{fk}{2}\mathrm{Ma}^2\frac{dx}{D} + k\frac{\mathrm{Ma}^2}{2}\frac{d(V^2)}{V^2} = 0 \tag{11.89}$$

Since $V = \mathrm{Ma}\, c = \mathrm{Ma}\sqrt{RTk}$, then

$$V^2 = \mathrm{Ma}^2 RTk$$

or

$$\frac{d(V^2)}{V^2} = \frac{d(\mathrm{Ma}^2)}{\mathrm{Ma}^2} + \frac{dT}{T} \tag{11.90}$$

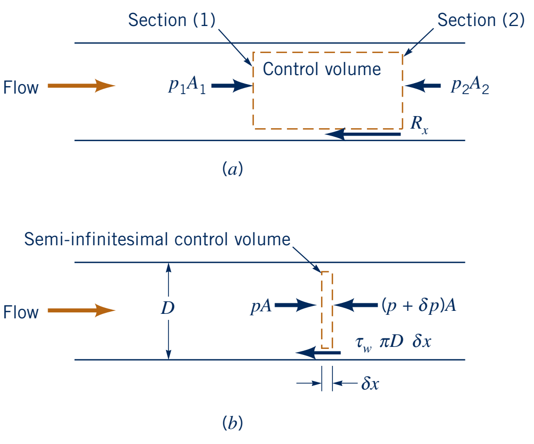

■ **Figure 11.19** ***(a)* Finite control volume. *(b)* Semi-infinitesimal control volume.**

The application of the energy equation (Eq. 5.69) to Fanno flow gave Eq. 11.74. If Eq. 11.74 is differentiated and divided by temperature, the result is

$$\frac{dT}{T} + \frac{d(V^2)}{2c_pT} = 0 \tag{11.91}$$

Substituting Eqs. 11.14, 11.36, and 11.46 into Eq. 11.91 yields

$$\frac{dT}{T} + \frac{k-1}{2}\mathrm{Ma}^2\frac{d(V^2)}{V^2} = 0 \tag{11.92}$$

which can be combined with Eq. 11.90 to form

$$\frac{d(V^2)}{V^2} = \frac{d(\mathrm{Ma}^2)/\mathrm{Ma}^2}{1 + [(k-1)/2]\mathrm{Ma}^2} \tag{11.93}$$

We can merge Eqs. 11.77, 11.79, and 11.90 to get

$$\frac{dp}{p} = \frac{1}{2}\frac{d(V^2)}{V^2} - \frac{d(\mathrm{Ma}^2)}{\mathrm{Ma}^2} \tag{11.94}$$

Consolidating Eqs. 11.94 and 11.89 leads to

$$\frac{1}{2}(1 + k\mathrm{Ma}^2)\frac{d(V^2)}{V^2} - \frac{d(\mathrm{Ma}^2)}{\mathrm{Ma}^2} + \frac{fk}{2}\mathrm{Ma}^2\frac{dx}{D} = 0 \tag{11.95}$$

Finally, incorporating Eq. 11.93 into Eq. 11.95 yields

$$\frac{(1-\mathrm{Ma}^2)\,d(\mathrm{Ma}^2)}{\{1 + [(k-1)/2]\mathrm{Ma}^2\}k\mathrm{Ma}^4} = f\frac{dx}{D} \tag{11.96}$$

Equation 11.96 can be integrated from one section to another in a Fanno flow duct. We elect to use the critical (*) state as a reference and to integrate Eq. 11.96 from an upstream state to the critical state. Thus

$$\int_{\mathrm{Ma}}^{\mathrm{Ma}^*=1} \frac{(1-\mathrm{Ma}^2)\,d(\mathrm{Ma}^2)}{\{1 + [(k-1)/2]\,\mathrm{Ma}^2\}k\mathrm{Ma}^4} = \int_{\ell}^{\ell^*} f\frac{dx}{D} \tag{11.97}$$

For Fanno flow, the Mach number is a function of the distance to the critical state.

where ℓ is length measured from an arbitrary but fixed upstream reference location to a section in the Fanno flow. For an approximate solution, we can assume that the friction factor is constant at an average value over the integration length, $\ell^* - \ell$. We also consider a constant value of k. Thus, we obtain from Eq. 11.97

$$\boxed{\frac{1}{k}\frac{(1-\mathrm{Ma}^2)}{\mathrm{Ma}^2} + \frac{k+1}{2k}\ln\left\{\frac{[(k+1)/2]\mathrm{Ma}^2}{1 + [(k-1)/2]\mathrm{Ma}^2}\right\} = \frac{f(\ell^* - \ell)}{D}} \tag{11.98}$$

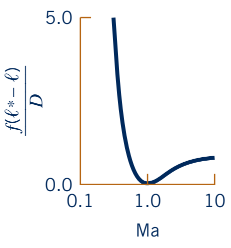

For a given gas, values of $f(\ell^* - \ell)/D$ can be tabulated as a function of Mach number for Fanno flow. For example, values of $f(\ell^* - \ell)/D$ for air ($k = 1.4$) Fanno flow are graphed as a function of Mach number in Fig. D.2 in Appendix D and in the figure in the margin. Note that the critical state does not have to exist in the actual Fanno flow being considered, since for any two sections in a given Fanno flow

$$\boxed{\frac{f(\ell^* - \ell_2)}{D} - \frac{f(\ell^* - \ell_1)}{D} = \frac{f}{D}(\ell_1 - \ell_2)} \tag{11.99}$$

The sketch in Fig. 11.20 illustrates the physical meaning of Eq. 11.99.

For a given Fanno flow (constant specific heat ratio, duct diameter, and friction factor) the length of duct required to change the Mach number from Ma_1 to Ma_2 can be determined from Eqs. 11.98 and 11.99 or a graph such as Fig. D.2. To get the values of other fluid properties in the Fanno flow field we need to develop more equations.

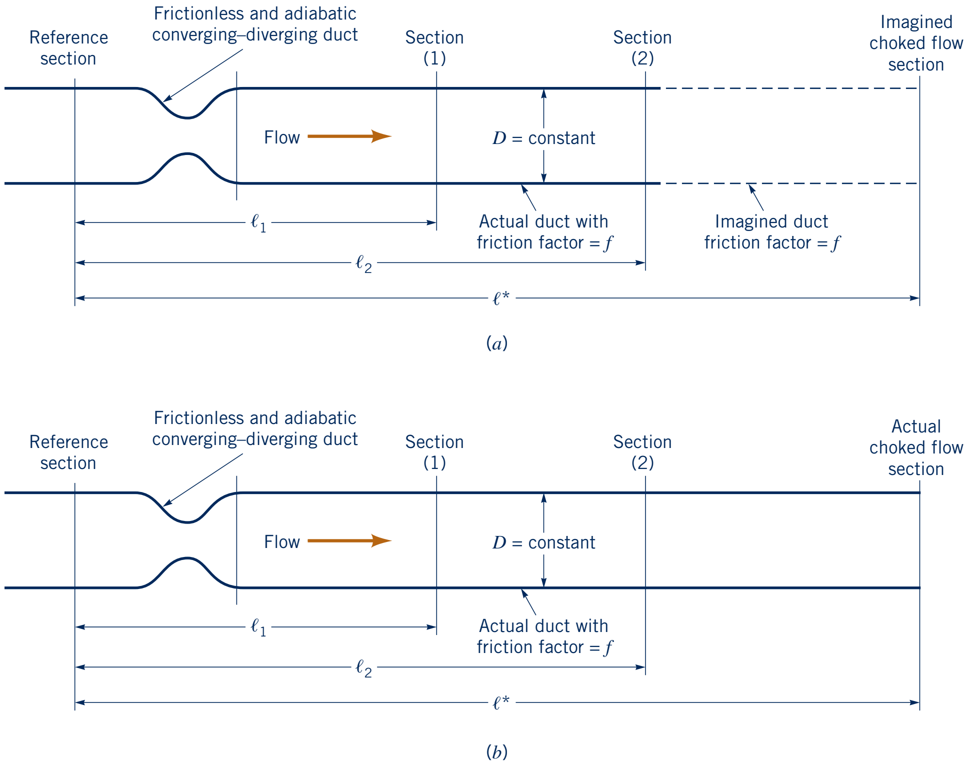

■ **Figure 11.20** ***(a)*** **Unchoked Fanno flow.** ***(b)*** **Choked Fanno flow.**

For Fanno flow, the length of duct needed to produce a given change in Mach number can be determined.

By consolidating Eqs. 11.90 and 11.92 we obtain

$$\frac{dT}{T} = -\frac{(k-1)}{2\{1 + [(k-1)/2]\text{Ma}^2\}}\, d(\text{Ma}^2) \tag{11.100}$$

Integrating Eq. 11.100 from any state upstream in a Fanno flow to the critical (*) state leads to

$$\boxed{\frac{T}{T^*} = \frac{(k+1)/2}{1 + [(k-1)/2]\text{Ma}^2}} \tag{11.101}$$

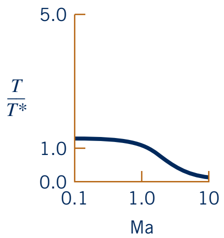

Equations 11.68 and 11.69 allow us to write

$$\frac{V}{V^*} = \frac{\text{Ma}\,\sqrt{RTk}}{\sqrt{RT^*k}} = \text{Ma}\sqrt{\frac{T}{T^*}} \tag{11.102}$$

Substituting Eq. 11.101 into Eq. 11.102 yields

$$\boxed{\frac{V}{V^*} = \left\{\frac{[(k+1)/2]\text{Ma}^2}{1 + [(k-1)/2]\text{Ma}^2}\right\}^{1/2}} \tag{11.103}$$

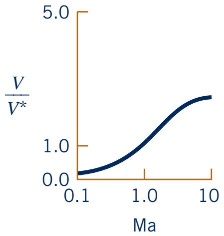

Equations 11.101 and 11.103 are graphed in the margin for air.

From the continuity equation (Eq. 11.40) we get for Fanno flow

$$\frac{\rho}{\rho^*} = \frac{V^*}{V} \tag{11.104}$$

Combining 11.104 and 11.103 results in

$$\frac{\rho}{\rho^*} = \left\{\frac{1 + [(k-1)/2]\text{Ma}^2}{[(k+1)/2]\text{Ma}^2}\right\}^{1/2} \tag{11.105}$$

The ideal gas equation of state (Eq. 11.1) leads to

$$\frac{p}{p^*} = \frac{\rho}{\rho^*}\frac{T}{T^*} \tag{11.106}$$

and merging Eqs. 11.106, 11.105, and 11.101 gives

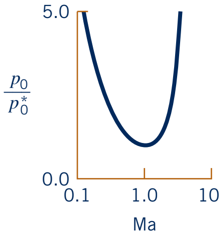

$$\boxed{\frac{p}{p^*} = \frac{1}{\text{Ma}}\left\{\frac{(k+1)/2}{1+[(k-1)/2]\text{Ma}^2}\right\}^{1/2}} \tag{11.107}$$

This relationship is graphed in the margin for air.

Finally, the stagnation pressure ratio can be written as

$$\frac{p_0}{p_0^*} = \left(\frac{p_0}{p}\right)\left(\frac{p}{p^*}\right)\left(\frac{p^*}{p_0^*}\right) \tag{11.108}$$

For Fanno flow, thermodynamic and flow properties can be calculated as a function of Mach number.

which by use of Eqs. 11.59 and 11.107 yields

$$\boxed{\frac{p_0}{p_0^*} = \frac{1}{\text{Ma}}\left[\left(\frac{2}{k+1}\right)\left(1+\frac{k-1}{2}\text{Ma}^2\right)\right]^{[(k+1)/2(k-1)]}} \tag{11.109}$$

Values of $f(\ell^* - \ell)/D$, T/T^*, V/V^*, p/p^*, and p_0/p_0^* for Fanno flow of air $(k = 1.4)$ are graphed as a function of Mach number (using Eqs. 11.99, 11.101, 11.103, 11.107, and 11.109) in Fig. D.2 of Appendix D. The usefulness of Fig. D.2 is illustrated in Examples 11.12, 11.13, and 11.14.

See Ref. 7 for additional compressible internal flow material.

EXAMPLE 11.12 Choked Fanno Flow

GIVEN Standard atmospheric air $[T_0 = 288\text{ K}, p_0 = 101\text{ kPa(abs)}]$ is drawn steadily through a frictionless, adiabatic converging nozzle into an adiabatic, constant area duct as shown in Fig. E11.12*a*. The duct is 2 m long and has an inside diameter of 0.1 m. The average friction factor for the duct is estimated as being equal to 0.02.

FIND What is the maximum mass flowrate through the duct? For this maximum flowrate, determine the values of static temperature, static pressure, stagnation temperature, stagnation pressure, and velocity at the inlet [section (1)] and exit [section (2)] of the constant area duct. Sketch a temperature–entropy diagram for this flow.

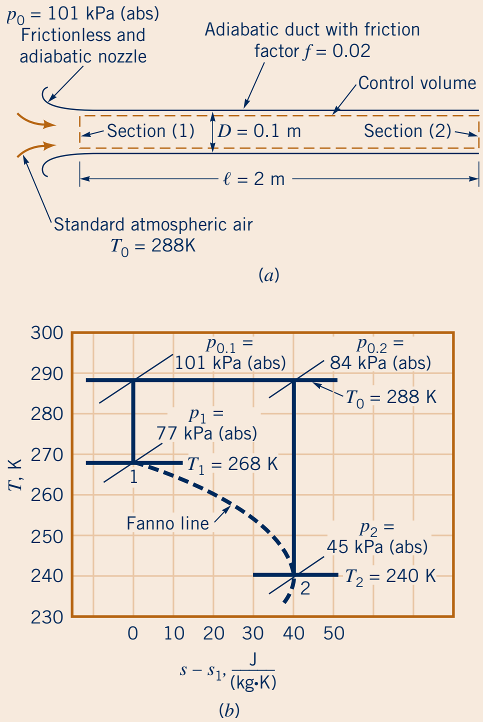

■ **Figure E11.12**

SOLUTION

We consider the flow through the converging nozzle to be isentropic and the flow through the constant area duct to be Fanno flow. A decrease in the pressure at the exit of the constant area duct (back pressure) causes the mass flowrate through the nozzle and the duct to increase. The flow throughout is subsonic. The maximum flowrate will occur when the back pressure is lowered to the extent that the constant area duct chokes and the Mach number at the duct exit is equal to 1. Any further decrease of back pressure will not affect the flowrate through the nozzle–duct combination.

For the maximum flowrate condition, the constant area duct must be choked, and

$$\frac{f(\ell^* - \ell_1)}{D} = \frac{f(\ell_2 - \ell_1)}{D} = \frac{(0.02)(2 \text{ m})}{(0.1 \text{ m})} = 0.4 \qquad \textbf{(1)}$$

With $k = 1.4$ for air and the above calculated value of $f(\ell^* - \ell_1)/D = 0.4$, we could use Eq. 11.98 to determine a value of Mach number at the entrance of the duct [section (1)]. With $k = 1.4$ and Ma_1 known, we could then rely on Eqs. 11.101, 11.103, 11.107, and 11.109 to obtain values of T_1/T^*, V_1/V^*, p_1/p^*, and $p_{0,1}/p_0^*$. Alternatively, for air ($k = 1.4$), we can use Fig. D.2 with $f(\ell^* - \ell_1)/D = 0.4$ and read off values of Ma_1, T_1/T^*, V_1/V^*, p_1/p^*, and $p_{0,1}/p_0^*$.

The pipe entrance Mach number, Ma_1, also represents the Mach number at the throat (and exit) of the isentropic, converging nozzle. Thus, the isentropic flow equations of Section 11.4 or Fig. D.1 can be used with Ma_1. We use Fig. D.1 in this example.

With Ma_1 known, we can enter Fig. D.1 and get values of T_1/T_0, p_1/p_0, and ρ_1/ρ_0. Through the isentropic nozzle, the values of T_0, p_0, and ρ_0 are each constant, and thus T_1, p_1, and ρ_1 can be readily obtained.

Since T_0 also remains constant through the constant area duct (see Eq. 11.75), we can use Eq. 11.63 to get T^*. Thus,

$$\frac{T^*}{T_0} = \frac{2}{k + 1} = \frac{2}{1.4 + 1} = 0.8333 \qquad \textbf{(2)}$$

Since $T_0 = 288$ K, we get from Eq. 2,

$$T^* = (0.8333)(288 \text{ K}) = 240 \text{ K} = T_2 \qquad \textbf{(3)} \quad \textbf{(Ans)}$$

With T^* known, we can calculate V^* from Eq. 11.36 as

$$\begin{aligned} V^* &= \sqrt{RT^*k} \\ &= \sqrt{[(286.9 \text{ J})/(\text{kg} \cdot \text{K})](240 \text{ K})(1.4)} \\ &= 310 \text{ (J/kg)}^{1/2} \end{aligned}$$

Thus, since $1 \text{ J/kg} = 1 \text{ N} \cdot \text{m/kg} = 1 \text{ (kg} \cdot \text{m/s}^2) \cdot \text{m/kg} = (\text{m/s})^2$, we obtain

$$V^* = 310 \text{ m/s} = V_2 \qquad \textbf{(4)} \quad \textbf{(Ans)}$$

Now V_1 can be obtained from V^* and V_1/V^*. Having A_1, ρ_1, and V_1 we can get the mass flowrate from

$$\dot{m} = \rho_1 A_1 V_1 \qquad \textbf{(5)}$$

Values of the other variables asked for can be obtained from the ratios mentioned.

Entering Fig. D.2 with $f(\ell^* - \ell)/D = 0.4$ we read

$$\text{Ma}_1 = 0.63 \qquad \textbf{(6)}$$

$$\frac{T_1}{T^*} = 1.1 \qquad \textbf{(7)}$$

$$\frac{V_1}{V^*} = 0.66 \qquad \textbf{(8)}$$

$$\frac{p_1}{p^*} = 1.7 \qquad \textbf{(9)}$$

$$\frac{p_{0,1}}{p_0^*} = 1.16 \qquad \textbf{(10)}$$

Entering Fig. D.1 with $\text{Ma}_1 = 0.63$ we read

$$\frac{T_1}{T_0} = 0.93 \qquad \textbf{(11)}$$

$$\frac{p_1}{p_{0,1}} = 0.76 \qquad \textbf{(12)}$$

$$\frac{\rho_1}{\rho_{0,1}} = 0.83 \qquad \textbf{(13)}$$

Thus, from Eqs. 4 and 8 we obtain

$$V_1 = (0.66)(310 \text{ m/s}) = 205 \text{ m/s} \qquad \textbf{(Ans)}$$

From Eq. 13 we get

$$\rho_1 = 0.83\rho_{0,1} = (0.83)(1.23 \text{ kg/m}^3) = 1.02 \text{ kg/m}^3$$

and from Eq. 5 we conclude that

$$\begin{aligned} \dot{m} &= (1.02 \text{ kg/m}^3)\left[\frac{\pi(0.1 \text{ m})^2}{4}\right](206 \text{ m/s}) \\ &= 1.65 \text{ kg/s} \qquad \textbf{(Ans)} \end{aligned}$$

From Eq. 11, it follows that

$$T_1 = (0.93)(288 \text{ K}) = 268 \text{ K} \qquad \textbf{(Ans)}$$

Equation 12 yields

$$p_1 = (0.76)[101 \text{ kPa(abs)}] = 77 \text{ kPa(abs)} \qquad \textbf{(Ans)}$$

The stagnation temperature, T_0, remains constant through this adiabatic flow at a value of

$$T_{0,1} = T_{0,2} = 288 \text{ K} \qquad \textbf{(Ans)}$$

The stagnation pressure, p_0, at the entrance of the constant area duct is the same as the constant value of stagnation pressure through the isentropic nozzle. Thus

$$p_{0,1} = 101 \text{ kPa(abs)} \qquad \textbf{(Ans)}$$

To obtain the duct exit pressure ($p_2 = p^*$) we can use Eqs. 9 and 12. Thus,

$$\begin{aligned} p_2 &= \left(\frac{p^*}{p_1}\right)\left(\frac{p_1}{p_{0,1}}\right)(p_{0,1}) = \left(\frac{1}{1.7}\right)(0.76)[101 \text{ kPa(abs)}] \\ &= 45 \text{ kPa(abs)} \qquad \textbf{(Ans)} \end{aligned}$$

For the duct exit stagnation pressure ($p_{0,2} = p_0^*$) we can use Eq. 10 as

$$\begin{aligned} p_{0,2} &= \left(\frac{p_0^*}{p_{0,1}}\right)(p_{0,1}) = \left(\frac{1}{1.16}\right)[101 \text{ kPa(abs)}] \\ &= 87.1 \text{ kPa(abs)} \qquad \textbf{(Ans)} \end{aligned}$$

The stagnation pressure, p_0, decreases in a Fanno flow because of friction.

COMMENT Use of graphs such as Figs. D.1 and D.2 illustrates the solution of a problem involving Fanno flow. The T–s diagram for this flow is shown in Fig. E.11.12b, where the entropy difference, $s_2 - s_1$, is obtained from Eq. 11.22.

EXAMPLE 11.13 Effect of Duct Length on Choked Fanno Flow

GIVEN The duct in Example 11.12 is shortened by 50%, but the duct discharge pressure is maintained at the choked flow value for Example 11.12, namely,

$$p_d = 45 \text{ kPa(abs)}$$

FIND Will shortening the duct cause the mass flowrate through the duct to increase or decrease? Assume that the average friction factor for the duct remains constant at a value of $f = 0.02$.

SOLUTION

We guess that the shortened duct will still choke and check our assumption by comparing p_d with p^*. If $p_d < p^*$, the flow is choked; if not, another assumption has to be made. For choked flow we can calculate the mass flowrate just as we did for Example 11.12. For unchoked flow, we will have to devise another strategy.

For choked flow

$$\frac{f(\ell^* - \ell_1)}{D} = \frac{(0.02)(1 \text{ m})}{0.1 \text{ m}} = 0.2$$

and from Fig. D.2, we read the values $\text{Ma}_1 = 0.70$ and $p_1/p^* = 1.5$. With $\text{Ma}_1 = 0.70$, we use Fig. D.1 and get

$$\frac{p_1}{p_0} = 0.72$$

Now the duct exit pressure $(p_2 = p^*)$ can be obtained from

$$p_2 = p^* = \left(\frac{p^*}{p_1}\right)\left(\frac{p_1}{p_{0,1}}\right)(p_{0,1})$$

$$= \left(\frac{1}{1.5}\right)(0.72)[101 \text{ kPa(abs)}] = 48.5 \text{ kPa(abs)}$$

and we see that $p_d < p^*$. Our assumption of choked flow is justified. The pressure at the exit plane is greater than the surrounding pressure outside the duct exit. The final drop of pressure from 48.5 kPa(abs) to 45 kPa(abs) involves complicated three-dimensional flow downstream of the exit.

To determine the mass flowrate we use

$$\dot{m} = \rho_1 A_1 V_1 \tag{1}$$

The density at section (1) is obtained from

$$\frac{\rho_1}{\rho_{0,1}} = 0.79 \tag{2}$$

which is read in Fig. D.1 for $\text{Ma}_1 = 0.7$. Thus,

$$\rho_1 = (0.79)(1.23 \text{ kg/m}^3) = 0.97 \text{ kg/m}^3 \tag{3}$$

We get V_1 from

$$\frac{V_1}{V^*} = 0.73 \tag{4}$$

from Fig. D.2 for $\text{Ma}_1 = 0.7$. The value of V^* is the same as it was in Example 11.12, namely,

$$V^* = 310 \text{ m/s} \tag{5}$$

Thus, from Eqs. 4 and 5 we obtain

$$V_1 = (0.73)(310) = 226 \text{ m/s} \tag{6}$$

and from Eqs. 1, 3, and 6 we get

$$\dot{m} = (0.97 \text{ kg/m}^3)\left[\frac{\pi(0.1\text{m})^2}{4}\right](226 \text{ m/s})$$

$$= 1.73 \text{ kg/s} \qquad \textbf{(Ans)}$$

The mass flowrate associated with a shortened tube is larger than the mass flowrate for the longer tube, $\dot{m} = 1.65$ kg/s. This trend is general for subsonic Fanno flow.

COMMENT For the same upstream stagnation state and downstream pressure, the mass flowrate for the Fanno flow will decrease with increase in length of duct for subsonic flow. Equivalently, if the length of the duct remains the same but the wall friction is increased, the mass flowrate will decrease.

EXAMPLE 11.14 Unchoked Fanno Flow

GIVEN The same flowrate obtained in Example 11.12 ($\dot{m} = 1.65$ kg/s) is desired through the shortened duct of Example 11.13 ($\ell_2 - \ell_1 = 1$ m). Assume f remains constant at a value of 0.02.

FIND Determine the Mach number at the exit of the duct, M_2, and the back pressure, p_2, required.

SOLUTION

Since the mass flowrate of Example 11.12 is desired, the Mach number and other properties at the entrance of the constant area duct remain at the values determined in Example 11.12. Thus, from Example 11.12, $\text{Ma}_1 = 0.63$ and from Fig. D.2

$$\frac{f(\ell^* - \ell_1)}{D} = 0.4$$

For this example,

$$\frac{f(\ell_2 - \ell_1)}{D} = \frac{f(\ell^* - \ell_1)}{D} - \frac{f(\ell^* - \ell_2)}{D}$$

or

$$\frac{(0.02)(1\text{ m})}{0.1\text{ m}} = 0.4 - \frac{f(\ell^* - \ell_2)}{D}$$

so that

$$\frac{f(\ell^* - \ell_2)}{D} = 0.2 \qquad \textbf{(1)}$$

By using the value from Eq. 1 and Fig. D.2, we get

$$\text{Ma}_2 = 0.70 \qquad \textbf{(Ans)}$$

and

$$\frac{p_2}{p^*} = 1.5 \qquad \textbf{(2)}$$

We obtain p_2 from

$$p_2 = \left(\frac{p_2}{p^*}\right)\left(\frac{p^*}{p_1}\right)\left(\frac{p_1}{p_{0,1}}\right)(p_{0,1})$$

where p_2/p^* is given in Eq. 2 and p^*/p_1, $p_1/p_{0,1}$, and $p_{0,1}$ are the same as they were in Example 11.12. Thus,

$$p_2 = (1.5)\left(\frac{1}{1.7}\right)(0.76)[101\text{ kPa(abs)}]$$
$$= 68.0\text{ kPa(abs)} \qquad \textbf{(Ans)}$$

COMMENT A larger back pressure [68.0 kPa(abs)] than the one associated with choked flow through a Fanno duct [45 kPa(abs)] will maintain the same flowrate through a shorter Fanno duct with the same friction coefficient. The flow through the shorter duct is not choked. It would not be possible to maintain the same flowrate through a Fanno duct longer than the choked one with the same friction coefficient, regardless of what back pressure is used.

11.5.2 Frictionless Constant Area Duct Flow with Heat Transfer (Rayleigh Flow)

Rayleigh flow involves heat transfer with no wall friction and constant cross-sectional area.

Consider the steady, one-dimensional, and frictionless flow of an ideal gas through the constant area duct with heat transfer illustrated in Fig. 11.21. This is ***Rayleigh flow***. Application of the linear momentum equation (Eq. 5.22) to the Rayleigh flow through the finite control volume sketched in Fig. 11.21 results in

$$p_1 A_1 + \dot{m} V_1 = p_2 A_2 + \dot{m} V_2 + \overset{0\text{(frictionless flow)}}{\cancel{R_x}}$$

or

$$p + \frac{(\rho V)^2}{\rho} = \text{constant} \qquad \textbf{(11.110)}$$

Use of the ideal gas equation of state (Eq. 11.1) in Eq. 11.110 leads to

$$p + \frac{(\rho V)^2 RT}{p} = \text{constant} \qquad \textbf{(11.111)}$$

Since the flow cross-sectional area remains constant for Rayleigh flow, from the continuity equation (Eq. 11.40) we conclude that

$$\rho V = \text{constant}$$

For a given Rayleigh flow, the constant in Eq. 11.111, the density–velocity product, ρV, and the ideal gas constant are all fixed. Thus, Eq. 11.111 can be used to determine values of fluid temperature corresponding to the local pressure in a Rayleigh flow.

To construct a temperature–entropy diagram for a given Rayleigh flow, we can use Eq. 11.76, which was developed earlier from the second $T\,ds$ relationship. Equations 11.111 and 11.76 can be solved simultaneously to obtain the curve sketched in Fig. 11.22. Curves like the one in Fig. 11.22 are called *Rayleigh lines*.

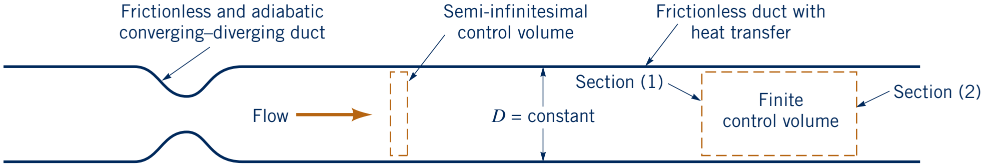

■ **Figure 11.21** **Rayleigh flow.**

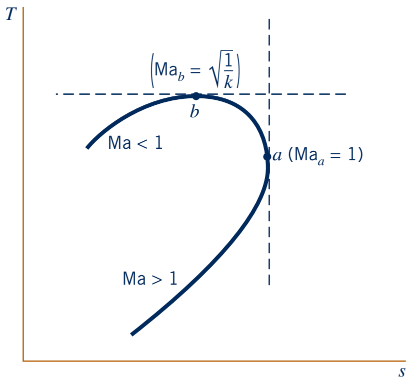

■ **Figure 11.22** Rayleigh line.

EXAMPLE 11.15 Frictionless, Constant Area Compressible Flow with Heat Transfer (Rayleigh Flow)

GIVEN Air ($k = 1.4$) enters [section (1)] a frictionless, constant flow cross-sectional area duct with the following properties (the same as in Example 11.11):

$$T_0 = 288 \text{ K}$$
$$T_1 = 286 \text{ K}$$
$$p_1 = 99 \text{ kPa}$$

FIND For Rayleigh flow, determine corresponding values of fluid temperature and entropy change for various levels of downstream pressure and plot the related Rayleigh line.

SOLUTION

To plot the Rayleigh line asked for, use Eq. 11.111

$$p + \frac{(\rho V)^2 RT}{p} = \text{constant} \tag{1}$$

and Eq. 11.76

$$s - s_1 = c_p \ln \frac{T}{T_1} - R \ln \frac{p}{p_1} \tag{2}$$

to construct a table of values of temperature and entropy change corresponding to different levels of pressure downstream in a Rayleigh flow.

Use the value of ideal gas constant for air from Table 1.4

$$R = 286.9 \text{ J/kg} \cdot \text{K}$$

and the value of specific heat at constant pressure for air from Example 11.11, namely,

$$c_p = 1004 \text{ J/kg} \cdot \text{K}$$

Also, from Example 11.11, $\rho V = 81.8 \text{ kg/m}^2 \cdot \text{s}$. For the given inlet [section (1)] conditions, we get

$$\frac{RT_1}{p_1} = \frac{(286.9 \text{ J/kg} \cdot \text{K})(286 \text{ K})}{99 \times 10^3 \text{ Pa}} = 0.8 \text{ m}^3/\text{kg}$$

Thus, from Eq. 1 we get

$$p + \frac{(\rho V)^2 RT}{p} = 99 \text{ kPa} + (286.9 \text{ J/kg} \cdot \text{K})^2 (0.8 \text{ m}^3/\text{kg})$$
$$= 99 \text{ kPa} + 5353 \text{ kg/m} \cdot \text{s}^2 = \text{constant}$$

or, since $1 \text{ kg/m} \cdot \text{s}^2 = \text{N/m}^2$

$$p + \frac{(\rho V)^2 RT}{p} = 99 \times 10^3 \text{ kPa} + (5353 \times 10^3 \text{ kPa})$$
$$= 104 \text{ kPa} = \text{constant} \tag{3}$$

With the downstream pressure of $p = 93$ kPa, we can obtain the downstream temperature by using Eq. 3 with the fact that

$$\frac{(\rho V)^2 R}{p} = \frac{(81.8 \text{ kg/m}^2 \cdot \text{s})(286.9 \text{ J/kg} \cdot \text{K})}{93 \times 10^3 \text{ Pa}} = 20.6 \text{ (N/m}^2\text{)/K}$$

Hence, from Eq. 3,

$$93 \times 10^3 \text{ Pa} + [20.6 \text{ (N/m}^2\text{)/K}]\, T = 104 \text{ kPa}$$

or

$$T = 534 \text{ K}$$

From Eq. 2 with the downstream pressure $p = 93$ kPa and temperature $T = 534$ K we get

$$s - s_1 = (1004 \text{ J/kg} \cdot \text{K}) \ln \left(\frac{534 \text{ K}}{286 \text{ K}}\right) - (286.9 \text{ J/kg} \cdot \text{K}) \ln \left(\frac{93{,}000 \text{ Pa}}{99{,}000 \text{ Pa}}\right)$$

$$s - s_1 = 645 \text{ J/kg} \cdot \text{K}$$

By proceeding as outlined above, we can construct the table of values shown below and graph the Rayleigh line of Fig. E11.15.

p (kPa)	T (K)	$s - s_1$ [J/kg · K]
93	534	645
86	807	1082
79	1028	1349
72	1199	1530
62	1356	1697
55	1404	1766
52	1409	1786
51.5	1409	1789
48	1400	1802
43	1366	1809
41	1346	1808
38	1306	1800
34	1240	1799
31	1179	1755
28	1109	1723
14	656	1395
7	354	974

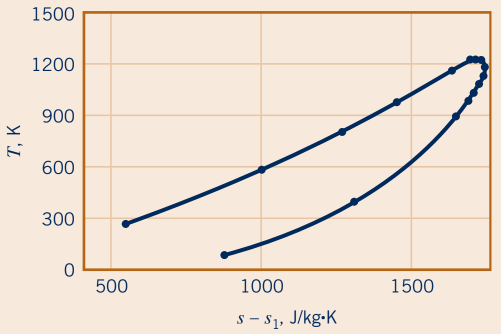

■ **Figure E11.15**

COMMENT Depending on whether the flow is being heated or cooled, it can proceed in either direction along the curve.

The maximum entropy state on the Rayleigh line corresponds to sonic conditions.

At point a on the Rayleigh line of Fig. 11.22, $ds/dT = 0$. To determine the physical importance of point a, we analyze further some of the governing equations. By differentiating the linear momentum equation for Rayleigh flow (Eq. 11.110), we obtain

$$dp = -\rho V\, dV$$

or

$$\frac{dp}{\rho} = -V\, dV \tag{11.112}$$

Combining Eq. 11.112 with the second $T\, ds$ equation (Eq. 11.18) leads to

$$T\, ds = d\check{h} + V\, dV \tag{11.113}$$

For an ideal gas (Eq. 11.7) $d\check{h} = c_p\, dT$. Thus, substituting Eq. 11.7 into Eq. 11.113 gives

$$T\, ds = c_p\, dT + V\, dV$$

or

$$\frac{ds}{dT} = \frac{c_p}{T} + \frac{V}{T}\frac{dV}{dT} \tag{11.114}$$

Consolidation of Eqs. 11.114, 11.112 (linear momentum), 11.1, 11.77 (differentiated equation of state), and 11.79 (continuity) leads to

$$\frac{ds}{dT} = \frac{c_p}{T} + \frac{V}{T}\frac{1}{[(T/V) - (V/R)]} \tag{11.115}$$

Hence, at state a where $ds/dT = 0$, Eq. 11.115 reveals that

$$V_a = \sqrt{RT_a k} \tag{11.116}$$

Comparison of Eqs. 11.116 and 11.36 tells us that the Mach number at state a is equal to 1,

$$\mathrm{Ma}_a = 1 \tag{11.117}$$

At point b on the Rayleigh line of Fig. 11.22, $dT/ds = 0$. From Eq. 11.115 we get

$$\frac{dT}{ds} = \frac{1}{ds/dT} = \frac{1}{(c_p/T) + (V/T)[(T/V) - (V/R)]^{-1}}$$

which for $dT/ds = 0$ (point b) gives

$$\mathrm{Ma}_b = \sqrt{\frac{1}{k}} \qquad \textbf{(11.118)}$$

The flow at point b is subsonic ($\mathrm{Ma}_b < 1.0$). Recall that $k > 1$ for any gas.

To learn more about Rayleigh flow, we need to consider the energy equation in addition to the equations already used. Application of the energy equation (Eq. 5.69) to the Rayleigh flow through the finite control volume of Fig. 11.21 yields

$$\dot{m}\left[\check{h}_2 - \check{h}_1 + \frac{V_2^2 - V_1^2}{2} + \overbrace{\cancel{g(z_2 - z_1)}}^{\text{0 (negligibly small for gas flow)}}\right] = \dot{Q}_{\substack{\text{net}\\ \text{in}}} + \overbrace{\cancel{\dot{W}_{\substack{\text{shaft}\\ \text{net in}}}}}^{\text{0 (flow is steady throughout)}}$$

or in differential form for Rayleigh flow through the semi-infinitesimal control volume of Fig. 11.21

$$d\check{h} + V\,dV = \delta q \qquad \textbf{(11.119)}$$

where δq is the heat transfer per unit mass of fluid in the semi-infinitesimal control volume.

By using $d\check{h} = c_p\,dT = Rk\,dT/(k-1)$ in Eq. 11.119, we obtain

$$\frac{dV}{V} = \frac{\delta q}{c_p T}\left[\frac{V}{T}\frac{dT}{dV} + \frac{V^2(k-1)}{kRT}\right]^{-1} \qquad \textbf{(11.120)}$$

Thus, by combining Eqs. 11.36 (ideal gas speed of sound), 11.46 (Mach number), 11.1 and 11.77 (ideal gas equation of state), 11.79 (continuity), and 11.112 (linear momentum) with Eq. 11.120 (energy) we get

$$\frac{dV}{V} = \frac{\delta q}{c_p T}\frac{1}{(1 - \mathrm{Ma}^2)} \qquad \textbf{(11.121)}$$

With the help of Eq. 11.121, we see clearly that when the Rayleigh flow is subsonic ($\mathrm{Ma} < 1$), fluid heating ($\delta q > 0$) increases fluid velocity while fluid cooling ($\delta q < 0$) decreases fluid velocity. When Rayleigh flow is supersonic ($\mathrm{Ma} > 1$), fluid heating decreases fluid velocity and fluid cooling increases fluid velocity.

Fluid temperature reduction can accompany heating a subsonic Rayleigh flow.

The second law of thermodynamics states that, based on experience, entropy increases with heating and decreases with cooling. With this additional insight provided by the conservation of energy principle and the second law of thermodynamics, we can say more about the Rayleigh line in Fig. 11.22. A summary of the qualitative aspects of Rayleigh flow is outlined in Table 11.2 and Fig. 11.23. Along the upper portion of the line, which includes point b, the flow is subsonic. Heating the fluid results in flow acceleration to a maximum Mach number of 1 at point a. Note that between points b and a along the Rayleigh line, heating the fluid results in a temperature decrease and cooling the fluid leads to a temperature increase. This trend is not surprising if we consider the stagnation temperature and fluid velocity changes that occur between points a and b when the fluid is heated or cooled. Along the lower portion of the Rayleigh curve the flow is supersonic. Rayleigh flows may or may not be choked. The amount of heating or cooling involved determines what will happen in a specific instance. As with Fanno flows, an abrupt deceleration from supersonic flow to subsonic flow across a normal shock wave can also occur in Rayleigh flows.

Table 11.2
Summary of Rayleigh Flow Characteristics

	Heating	Cooling
$\mathrm{Ma} < 1$	Acceleration	Deceleration
$\mathrm{Ma} > 1$	Deceleration	Acceleration

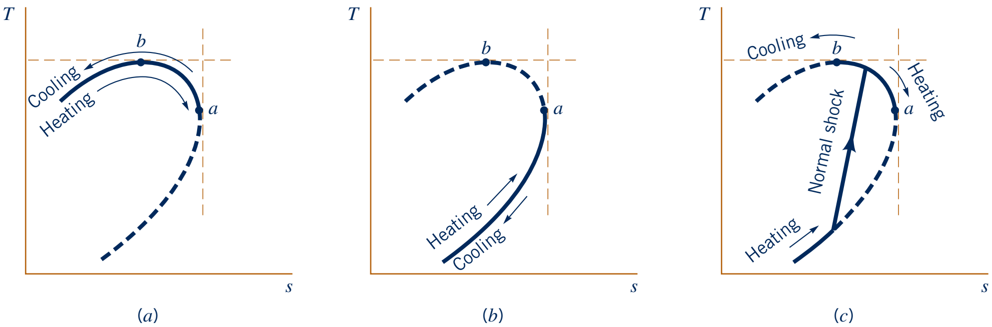

■ **Figure 11.23** **(*a*) Subsonic Rayleigh flow. (*b*) Supersonic Rayleigh flow. (*c*) Normal shock in a Rayleigh flow.**

To quantify Rayleigh flow behavior we need to develop appropriate forms of the governing equations. We elect to use the state of the Rayleigh flow fluid at point *a* of Fig. 11.22 as the reference state. As shown earlier, the Mach number at point *a* is 1. Even though the Rayleigh flow being considered may not choke and state *a* is not achieved by the flow, this reference state is useful.

If we apply the linear momentum equation (Eq. 11.110) to Rayleigh flow between any upstream section and the section, actual or imagined, where state *a* is attained, we get

$$p + \rho V^2 = p_a + \rho_a V_a^2$$

or

$$\frac{p}{p_a} + \frac{\rho V^2}{p_a} = 1 + \frac{\rho_a}{p_a} V_a^2 \tag{11.122}$$

By substituting the ideal gas equation of state (Eq. 11.1) into Eq. 11.122 and making use of the ideal gas speed-of-sound equation (Eq. 11.36) and the definition of Mach number (Eq. 11.46), we obtain

$$\boxed{\frac{p}{p_a} = \frac{1 + k}{1 + k\text{Ma}^2}} \tag{11.123}$$

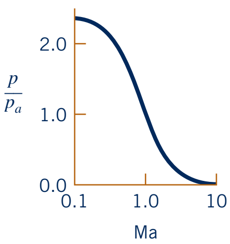

This relationship is graphed in the margin for air.

From the ideal gas equation of state (Eq. 11.1) we conclude that

$$\frac{T}{T_a} = \frac{p}{p_a}\frac{\rho_a}{\rho} \tag{11.124}$$

Conservation of mass (Eq. 11.40) with constant A gives

$$\frac{\rho_a}{\rho} = \frac{V}{V_a} \tag{11.125}$$

which when combined with Eqs. 11.36 (ideal gas speed of sound) and 11.46 (Mach number definition) gives

$$\frac{\rho_a}{\rho} = \text{Ma}\sqrt{\frac{T}{T_a}} \tag{11.126}$$

Combining Eqs. 11.124 and 11.126 leads to

$$\frac{T}{T_a} = \left(\frac{p}{p_a}\text{Ma}\right)^2 \tag{11.127}$$

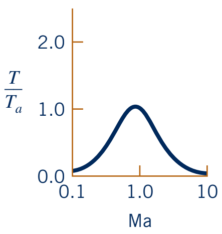

which when combined with Eq. 11.123 gives (also see margin figure)

$$\boxed{\frac{T}{T_a} = \left[\frac{(1 + k)\text{Ma}}{1 + k\text{Ma}^2}\right]^2} \tag{11.128}$$

From Eqs. 11.125, 11.126, and 11.128 we see that

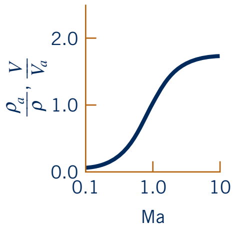

$$\boxed{\frac{\rho_a}{\rho} = \frac{V}{V_a} = \text{Ma}\left[\frac{(1 + k)\text{Ma}}{1 + k\text{Ma}^2}\right]} \tag{11.129}$$

This relationship is graphed in the margin for air.

The energy equation (Eq. 5.69) tells us that because of the heat transfer involved in Rayleigh flows, the stagnation temperature varies. We note that

$$\frac{T_0}{T_{0,a}} = \left(\frac{T_0}{T}\right)\left(\frac{T}{T_a}\right)\left(\frac{T_a}{T_{0,a}}\right) \tag{11.130}$$

Unlike Fanno flow, the stagnation temperature in Rayleigh flow varies.

We can use Eq. 11.56 (developed earlier for steady, isentropic, ideal gas flow) to evaluate T_0/T and $T_a/T_{0,a}$ because these two temperature ratios, by definition of the stagnation state, involve isentropic processes. Equation 11.128 can be used for T/T_a. Thus, consolidating Eqs. 11.130, 11.56, and 11.128 we obtain

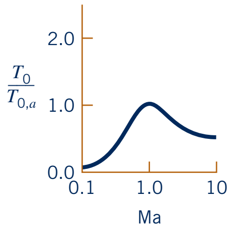

$$\boxed{\frac{T_0}{T_{0,a}} = \frac{2(k + 1)\text{Ma}^2\left(1 + \dfrac{k - 1}{2}\text{Ma}^2\right)}{(1 + k\text{Ma}^2)^2}} \tag{11.131}$$

This relationship is graphed in the margin for air.

Finally, we observe that

$$\frac{p_0}{p_{0,a}} = \left(\frac{p_0}{p}\right)\left(\frac{p}{p_a}\right)\left(\frac{p_a}{p_{0,a}}\right) \tag{11.132}$$

We can use Eq. 11.59 developed earlier for steady, isentropic, ideal gas flow to evaluate p_0/p and $p_a/p_{0,a}$ because these two pressure ratios, by definition, involve isentropic processes. Equation 11.123 can be used for p/p_a. Together, Eqs. 11.59, 11.123, and 11.132 give

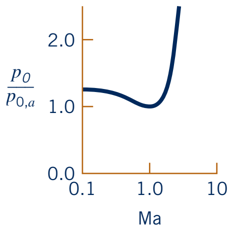

$$\boxed{\frac{p_0}{p_{0,a}} = \frac{(1 + k)}{(1 + k\text{Ma}^2)}\left[\left(\frac{2}{k + 1}\right)\left(1 + \frac{k - 1}{2}\text{Ma}^2\right)\right]^{k/(k-1)}} \tag{11.133}$$

This relationship is graphed in the margin for air.

Values of p/p_a, T/T_a, ρ/ρ_a or V/V_a, $T_0/T_{0,a}$, and $p_0/p_{0,a}$ are graphed in Fig. D.3 of Appendix D as a function of Mach number for Rayleigh flow of air ($k = 1.4$). The values in Fig. D.3 were calculated from Eqs. 11.123, 11.128, 11.129, 11.131, and 11.133. The usefulness of Fig. D.3 is illustrated in Example 11.16.

See Ref. 7 for a more advanced treatment of internal flows with heat transfer.

EXAMPLE 11.16 Effect of Mach Number and Heating/Cooling for Rayleigh Flow

GIVEN The information in Table 11.2 shows us that subsonic Rayleigh flow accelerates when heated and decelerates when cooled. Supersonic Rayleigh flow behaves just opposite to subsonic Rayleigh flow; it decelerates when heated and accelerates when cooled.

FIND Using Fig. D.3 for air ($k = 1.4$), state whether velocity, Mach number, static temperature, stagnation temperature, static pressure, and stagnation pressure increase or decrease as subsonic and supersonic Rayleigh flow is (a) heated, (b) cooled.

Solution

Acceleration occurs when V/V_a in Fig. D.3 increases. For deceleration, V/V_a decreases. From Fig. D.3 and Table 11.2 the following chart can be constructed.

From the Rayleigh flow trends summarized in the table below, we note that heating affects Rayleigh flows much like friction affects Fanno flows. Heating and friction both accelerate subsonic flows and decelerate supersonic flows. More importantly, both heating and friction cause the stagnation pressure to decrease. Since stagnation pressure loss is considered undesirable in terms of fluid mechanical efficiency, heating a fluid flow must be accomplished with this loss in mind.

COMMENT Note that for a small range of Mach numbers cooling actually results in a rise in temperature, T.

	Heating		Cooling	
	Subsonic	**Supersonic**	**Subsonic**	**Supersonic**
V	Increase	Decrease	Decrease	Increase
Ma	Increase	Decrease	Decrease	Increase
T	Increase for $0 \leq \text{Ma} \leq \sqrt{1/k}$ Decrease for $\sqrt{1/k} \leq \text{Ma} \leq 1$	Increase	Decrease for $0 \leq \text{Ma} \leq \sqrt{1/k}$ Increase for $\sqrt{1/k} \leq \text{Ma} \leq 1$	Decrease
T_0	Increase	Increase	Decrease	Decrease
p	Decrease	Increase	Increase	Decrease
p_0	Decrease	Decrease	Increase	Increase

11.5.3 Normal Shock Waves

V11.8 Blast waves

As mentioned earlier, normal shock waves can occur in supersonic flows through converging–diverging and constant area ducts. Past experience suggests that normal shock waves involve deceleration from a supersonic flow to a subsonic flow, a pressure rise, and an increase of entropy. To develop the equations that verify this observed behavior of flows across a normal shock, we apply first principles to the flow through a control volume that completely surrounds a normal shock wave (see Fig. 11.24). We consider the normal shock and thus the control volume to be infinitesimally thin and stationary.

For steady flow through the control volume of Fig. 11.24, the conservation of mass principle yields

$$\rho V = \text{constant} \tag{11.134}$$

because the flow cross-sectional area remains essentially constant within the infinitesimal thickness of the normal shock. Note that Eq. 11.134 is identical to the continuity equation used for Fanno and Rayleigh flows considered earlier.

Normal shock waves are assumed to be infinitesimally thin discontinuities.

The friction force acting on the contents of the infinitesimally thin control volume surrounding the normal shock is considered to be negligibly small. Also for ideal gas flow, the effect of gravity is neglected. Thus, the linear momentum equation (Eq. 5.22) describing steady gas flow through the control volume of Fig. 11.24 is

$$p + \rho V^2 = \text{constant}$$

or for an ideal gas for which $p = \rho RT$,

$$p + \frac{(\rho V)^2 RT}{p} = \text{constant} \tag{11.135}$$

Equation 11.135 is the same as the linear momentum equation for Rayleigh flow, which was derived earlier (Eq. 11.111).

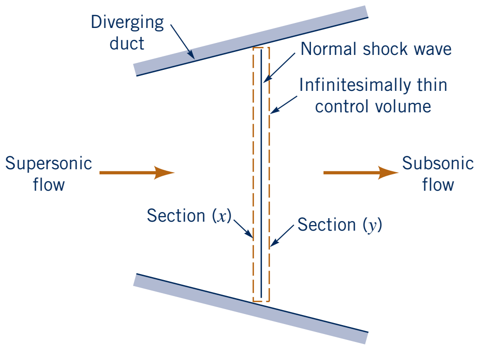

■ **Figure 11.24 Normal shock control volume.**

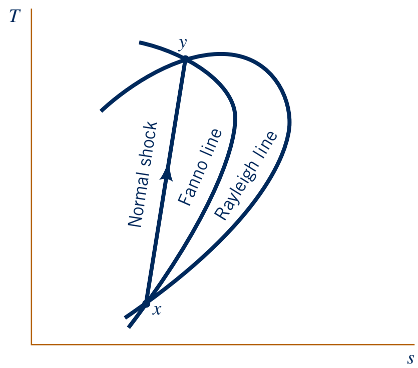

■ **Figure 11.25 The relationship between a normal shock and Fanno and Rayleigh lines.**

For the control volume containing the normal shock, no shaft work is involved and the heat transfer is assumed negligible. Thus, the energy equation (Eq. 5.69) can be applied to steady gas flow through the control volume of Fig. 11.24 to obtain

$$\check{h} + \frac{V^2}{2} = \check{h}_0 = \text{constant}$$

or, for an ideal gas, since $\check{h} - \check{h}_0 = c_p(T - T_0)$ and $p = \rho RT$

$$T + \frac{(\rho V)^2 T^2}{2c_p(p^2/R^2)} = T_0 = \text{constant} \tag{11.136}$$

Equation 11.136 is identical to the energy equation for Fanno flow analyzed earlier (Eq. 11.75).

The energy equation for Fanno flow and the momentum equation for Rayleigh flow are valid for flow across normal shocks.

The $T\,ds$ relationship previously used for ideal gas flow (Eq. 11.22) is valid for the flow through the normal shock (Fig. 11.24) because it (Eq. 11.22) is an ideal gas property relationship.

From the analyses in the previous paragraphs, it is apparent that the steady flow of an ideal gas across a normal shock is governed by some of the same equations used for describing both Fanno and Rayleigh flows (energy equation for Fanno flows and momentum equation for Rayleigh flow). Thus, for a given density–velocity product (ρV), gas (R, k), and conditions at the inlet of the normal shock (T_x, p_x, and s_x), the conditions downstream of the shock (state y) will be on both a Fanno line and a Rayleigh line that pass through the inlet state (state x), as is illustrated in Fig. 11.25. To conform with common practice we designate the states upstream and downstream of the normal shock with x and y instead of numerals 1 and 2. The Fanno and Rayleigh lines describe more of the flow field than just in the vicinity of the normal shock when Fanno and Rayleigh flows are actually involved (solid lines in Figs. 11.26*a* and 11.26*b*). Otherwise, these lines (dashed lines in Figs. 11.26*a*, 11.26*b*, and 11.26*c*) are useful mainly as a way to better visualize how the governing equations combine to yield a solution to the normal shock flow problem.

The second law of thermodynamics requires that entropy must increase across a normal shock wave. This law and sketches of the Fanno line and Rayleigh line intersections, like those of Figs. 11.25 and 11.26, persuade us to conclude that flow across a normal shock can only proceed from supersonic to subsonic flow. Similarly, in open-channel flows (see Chapter 10) the flow across a hydraulic jump proceeds from supercritical to subcritical conditions.

Since the states upstream and downstream of a normal shock wave are represented by the supersonic and subsonic intersections of actual and/or imagined Fanno and Rayleigh lines, we should be able to use equations developed earlier for Fanno and Rayleigh flows to quantify normal shock flow. For example, for the Rayleigh line of Fig. 11.26*b*

$$\frac{p_y}{p_x} = \left(\frac{p_y}{p_a}\right)\left(\frac{p_a}{p_x}\right) \tag{11.137}$$

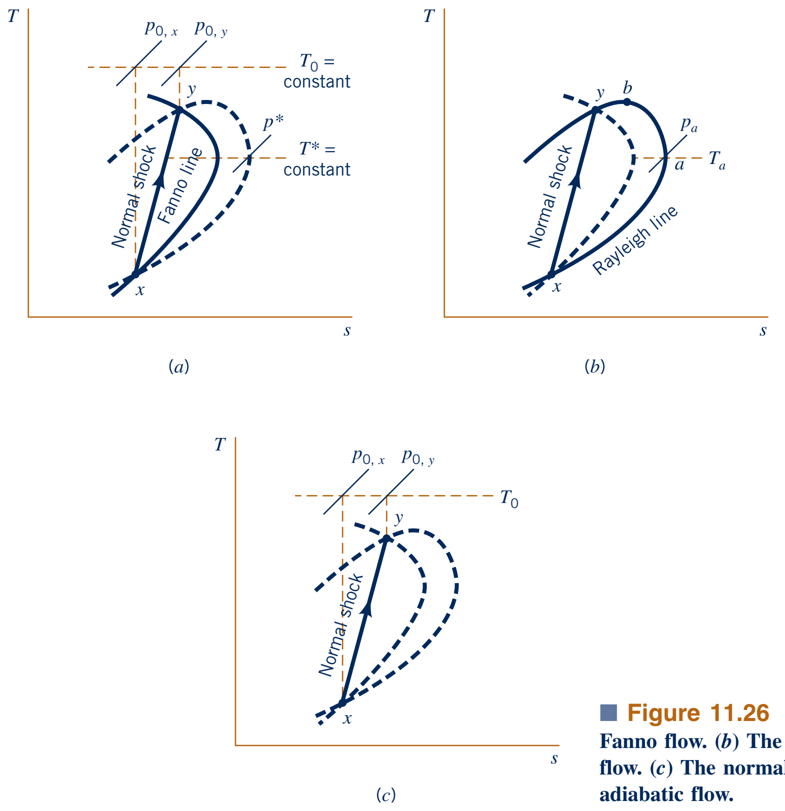

■ **Figure 11.26** (*a*) **The normal shock in a Fanno flow.** (*b*) **The normal shock in a Rayleigh flow.** (*c*) **The normal shock in a frictionless and adiabatic flow.**

But from Eq. 11.123 for Rayleigh flow we get

$$\frac{p_y}{p_a} = \frac{1 + k}{1 + k\text{Ma}_y^2} \tag{11.138}$$

and

$$\frac{p_x}{p_a} = \frac{1 + k}{1 + k\text{Ma}_x^2} \tag{11.139}$$

Thus, by combining Eqs. 11.137, 11.138, and 11.139 we get

Ratios of thermodynamic properties across a normal shock are functions of the Mach numbers.

$$\boxed{\frac{p_y}{p_x} = \frac{1 + k\text{Ma}_x^2}{1 + k\text{Ma}_y^2}} \tag{11.140}$$

Equation 11.140 can also be derived starting with

$$\frac{p_y}{p_x} = \left(\frac{p_y}{p^*}\right)\left(\frac{p^*}{p_x}\right)$$

and using the Fanno flow equation (Eq. 11.107)

$$\frac{p}{p^*} = \frac{1}{\text{Ma}}\left\{\frac{(k+1)/2}{1 + [(k-1)/2]\text{Ma}^2}\right\}^{1/2}$$

As might be expected, Eq. 11.140 can be obtained directly from the linear momentum equation

$$p_x + \rho_x V_x^2 = p_y + \rho_y V_y^2$$

since $\rho V^2/p = V^2/RT = kV^2/RTk = k\,\text{Ma}^2$.

For the Fanno flow of Fig. 11.26*a*,

$$\frac{T_y}{T_x} = \left(\frac{T_y}{T^*}\right)\left(\frac{T^*}{T_x}\right) \tag{11.141}$$

From Eq. 11.101 for Fanno flow we get

$$\frac{T_y}{T^*} = \frac{(k+1)/2}{1 + [(k-1)/2]\text{Ma}_y^2} \tag{11.142}$$

and

$$\frac{T_x}{T^*} = \frac{(k+1)/2}{1 + [(k-1)/2]\text{Ma}_x^2} \tag{11.143}$$

A consolidation of Eqs. 11.141, 11.142, and 11.143 gives

$$\boxed{\frac{T_y}{T_x} = \frac{1 + [(k-1)/2]\text{Ma}_x^2}{1 + [(k-1)/2]\text{Ma}_y^2}} \tag{11.144}$$

We seek next to develop an equation that will allow us to determine the Mach number downstream of the normal shock, Ma_y, when the Mach number upstream of the normal shock, Ma_x, is known. From the ideal gas equation of state (Eq. 11.1), we can form

$$\frac{p_y}{p_x} = \left(\frac{T_y}{T_x}\right)\left(\frac{\rho_y}{\rho_x}\right) \tag{11.145}$$

Using the continuity equation

$$\rho_x V_x = \rho_y V_y$$

with Eq. 11.145 we obtain

$$\frac{p_y}{p_x} = \left(\frac{T_y}{T_x}\right)\left(\frac{V_x}{V_y}\right) \tag{11.146}$$

When combined with the Mach number definition (Eq. 11.46) and the ideal gas speed-of-sound equation (Eq. 11.36), Eq. 11.146 becomes

$$\frac{p_y}{p_x} = \left(\frac{T_y}{T_x}\right)^{1/2}\left(\frac{\text{Ma}_x}{\text{Ma}_y}\right) \tag{11.147}$$

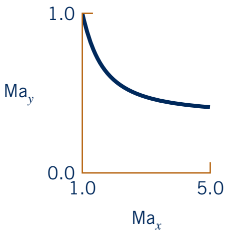

Thus, Eqs. 11.147 and 11.144 lead to

$$\frac{p_y}{p_x} = \left\{\frac{1 + [(k-1)/2]\text{Ma}_x^2}{1 + [(k-1)/2]\text{Ma}_y^2}\right\}^{1/2}\frac{\text{Ma}_x}{\text{Ma}_y} \tag{11.148}$$

which can be merged with Eq. 11.140 to yield

$$\boxed{\text{Ma}_y^2 = \frac{\text{Ma}_x^2 + [2/(k-1)]}{[2k/(k-1)]\text{Ma}_x^2 - 1}} \tag{11.149}$$

The flow changes from supersonic to subsonic across a normal shock.

This relationship is graphed in the margin for air.

Thus, we can use Eq. 11.149 to calculate values of Mach number downstream of a normal shock from a known Mach number upstream of the shock. As suggested by Fig. 11.26, to have a normal shock we must have $\text{Ma}_x > 1$. From Eq. 11.149 we find that $\text{Ma}_y < 1$.

If we combine Eqs. 11.149 and 11.140, we get

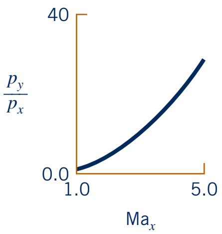

$$\boxed{\frac{p_y}{p_x} = \frac{2k}{k+1}\text{Ma}_x^2 - \frac{k-1}{k+1}} \tag{11.150}$$

This relationship is graphed in the margin for air.

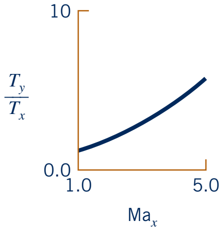

This equation allows us to calculate the pressure ratio across a normal shock from a known upstream Mach number. Similarly, taking Eqs. 11.149 and 11.144 together we obtain

$$\boxed{\frac{T_y}{T_x} = \frac{\{1 + [(k-1)/2]\mathrm{Ma}_x^2\}\{[2k/(k-1)]\mathrm{Ma}_x^2 - 1\}}{\{(k+1)^2/[2(k-1)]\}\mathrm{Ma}_x^2}} \tag{11.151}$$

This relationship is graphed in the margin for air.

From the continuity equation (Eq. 11.40), we have for flow across a normal shock

$$\frac{\rho_y}{\rho_x} = \frac{V_x}{V_y} \tag{11.152}$$

and from the ideal gas equation of state (Eq. 11.1)

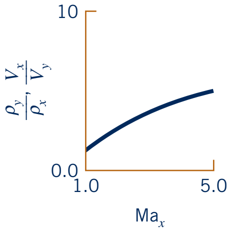

$$\frac{\rho_y}{\rho_x} = \left(\frac{p_y}{p_x}\right)\left(\frac{T_x}{T_y}\right) \tag{11.153}$$

Thus, by combining Eqs. 11.152, 11.153, 11.150, and 11.151, we get

$$\boxed{\frac{\rho_y}{\rho_x} = \frac{V_x}{V_y} = \frac{(k+1)\mathrm{Ma}_x^2}{(k-1)\mathrm{Ma}_x^2 + 2}} \tag{11.154}$$

This relationship is graphed in the margin for air.

The stagnation pressure ratio across the shock can be determined by combining

$$\frac{p_{0,y}}{p_{0,x}} = \left(\frac{p_{0,y}}{p_y}\right)\left(\frac{p_y}{p_x}\right)\left(\frac{p_x}{p_{0,x}}\right) \tag{11.155}$$

with Eqs. 11.59, 11.149, and 11.150 to get

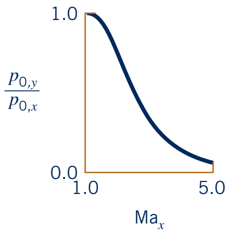

$$\boxed{\frac{p_{0,y}}{p_{0,x}} = \frac{\left(\dfrac{k+1}{2}\mathrm{Ma}_x^2\right)^{k/(k-1)}\left(1 + \dfrac{k-1}{2}\mathrm{Ma}_x^2\right)^{k/(1-k)}}{\left(\dfrac{2k}{k+1}\mathrm{Ma}_x^2 - \dfrac{k-1}{k+1}\right)^{1/(k-1)}}} \tag{11.156}$$

This relationship is graphed in the margin for air.

Figure D.4 in Appendix D graphs values of downstream Mach numbers, Ma_y, pressure ratio, p_y/p_x, temperature ratio, T_y/T_x, density ratio, ρ_y/ρ_x, or velocity ratio, V_x/V_y, and stagnation pressure ratio, $p_{0,y}/p_{0,x}$, as a function of upstream Mach number, Ma_x, for the steady flow across a normal shock wave of an ideal gas having a specific heat ratio $k = 1.4$. These values were calculated from Eqs. 11.149, 11.150, 11.151, 11.154, and 11.156.

Important trends associated with the steady flow of an ideal gas across a normal shock wave can be determined by studying Fig. D.4. These trends are summarized in Table 11.3.

Examples 11.17 and 11.18 illustrate how Fig. D.4 can be used to solve fluid flow problems involving normal shock waves.

Across a normal shock the values of some parameters increase, some remain constant, and some decrease.

■ **Table 11.3**
Summary of Normal Shock Wave Characteristics

Variable	Change Across Normal Shock Wave
Mach number	Decrease
Static pressure	Increase
Stagnation pressure	Decrease
Static temperature	Increase
Stagnation temperature	Constant
Density	Increase
Velocity	Decrease

EXAMPLE 11.17 Stagnation Pressure Drop across a Normal Shock

GIVEN Designers involved with fluid mechanics work hard at minimizing loss of available energy in their designs. Adiabatic, frictionless flows involve no loss in available energy. Entropy remains constant for these idealized flows. Adiabatic flows with friction involve available energy loss and entropy increase. Generally, larger entropy increases imply larger losses.

FIND For normal shocks, show that the stagnation pressure drop (and thus loss) is larger for higher Mach numbers.

SOLUTION

We assume that air ($k = 1.4$) behaves as a typical gas and use Fig. D.4 to respond to the above-stated requirements. Since

$$1 - \frac{p_{0,y}}{p_{0,x}} = \frac{p_{0,x} - p_{0,y}}{p_{0,x}}$$

we can construct the following table with values of $p_{0,y}/p_{0,x}$ from Fig. D.4.

COMMENT When the Mach number of the flow entering the shock is low, say $\text{Ma}_x = 1.2$, the flow across the shock is nearly isentropic and the loss in stagnation pressure is small. However, as shown in Fig. E11.17, at larger Mach numbers, the entropy change across the normal shock rises dramatically and the stagnation pressure drop across the shock is appreciable. If a shock occurs at $\text{Ma}_x = 2.5$, only about 50% of the upstream stagnation pressure is recovered.

In devices where supersonic flows occur, for example, high-performance aircraft engine inlet ducts and high-speed wind tunnels, designers attempt to prevent shock formation, or if shocks must occur, they design the flow path so that shocks are positioned where they are weak (small Mach number).

Of interest also is the static pressure rise that occurs across a normal shock. These static pressure ratios, p_y/p_x, obtained from Fig. D.4 are shown in the table for a few Mach numbers. For a developing boundary layer, any pressure rise in the flow direction is considered as an adverse pressure gradient that can possibly cause flow separation (see Section 9.2.6). Thus, shock–boundary layer interactions are of great concern to designers of high-speed flow devices.

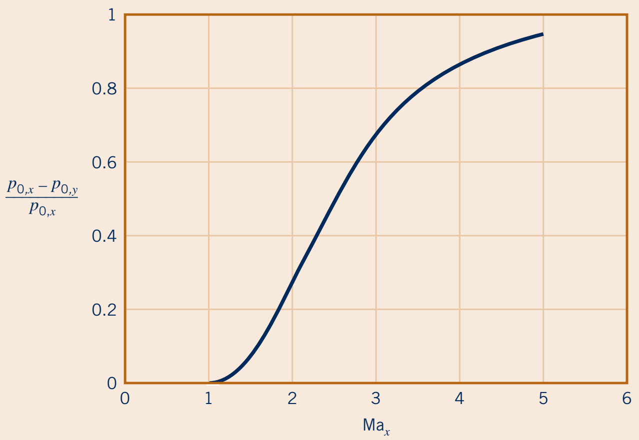

■ **Figure E11.17**

Ma_x	$p_{0,y}/p_{0,x}$	$\frac{p_{0,x} - p_{0,y}}{p_{0,x}}$
1.0	1.0	0
1.2	0.99	0.01
1.5	0.93	0.07
2.0	0.72	0.28
2.5	0.50	0.50
3.0	0.33	0.67
3.5	0.21	0.79
4.0	0.14	0.86
5.0	0.06	0.94

Ma_x	p_y/p_x
1.0	1.0
1.2	1.5
1.5	2.5
2.0	4.5
3.0	10
4.0	18
5.0	29

EXAMPLE 11.18 Supersonic Flow Pitot Tube

GIVEN A total pressure probe is inserted into a supersonic air flow. A shock wave forms just upstream of the impact hole and head as illustrated in Fig. E11.18. The probe measures a total pressure of 414 kPa. The stagnation temperature at the probe head is 555 K. The static pressure upstream of the shock is measured with a wall tap to be 82 kPa.

FIND Determine the Mach number and velocity of the flow.

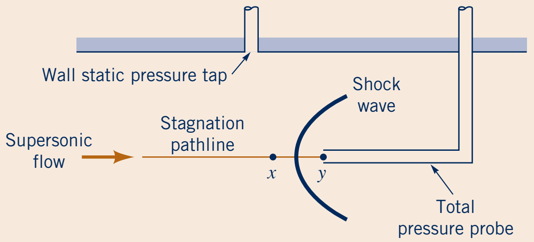

■ **Figure E11.18**

Solution

We assume that the flow along the stagnation pathline is isentropic except across the shock. Also, the shock is treated as a normal shock. Thus, in terms of the data we have

$$\frac{p_{0,y}}{p_x} = \left(\frac{p_{0,y}}{p_{0,x}}\right)\left(\frac{p_{0,x}}{p_x}\right) \tag{1}$$

where $p_{0,y}$ is the stagnation pressure measured by the probe, and p_x is the static pressure measured by the wall tap. The stagnation pressure upstream of the shock, $p_{0,x}$, is not measured.

Combining Eqs. 1, 11.156, and 11.59 we obtain

$$\frac{p_{0,y}}{p_x} = \frac{\{[(k+1)/2]\text{Ma}_x^2\}^{k/(k-1)}}{\{[2k/(k+1)]\text{Ma}_x^2 - [(k-1)/(k+1)]\}^{1/(k-1)}} \tag{2}$$

which is called the *Rayleigh Pitot-tube formula*. Values of $p_{0,y}/p_x$ from Eq. 2 are considered important enough to be included in Fig. D.4 for $k = 1.4$. Thus, for $k = 1.4$ and

$$\frac{p_{0,y}}{p_x} = \frac{414 \text{ kPa}}{82 \text{ kPa}} = 5$$

we use Fig. D.4 (or Eq. 2) to ascertain that

$$\text{Ma}_x = 1.9 \qquad \textbf{(Ans)}$$

To determine the flow velocity we need to know the static temperature upstream of the shock, since Eqs. 11.36 and 11.46 can be used to yield

$$V_x = \text{Ma}_x c_x = \text{Ma}_x \sqrt{RT_x k} \tag{3}$$

The stagnation temperature downstream of the shock was measured and found to be

$$T_{0,y} = 555 \text{ K}$$

Since the stagnation temperature remains constant across a normal shock (see Eq. 11.136),

$$T_{0,x} = T_{0,y} = 555 \text{ K}$$

For the isentropic flow upstream of the shock, Eq. 11.56 or Fig. D.1 can be used. For $\text{Ma}_x = 1.9$,

$$\frac{T_x}{T_{0,x}} = 0.59$$

or

$$T_x = (0.59)(555 \text{ K}) = 327 \text{ K}$$

With Eq. 3 we obtain

$$V_x = 1.87\sqrt{(286.9 \text{ J/kg}\cdot\text{K})(327 \text{ K})(1.4)}$$
$$= 678 \text{ m/s} \qquad \textbf{(Ans)}$$

COMMENT Application of the incompressible flow Pitot tube results (see Section 3.5) would give highly inaccurate results because of the large pressure and density changes involved.

Example 11.19 Normal Shock in a Converging–Diverging Duct

GIVEN Consider the converging–diverging duct of Example 11.8.

FIND Determine the ratio of back pressure to inlet stagnation pressure, $p_{\text{III}}/p_{0,x}$ (see Fig. 11.13), that will result in a standing normal shock at the exit ($x = +0.5$ m) of the duct. What value of the ratio of back pressure to inlet stagnation pressure would be required to position the shock at $x = +0.3$ m? Show related temperature–entropy diagrams for these flows.

Solution

For supersonic, isentropic flow through the nozzle to just upstream of the standing normal shock at the duct exit, we have from the table of Example 11.8 at $x = +0.5$ m

$$\text{Ma}_x = 2.8$$

and

$$\frac{p_x}{p_{0,x}} = 0.04$$

From Fig. D.4 for $\text{Ma}_x = 2.8$ we obtain

$$\frac{p_y}{p_x} = 9.0$$

Thus,

$$\frac{p_y}{p_{0,x}} = \left(\frac{p_y}{p_x}\right)\left(\frac{p_x}{p_{0,x}}\right) = (9.0)(0.04)$$
$$= 0.36 = \frac{p_{\text{III}}}{p_{0,x}} \qquad \textbf{(Ans)}$$

When the ratio of duct back pressure to inlet stagnation pressure, $p_{\text{III}}/p_{0,x}$, is set equal to 0.36, the air will accelerate through the converging–diverging duct to a Mach number of 2.8 at the duct exit. The air will subsequently decelerate to a subsonic flow across a normal shock at the duct exit. The stagnation pressure ratio across the normal shock, $p_{0,y}/p_{0,x}$, is 0.38 (Fig. D.4 for

$Ma_x = 2.8$). A considerable amount of available energy is lost across the shock.

For a normal shock at $x = +0.3$ m, we note from the table of Example 11.8 that $Ma_x = 2.14$ and

$$\frac{p_x}{p_{0,x}} = 0.10 \quad (1)$$

From Fig. D.4 for $Ma_x = 2.14$ we obtain $p_y/p_x = 5.2$, $Ma_y = 0.56$, and

$$\frac{p_{0,y}}{p_{0,x}} = 0.66 \quad (2)$$

From Fig. D.1 for $Ma_y = 0.56$ we get

$$\frac{A_y}{A^*} = 1.24 \quad (3)$$

For $x = +0.3$ m, the ratio of duct exit area to local area (A_2/A_y) is, using the area equation from Example 11.8,

$$\frac{A_2}{A_y} = \frac{0.1 + (0.5)^2}{0.1 + (0.3)^2} = 1.842 \quad (4)$$

Using Eqs. 3 and 4 we get

$$\frac{A_2}{A^*} = \left(\frac{A_y}{A^*}\right)\left(\frac{A_2}{A_y}\right) = (1.24)(1.842) = 2.28$$

Note that for the isentropic flow upstream of the shock, $A^* = 0.10$ m^2 (the actual throat area), while for the isentropic flow downstream of the shock, $A^* = A_2/2.28 = 0.35$ m^2$/2.28 = 0.15$ m^2. With $A_2/A^* = 2.28$ we use Fig. D.1 and find $Ma_2 = 0.26$ and

$$\frac{p_2}{p_{0,y}} = 0.95 \quad (5)$$

Combining Eqs. 2 and 5 we obtain

$$\frac{p_2}{p_{0,x}} = \left(\frac{p_2}{p_{0,y}}\right)\left(\frac{p_{0,y}}{p_{0,x}}\right) = (0.95)(0.66) = 0.63 \quad \textbf{(Ans)}$$

When the back pressure, p_2, is set equal to 0.63 times the inlet stagnation pressure, $p_{0,x}$, the normal shock will be positioned at $x = +0.3$ m. The corresponding $T-s$ diagrams are shown in Figs. E11.19*a* and E11.19*b*.

COMMENT Note that $p_2/p_{0,x} = 0.63$ is less than the value of this ratio for subsonic isentropic flow through the converging–diverging duct, $p_2/p_0 = 0.98$ (from Example 11.8) and is larger than $p_{III}/p_{0,x} = 0.36$, for duct flow with a normal shock at the exit (see Fig. 11.13). Also the stagnation pressure ratio with the shock at $x = +0.3$ m, $p_{0,y}/p_{0,x} = 0.66$, is much greater than the stagnation pressure ratio, 0.38, when the shock occurs at the exit ($x = +0.5$ m) of the duct.

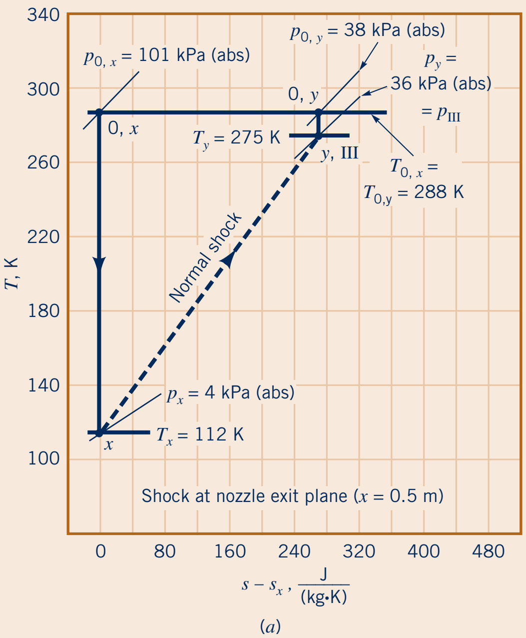

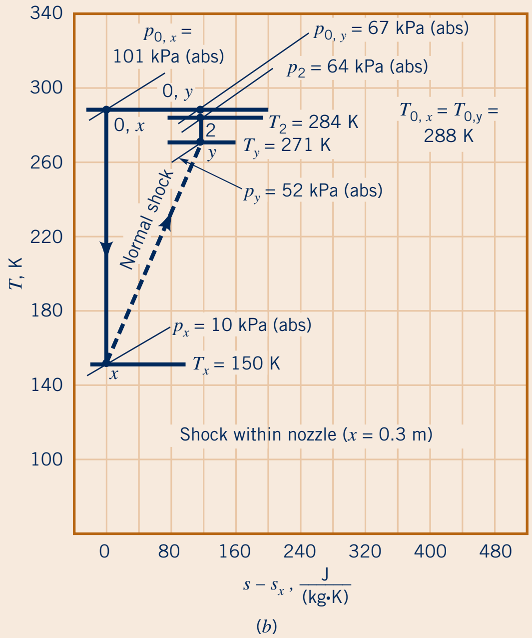

■ **Figure E11.19**

11.6 Analogy between Compressible and Open-Channel Flows

During a first course in fluid mechanics, students rarely study both open-channel flows (Chapter 10) and compressible flows. This is unfortunate because these two kinds of flows are strikingly similar in several ways. Furthermore, the analogy between open-channel and compressible flows is useful because important two-dimensional compressible flow phenomena can be simply and inexpensively demonstrated with a shallow, open-channel flow field in a *ripple tank* or *water table*.

The propagation of weak pressure pulses (sound waves) in a compressible flow can be considered to be comparable to the movement of small-amplitude waves on the surface of an open-channel flow. In each case—two-dimensional compressible flow and open-channel flow—the influence of flow velocity on wave pattern is similar. When the flow velocity is less than the wave speed, wave fronts can move upstream of the wave source and the flow is subsonic (compressible flow) or subcritical (open-channel flow). When the flow velocity is equal to the wave speed, wave fronts cannot move upstream of the wave source and the flow is sonic (compressible flow) or critical (open-channel flow). When the flow velocity is greater than the wave speed, the flow is supersonic (compressible flow) or supercritical (open-channel flow). Normal shocks can occur in supersonic compressible flows. Hydraulic jumps can occur in supercritical open-channel flows. Comparison of the characteristics of normal shocks (Section 11.5.3) and hydraulic jumps (Section 10.6.1) suggests a strong resemblance and thus analogy between the two phenomena.

Compressible gas flows and open-channel liquid flows are strikingly similar in several ways.

For compressible flows a meaningful dimensionless variable is the Mach number, where

$$\mathrm{Ma} = \frac{V}{c} \tag{11.46}$$

In open-channel flows, an important dimensionless variable is the Froude number, where

$$\mathrm{Fr} = \frac{V_{oc}}{\sqrt{gy}} \tag{11.157}$$

The velocity of the channel flow is V_{oc}, the acceleration of gravity is g, and the depth of the flow is y. Since the speed of a small-amplitude wave on the surface of an open-channel flow, c_{oc}, is (see Section 10.2.1)

$$c_{oc} = \sqrt{gy} \tag{11.158}$$

we conclude that

$$\mathrm{Fr} = \frac{V_{oc}}{c_{oc}} \tag{11.159}$$

From Eqs. 11.46 and 11.159 we see the similarity between Mach number (compressible flow) and Froude number (open-channel flow).

For compressible flow, the continuity equation is

$$\rho A V = \text{constant} \tag{11.160}$$

where V is the flow velocity, ρ is the fluid density, and A is the flow cross-sectional area. For an open-channel flow, conservation of mass leads to

$$ybV_{oc} = \text{constant} \tag{11.161}$$

where V_{oc} is the flow velocity, and y and b are the depth and width of the open-channel flow. Comparing Eqs. 11.160 and 11.161 we note that if flow velocities are considered similar and flow area, A, and channel width, b, are considered similar, then compressible flow density, ρ, is analogous to open-channel flow depth, y.

It should be pointed out that the similarity between Mach number and Froude number is generally not exact. If compressible flow and open-channel flow velocities are considered to be similar, then it follows that for Mach number and Froude number similarity the wave speeds c and c_{oc} must also be similar.

From the development of the equation for the speed of sound in an ideal gas (see Eqs. 11.34 and 11.35) we have for the compressible flow

$$c = \sqrt{(\text{constant})\, k\rho^{k-1}} \tag{11.162}$$

From Eqs. 11.162 and 11.158, we see that if y is to be similar to ρ as suggested by comparing Eqs. 11.160 and 11.161, then k should be equal to 2. Typically $k = 1.4$ or 1.67, not 2. This limitation to exactness is, however, usually not serious enough to compromise the benefits of the analogy between compressible and open-channel flows.

11.7 Two-Dimensional Compressible Flow

A brief introduction to two-dimensional compressible flow is included here for those who are interested. We begin with a consideration of supersonic flow over a wall with a small change of direction as sketched in Fig. 11.27.

We apply the component of the linear momentum equation (Eq. 5.22) parallel to the Mach wave to the flow across the Mach wave. (See Eq. 11.39 for the definition of a Mach wave.) The result is that the component of velocity parallel to the Mach wave is constant across the Mach wave. That is, $V_{t1} = V_{t2}$. Thus, from the simple velocity triangle construction indicated in Fig. 11.27, we conclude that the flow accelerates because of the change in direction of the flow. If several changes in wall direction are involved as shown in Fig. 11.28, then the supersonic flow accelerates (expands) because of the changes in flow direction across the Mach waves (also called *expansion* waves). Each Mach wave makes an appropriately smaller angle α with the upstream wall because of the increase in Mach number that occurs with each direction change (see Section 11.3). A rounded expansion corner may be considered as a series of infinitesimal changes in direction. Conversely, even sharp corners are actually rounded when viewed on a small enough scale. Thus, expansion fans as illustrated in Fig. 11.29 are commonly used for supersonic flow around a "sharp" corner. If the flow across the Mach waves is considered to be isentropic, then Eq. 11.42 suggests that the increase in flow speed is accompanied by a decrease in static pressure.

Supersonic flows accelerate across expansion Mach waves.

When the change in supersonic flow direction involves the change in wall orientation sketched in Fig. 11.30, compression rather than expansion occurs. The flow decelerates and the static pressure increases across the Mach wave. For several changes in wall direction, as indicated in Fig. 11.31, several Mach waves occur, each at an appropriately larger angle α with the upstream wall. A rounded compression corner may be considered as a series of infinitesimal changes in

V11.9 Wedge oblique shocks and expansions

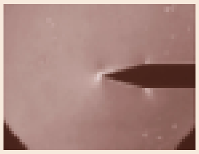

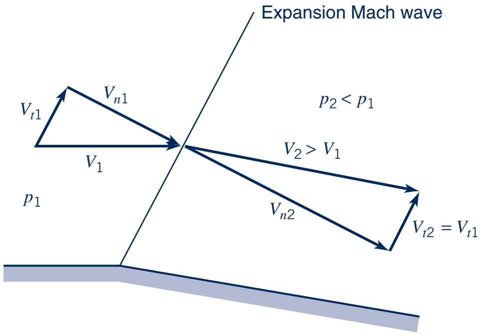

Figure 11.27 **Flow acceleration across a Mach wave.**

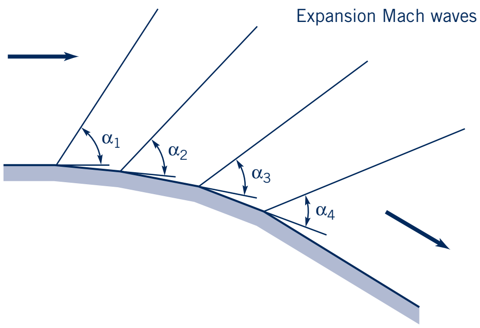

Figure 11.28 **Flow acceleration across Mach waves.**

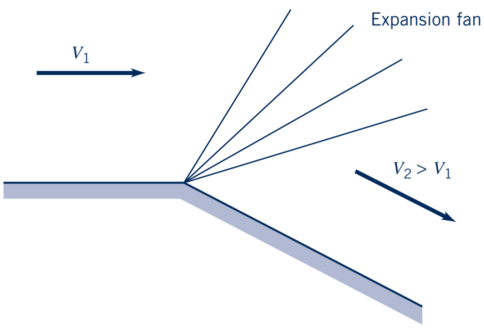

Figure 11.29 **Corner expansion fan.**

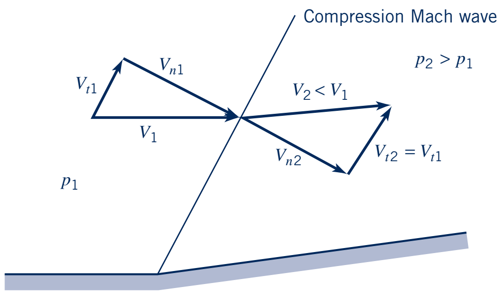

Figure 11.30 **Flow deceleration across a Mach wave.**

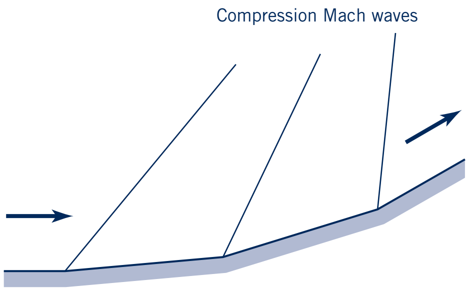

■ **Figure 11.31** **Flow deceleration across Mach waves.**

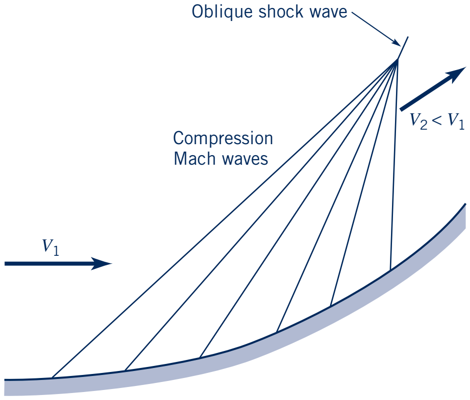

■ **Figure 11.32** **Oblique shock wave.**

V11.10 Bullet oblique shocks

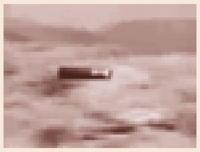

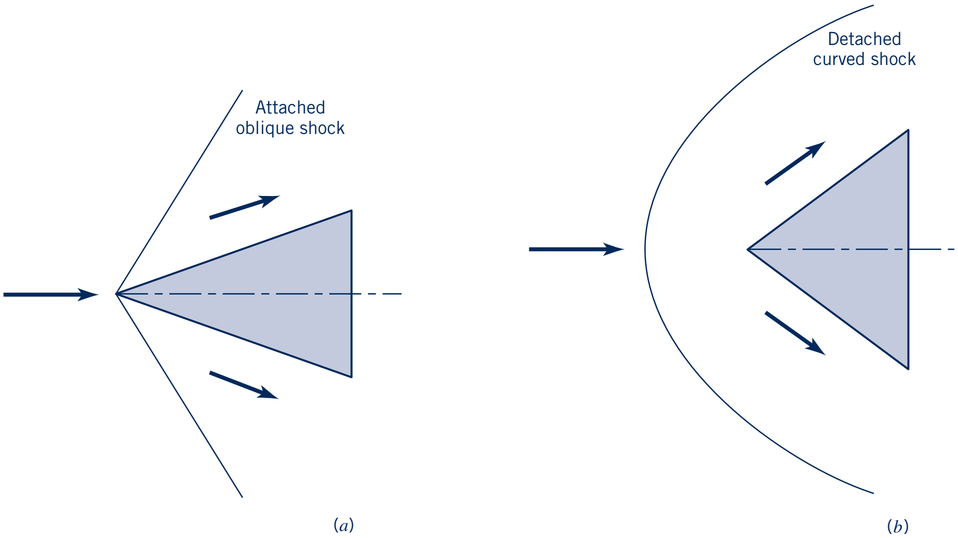

■ **Figure 11.33** **Supersonic flow over a wedge: (*a*) Smaller wedge angle results in attached oblique shock. (*b*) Large wedge angle results in detached curved shock.**

V11.11 Space Shuttle oblique shocks

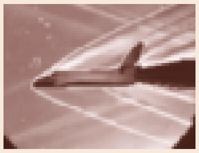

direction and even sharp corners are actually rounded. Mach waves or compression waves can coalesce to form an oblique shock wave as shown in Fig. 11.32.

The above discussion of compression waves can be usefully extended to supersonic flow impinging on an object. For example, for supersonic flow incident on a wedge-shaped leading edge (see Fig. 11.33), an attached oblique shock can form as suggested in Fig. 11.33*a*. For the same incident Mach number but with a larger wedge angle, a detached curved shock as sketched in Fig. 11.33*b* can result. In Example 11.19, we considered flow along a stagnation pathline across a detached curved shock to be identical to flow across a normal shock wave.

From this brief look at two-dimensional supersonic flow, one can easily conclude that the extension of these concepts to flows over immersed objects and within ducts can be exciting, especially if three-dimensional effects are considered. Reference 6 provides much more on this subject than could be included here.

11.8 Chapter Summary and Study Guide

In this chapter, consideration is given to the flow of gas involving substantial changes in fluid density caused mainly by high speeds. While the flow of liquids may most often be considered of constant density or incompressible over a wide range of speeds, the flow of gases and vapors

compressible flow
ideal gas
internal energy
enthalpy
specific heat ratio
entropy
adiabatic
isentropic
Mach number
speed of sound
stagnation pressure
subsonic
sonic
Mach wave
supersonic
Mach cone
transonic flows
hypersonic flows
converging–diverging duct
throat
temperature–entropy (T–s) diagram
choked flow
critical state
critical pressure ratio
normal shock wave
oblique shock wave
expansion wave
overexpanded
underexpanded
nonisentropic flow
Fanno flow
Rayleigh flow

may involve substantial fluid density changes at higher speeds. At lower speeds, gas and vapor density changes are not appreciable, and so these flows may be treated as incompressible.

Since fluid density and other fluid property changes are significant in compressible flows, property relationships are important. An ideal gas, with well-defined fluid property relationships, is used as an approximation of an actual gas. This profound simplification still allows useful conclusions to be made about compressible flows.

The Mach number is a key variable in compressible flow theory. Most easily understood as the ratio of the local speed of flow and the speed of sound in the flowing fluid, it is a measure of the extent to which the flow is compressible or not. It is used to define categories of compressible flows, which range from subsonic (Mach number less than 1) to supersonic (Mach number greater than 1). The speed of sound in a truly incompressible fluid is infinite, so the Mach numbers associated with liquid flows are generally low.

The notion of an isentropic or constant entropy flow is introduced. The most important isentropic flow is one that is adiabatic (no heat transfer to or from the flowing fluid) and frictionless (zero viscosity). This simplification, like the one associated with approximating real gases with an ideal gas, leads to useful results including trends associated with accelerating and decelerating flows through converging, diverging, and converging–diverging flow paths. Phenomena including flow choking, acceleration in a diverging passage, deceleration in a converging passage, and the achievement of supersonic flows are discussed.

Three major nonisentropic compressible flows considered in this chapter are Fanno flows, Rayleigh flows, and flows across normal shock waves. Unusual outcomes include the conclusions that friction can accelerate a subsonic Fanno flow, heating can result in fluid temperature reduction in a subsonic Rayleigh flow, and a flow can decelerate from supersonic flow to subsonic flow across a very small distance. The value of temperature–entropy (T–s) diagramming of flows to better understand them is demonstrated.

Numerous formulas describing a variety of ideal gas compressible flows are derived. These formulas can be easily solved with computers. However, to provide the learner with a better grasp of the details of a compressible flow process, a graphical approach, albeit approximate, is used.

The striking analogy between compressible and open-channel flows leads to a brief discussion of the usefulness of a ripple tank or water table to simulate compressible flows.

Expansion and compression Mach waves associated with two-dimensional compressible flows are introduced, as is the formation of oblique shock waves from compression Mach waves.

The following checklist provides a study guide for this chapter. When your study of the entire chapter and end-of-chapter exercises is completed, you should be able to

- write out the meanings of the terms listed here in the margin and understand each of the related concepts. These terms are particularly important and are set in ***italic, bold, and color*** type in the text.
- estimate the change in ideal gas properties in a compressible flow.
- calculate Mach number value for a specific compressible flow.
- estimate when a flow may be considered incompressible and when it must be considered compressible to preserve accuracy.
- estimate details of isentropic flows of an ideal gas though converging, diverging, and converging–diverging passages.
- estimate details of nonisentropic Fanno and Rayleigh flows and flows across normal shock waves.
- explain the analogy between compressible and open-channel flows.

Some of the important equations in this chapter are:

Ideal gas equation of state	$\rho = \dfrac{p}{RT}$	**(11.1)**
Internal energy change	$\check{u}_2 - \check{u}_1 = c_v(T_2 - T_1)$	**(11.5)**
Enthalpy	$\check{h} = \check{u} + \dfrac{p}{\rho}$	**(11.6)**

Enthalpy change	$\check{h}_2 - \check{h}_1 = c_p(T_2 - T_1)$	**(11.9)**
Specific heat difference	$c_p - c_v = R$	**(11.12)**
Specific heat ratio	$k = \dfrac{c_p}{c_v}$	**(11.13)**
Specific heat at constant pressure	$c_p = \dfrac{Rk}{k - 1}$	**(11.14)**
Specific heat at constant volume	$c_v = \dfrac{R}{k - 1}$	**(11.15)**
First $T\,ds$ equation	$T\,ds = d\check{u} + p\,d\left(\dfrac{1}{\rho}\right)$	**(11.16)**
Second $T\,ds$ equation	$T\,ds = d\check{h} - \left(\dfrac{1}{\rho}\right)dp$	**(11.18)**
Entropy change	$s_2 - s_1 = c_v \ln \dfrac{T_2}{T_1} + R \ln \dfrac{\rho_1}{\rho_2}$	**(11.21)**
Entropy change	$s_2 - s_1 = c_p \ln \dfrac{T_2}{T_1} - R \ln \dfrac{p_2}{p_1}$	**(11.22)**
Isentropic flow	$\dfrac{p}{\rho^k} = \text{constant}$	**(11.25)**
Speed of sound	$c = \sqrt{\left(\dfrac{\partial p}{\partial \rho}\right)_s}$	**(11.34)**
Speed of sound in gas	$c = \sqrt{RTk}$	**(11.36)**
Speed of sound in liquid	$c = \sqrt{\dfrac{E_v}{\rho}}$	**(11.38)**
Mach cone angle	$\sin \alpha = \dfrac{c}{V} = \dfrac{1}{\text{Ma}}$	**(11.39)**
Mach number	$\text{Ma} = \dfrac{V}{c}$	**(11.46)**
Isentropic flow	$\dfrac{dV}{V} = -\dfrac{dA}{A}\dfrac{1}{(1 - \text{Ma}^2)}$	**(11.48)**
Isentropic flow	$\dfrac{d\rho}{\rho} = \dfrac{dA}{A}\dfrac{\text{Ma}^2}{(1 - \text{Ma}^2)}$	**(11.49)**
Isentropic flow	$\dfrac{T}{T_0} = \dfrac{1}{1 + [(k-1)/2]\text{Ma}^2}$	**(11.56)**
Isentropic flow	$\dfrac{p}{p_0} = \left\{\dfrac{1}{1 + [(k-1)/2]\text{Ma}^2}\right\}^{k/(k-1)}$	**(11.59)**
Isentropic flow	$\dfrac{\rho}{\rho_0} = \left\{\dfrac{1}{1 + [(k-1)/2]\text{Ma}^2}\right\}^{1/(k-1)}$	**(11.60)**
Isentropic flow-critical pressure ratio	$\dfrac{p^*}{p_0} = \left(\dfrac{2}{k+1}\right)^{k/(k-1)}$	**(11.61)**
Isentropic flow-critical temperature ratio	$\dfrac{T^*}{T_0} = \dfrac{2}{k+1}$	**(11.63)**

Isentropic flow	$\dfrac{A}{A^*} = \dfrac{1}{\text{Ma}}\left\{\dfrac{1 + [(k-1)/2]\text{Ma}^2}{1 + [(k-1)/2]}\right\}^{(k+1)/[2(k-1)]}$	**(11.71)**
Fanno flow	$\dfrac{1}{k}\dfrac{(1 - \text{Ma}^2)}{\text{Ma}^2} + \dfrac{k+1}{2k}\ln\left\{\dfrac{[(k+1)/2]\text{Ma}^2}{1 + [(k-1)/2]\text{Ma}^2}\right\} = \dfrac{f(\ell^* - \ell)}{D}$	**(11.98)**
Fanno flow	$\dfrac{T}{T^*} = \dfrac{(k+1)/2}{1 + [(k-1)/2]\text{Ma}^2}$	**(11.101)**
Fanno flow	$\dfrac{V}{V^*} = \left\{\dfrac{[(k+1)/2]\text{Ma}^2}{1 + [(k-1)/2]\text{Ma}^2}\right\}^{1/2}$	**(11.103)**
Fanno flow	$\dfrac{p}{p^*} = \dfrac{1}{\text{Ma}}\left\{\dfrac{(k+1)/2}{1 + [(k-1)/2]\text{Ma}^2}\right\}^{1/2}$	**(11.107)**
Fanno flow	$\dfrac{p_0}{p_0^*} = \dfrac{1}{\text{Ma}}\left[\left(\dfrac{2}{k+1}\right)\left(1 + \dfrac{k-1}{2}\text{Ma}^2\right)\right]^{[(k+1)/2(k-1)]}$	**(11.109)**
Rayleigh flow	$\dfrac{p}{p_a} = \dfrac{1+k}{1 + k\text{Ma}^2}$	**(11.123)**
Rayleigh flow	$\dfrac{T}{T_a} = \left[\dfrac{(1+k)\text{Ma}}{1 + k\text{Ma}^2}\right]^2$	**(11.128)**
Rayleigh flow	$\dfrac{\rho_a}{\rho} = \dfrac{V}{V_a} = \text{Ma}\left[\dfrac{(1+k)\text{Ma}}{1 + k\text{Ma}^2}\right]$	**(11.129)**
Rayleigh flow	$\dfrac{T_0}{T_{0,a}} = \dfrac{2(k+1)\text{Ma}^2\left(1 + \dfrac{k-1}{2}\text{Ma}^2\right)}{(1 + k\text{Ma}^2)^2}$	**(11.131)**
Rayleigh flow	$\dfrac{p_0}{p_{0,a}} = \dfrac{(1+k)}{(1 + k\text{Ma}^2)}\left[\left(\dfrac{2}{k+1}\right)\left(1 + \dfrac{k-1}{2}\text{Ma}^2\right)\right]^{k/(k-1)}$	**(11.133)**
Normal shock	$\text{Ma}_y^2 = \dfrac{\text{Ma}_x^2 + [2/(k-1)]}{[2k/(k-1)]\text{Ma}_x^2 - 1}$	**(11.149)**
Normal shock	$\dfrac{p_y}{p_x} = \dfrac{2k}{k+1}\text{Ma}_x^2 - \dfrac{k-1}{k+1}$	**(11.150)**
Normal shock	$\dfrac{T_y}{T_x} = \dfrac{\{1 + [(k-1)/2]\text{Ma}_x^2\}\{[2k/(k-1)]\text{Ma}_x^2 - 1\}}{\{(k+1)^2/[2(k-1)]\}\text{Ma}_x^2}$	**(11.151)**
Normal shock	$\dfrac{\rho_y}{\rho_x} = \dfrac{V_x}{V_y} = \dfrac{(k+1)\text{Ma}_x^2}{(k-1)\text{Ma}_x^2 + 2}$	**(11.154)**
Normal shock	$\dfrac{p_{0,y}}{p_{0,x}} = \dfrac{\left(\dfrac{k+1}{2}\text{Ma}_x^2\right)^{k/(k-1)}\left(1 + \dfrac{k-1}{2}\text{Ma}_x^2\right)^{k/(1-k)}}{\left(\dfrac{2k}{k+1}\text{Ma}_x^2 - \dfrac{k-1}{k+1}\right)^{1/(k-1)}}$	**(11.156)**

References

1. Coles, D., "Channel Flow of a Compressible Fluid," Summary description of film in *Illustrated Experiments in Fluid Mechanics, The NCFMF Book of Film Notes,* MIT Press, Cambridge, Mass., 1972.
2. Moran, M. J., and Shapiro, H. N., *Fundamentals of Engineering Thermodynamics,* 6th Ed., Wiley, New York, 2008.

3. Keenan, J. H., Chao, J., and Kaye, J., *Gas Tables,* 2nd Ed., Wiley, New York, 1980.
4. Shapiro, A. H., *The Dynamics and Thermodynamics of Compressible Fluid Flow,* Vol. 1, Wiley, New York, 1953.
5. Liepmann, H. W., and Roshko, A., *Elements of Gasdynamics,* Dover Publications, 2002.
6. Anderson, J. D., Jr., *Modern Compressible Flow with Historical Perspective,* 3rd Ed., McGraw-Hill, New York, 2003.
7. Greitzer, E. M., Tan, C. S., and Graf, M. B., *Internal Flow Concepts and Applications,* Cambridge University Press, UK, 2004.

Problem available in *WileyPLUS* at instructor's discretion.

GO Tutoring problem available in *WileyPLUS* at instructor's discretion.

Problem is related to a chapter video available in *WileyPLUS*.

* Problem to be solved with aid of programmable calculator or computer.

† Open-ended problem that requires critical thinking. These problems require various assumptions to provide the necessary input data. There are not unique answers to these problems.

Review Problems

Go to Appendix G (*WileyPLUS* or the book's website, www.wiley.com/college/munson) for a set of review problems with answers. Detailed solutions can be found in the *Student Solution Manual and Study Guide for Fundamentals of Fluid Mechanics,* by Munson et al. (© 2013 John Wiley and Sons, Inc.).

Conceptual Questions

11.1C You are watching fireworks on the Fourth of July and notice that you hear the sound of a firework exploding 2 seconds after you see the flash of the explosion. Approximately how far away are the fireworks?

a) About the length of a football field.
b) About one-half of a kilometer.
c) About a kilometer.
d) About two kilometers.

11.2C An object, shown as the dark circle below, is moving along and emitting sound waves. The sound waves that were emitted by the object at times −1 second (one second ago), −2 seconds, and −3 seconds are shown below.

If the Mach number of the object is equal to unity, which is the correct picture for the sound waves?

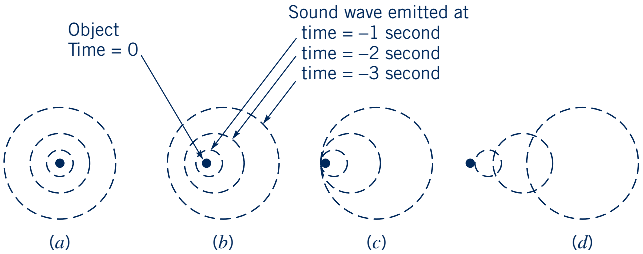

a) Picture A. b) Picture B. c) Picture C. d) Picture D.

Additional conceptual questions are available in *WileyPLUS* at the instructor's discretion.

Problems

Note: Unless specific values of required fluid properties are given in the problem statement, use the values found in the tables on the inside of the front cover. Answers to the even-numbered problems are listed at the end of the book. The Lab Problems as well as the videos that accompany problems can be accessed in *WileyPLUS* or the book's website, www.wiley.com/college/munson.

Section 11.1 Ideal Gas Relationships

11.1 Distinguish between flow of an ideal gas and inviscid flow of a fluid.

11.2 Compare the density of standard air listed in Table 1.4 with the value of standard air calculated with the ideal gas equation of state, and comment on what you discover.

11.3 Two kilogram mass of air is heated in a closed, rigid container from 25 °C, 103 kPa to 260 °C. Estimate the final pressure of the air and the entropy rise involved.

11.4 Air flows steadily between two sections in a duct. At section (1), the temperature and pressure are T_1 = 80 °C, p_1 = 301 kPa(abs), and at section (2), the temperature and pressure are T_2 = 180 °C, p_2 = 181 kPa(abs). Calculate the **(a)** change in internal energy between sections (1) and (2), **(b)** change in enthalpy between sections (1) and (2), **(c)** change in density between sections (1) and (2), and **(d)** change in entropy between sections (1) and (2). How would you estimate the loss of available energy between the two sections of this flow?

11.5 Determine, in SI units, nominal values of c_p and c_v for: **(a)** air, **(b)** carbon dioxide, **(c)** helium. Use information provided in Table 1.4.

11.6 As demonstrated in **Video V11.1** fluid density differences in a flow may be seen with the help of a schlieren optical system. Discuss what variables affect fluid density and the different ways in which a variable density flow can be achieved.

11.7 Describe briefly how a schlieren optical visualization system (**Videos V11.1** and **V11.5**, also Fig. 11.4) works. How else might density changes in a fluid flow be made visible to the eye?

11.8 Three kilograms of hydrogen contained in a nondeforming sealed vessel are cooled from 400 °C, 400 kPa(abs) until the hydrogen pressure is 100 kPa(abs). Calculate the change in internal energy, enthalpy, and entropy associated with this cooling process.

11.9 GO Helium is compressed isothermally from 121 kPa(abs) to 301 kPa(abs). Determine the entropy change associated with this process.

11.10 Air at 101.3 kPa and 20 °C is compressed adiabatically by a centrifugal compressor to a pressure of 690 kPa. What is the minimum temperature rise possible? Explain.

11.11 Methane is compressed adiabatically from 100 kPa(abs) and 25 °C to 200 kPa(abs). What is the minimum compressor exit temperature possible? Explain.

11.12 Air expands adiabatically through a turbine from a pressure and temperature of 1240 kPa, 615 K to a pressure of 101.3 kPa. If the actual temperature change is 85% of the ideal temperature change, determine the actual temperature of the expanded air and the actual enthalpy and entropy differences across the turbine.

11.13 An expression for the value of c_p for carbon dioxide as a function of temperature is

$$c_p = 1544 - \frac{3.44 \times 10^5}{T} + \frac{4.13 \times 10^6}{T^2}$$

where c_p is in J/kg·K and T is in kelvin. Compare the change in enthalpy of carbon dioxide using the constant value of c_p (see Table 1.4) with the change in enthalpy of carbon dioxide using the expression above, for $T_2 - T_1$ equal to **(a)** 5 K, **(b)** 555 K, **(c)** 1666 K. Set $T_1 = 300$ K.

Section 11.2 Mach Number and Speed of Sound

11.14 Confirm the speed of sound for air at 20 °C listed in Table B.2.

11.15 From Table B.1 we can conclude that the speed of sound in water at 20 °C is 1481 m/s. Is this value of c consistent with the value of bulk modulus, E_v, listed in Table 1.3?

11.16 If the observed speed of sound in steel is 5300 m/s, determine the bulk modulus of elasticity of steel in N/m^3. The density of steel is nominally 7790 kg/m^3. How does your value of E_v for steel compare with E_v for water at 15.6 °C? Compare the speeds of sound in steel, water, and air at standard atmospheric pressure and 15 °C and comment on what you observe.

11.17 If a high-performance aircraft is able to cruise at a Mach number of 3.0 at an altitude 24,384 m, how fast is this in m/s?

11.18 Compare values of the speed of sound in m/s at 20 °C in the following gases: **(a)** air, **(b)** carbon dioxide, **(c)** helium.

11.19 Determine the Mach number of a car moving in standard air at a speed of **(a)** 40 km/h, **(b)** 90 km/h, and **(c)** 160 km/h.

11.20 The flow of an ideal gas may be considered incompressible if the Mach number is less than 0.3. Determine the velocity level in m/s for Ma = 0.3 in the following gases: **(a)** standard air, **(b)** hydrogen at 20 °C.

Section 11.3 Categories of Compressible Flow

11.21 A schlieren photo of a bullet moving through air (see **Video V11.10**) at 101.3 kPa and 20 °C indicates a Mach cone angle of 28°. How fast was the bullet moving in m/s?

11.22 At a given instant of time, two pressure waves, each moving at the speed of sound, emitted by a point source moving with constant velocity in a fluid at rest are shown in Fig. P11.22. Determine the Mach number involved and indicate with a sketch the instantaneous location of the point source.

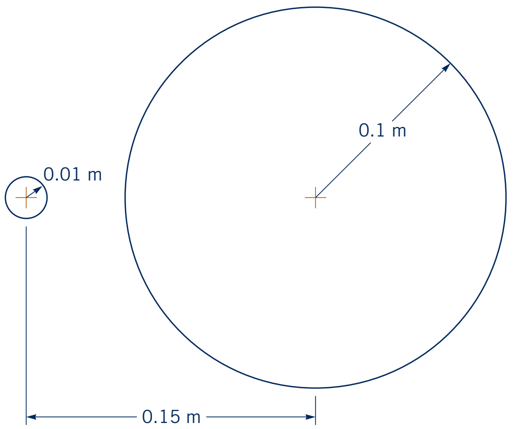

■ **Figure P11.22**

11.23 At a given instant of time, a pressure wave moving at the speed of sound, which is emitted by a point source moving with constant velocity along the line A–B in a fluid at rest, is shown in Fig. P11.23. If the point source Mach number is 0.8, sketch, for the given instant, the pressure wave emitted by the point source when it was at location B.

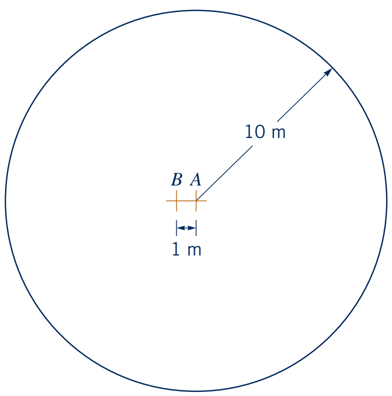

■ **Figure P11.23**

11.24 At a given instant of time, two pressure waves, each moving at the speed of sound, emitted by a point source moving with constant velocity in a fluid at rest, are shown in Fig. P11.24. Determine the Mach number involved and indicate with a sketch the instantaneous location of the point source.

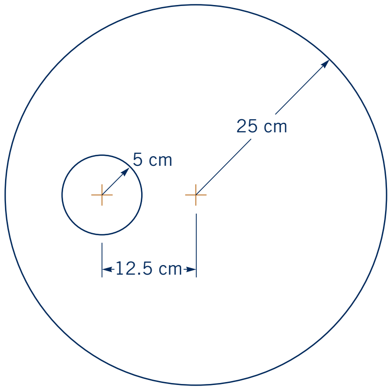

■ **Figure P11.24**

11.25 Sound waves are very small-amplitude pressure pulses that travel at the "speed of sound." Do very large-amplitude waves such as a blast wave caused by an explosion (see **Video V11.8**) travel less than, equal to, or greater than the speed of sound? Explain.

11.26 How would you estimate the distance between you and an approaching storm front involving lightning and thunder?

11.27 If a new Boeing 787 Dreamliner cruises at a Mach number of 0.87 at an altitude of 9144 m, how fast is this in m/s?

11.28 At the seashore, you observe a high-speed aircraft moving overhead at an elevation of 3048 m. You hear the plane 8 s after it passes directly overhead. Using a nominal air temperature of 4.4 °C, estimate the Mach number and speed of the aircraft.

11.29 Explain how you could vary the Mach number but not the Reynolds number in airflow past a sphere. For a constant Reynolds number of 300,000, estimate how much the drag coefficient will increase as the Mach number is increased from 0.3 to 1.0.

Section 11.4 Isentropic Flow of an Ideal Gas

11.30 Starting with the enthalpy form of the energy equation (Eq. 5.69), show that for isentropic flows, the stagnation temperature remains constant. Why is this important?

11.31 Starting with Eq. 11.52, prove that the stagnation enthalpy (and temperature) of an ideal gas remains constant during isentropic flow. Does this result fix the stagnation state for the flow? Explain. Using Eq. 5.69, comment on heat transfer and shaft work during any constant stagnation state process.

11.32 Air flows steadily and isentropically from standard atmospheric conditions to a receiver pipe through a converging duct. The cross-sectional area of the throat of the converging duct is $4.6 \times 10^{-3}\ \text{m}^2$. Determine the mass flowrate through the duct if the receiver pressure is **(a)** 68 kPa, **(b)** 34 kPa. Sketch temperature–entropy diagrams for situations **(a)** and **(b)**. Verify results obtained with values from the appropriate graph in Appendix D with calculations involving ideal gas equations. Is condensation of water vapor a concern? Explain.

11.33 Determine the critical pressure and temperature ratios for **(a)** air, **(b)** carbon dioxide, **(c)** helium.

11.34 Determine the static pressure to stagnation pressure ratio associated with the following motion in standard air: **(a)** a runner moving at the rate of 16 km/h, **(b)** a cyclist moving at the rate of 64 km/h, **(c)** a car moving at the rate of 104 km/h, **(d)** an airplane moving at the rate of 800 km/h.

11.35 The static pressure to stagnation pressure ratio at a point in a gas flow field is measured with a Pitot-static probe as being equal to 0.6. The stagnation temperature of the gas is 20 °C. Determine the flow speed in m/s and the Mach number if the gas is air. What error would be associated with assuming that the flow is incompressible?

11.36 The stagnation pressure and temperature of air flowing past a probe are 120 kPa(abs) and 100 °C, respectively. The air pressure is 80 kPa(abs). Determine the airspeed and the Mach number considering the flow to be **(a)** incompressible, **(b)** compressible.

11.37 The stagnation pressure indicated by a Pitot tube mounted on an airplane in flight is 45 kPa(abs). If the aircraft is cruising in standard atmosphere at an altitude of 10,000 m, determine the speed and Mach number involved.

11.38 GO Helium at 20 °C and 101.3 kPa in a large tank flows steadily and isentropically through a converging nozzle to a receiver pipe. The cross-sectional area of the throat of the converging passage is $4.6 \times 10^{-3}\ \text{m}^2$. Determine the mass flowrate through the duct if the receiver pressure is **(a)** 68 kPa, **(b)** 34 kPa. Sketch temperature–entropy diagrams for situations (a) and (b).

***11.39** An ideal gas enters subsonically and flows isentropically through a choked converging–diverging duct having a circular cross-sectional area A that varies with axial distance from the throat, x, according to the formula

$$A = 0.1 + x^2$$

where A is in square meters and x is in meters. For this flow situation, sketch the side view of the duct and graph the variation of Mach number, static temperature to stagnation temperature ratio, T/T_0, and static pressure to stagnation pressure ratio, p/p_0, through the duct from $x = -0.2$ m to $x = +0.2$ m. Also show the possible fluid states at $x = -0.2$ m, 0 m, and $+0.2$ m using temperature-entropy coordinates. Consider the gas as being helium (use $0.051 \leq \text{Ma} \leq 5.193$). Sketch on your pressure variation graph the nonisentropic paths that would occur with over- and underexpanded duct exit flows (see **Video V11.7**) and explain when they will occur. When will isentropic supersonic duct exit flow occur?

***11.40** An ideal gas enters supersonically and flows isentropically through the choked converging–diverging duct described in Problem 11.39. Graph the variation of Ma, T/T_0, and p/p_0 from the entrance to the exit sections of the duct for helium (use $0.051 \leq \text{Ma} \leq 5.193$). Show the possible fluid states at $x = -0.2$ m, 0 m, and $+0.2$ m using temperature–entropy coordinates. Sketch on your pressure variation graph the nonisentropic paths that would occur with over- and underexpanded duct exit flows (see **Video V11.7**) and explain when they will occur. When will isentropic supersonic duct exit flow occur?

11.41 An ideal gas is to flow isentropically from a large tank where the air is maintained at a temperature and pressure of 15 °C and 551 kPa to standard atmospheric discharge conditions. Describe in general terms the kind of duct involved and determine the duct exit Mach number and velocity in m/s if the gas is air.

11.42 An ideal gas flows isentropically through a converging–diverging nozzle. At a section in the converging portion of the nozzle, $A_1 = 0.1\ \text{m}^2$, $p_1 = 600$ kPa(abs), $T_1 = 20$ °C, and $\text{Ma}_1 = 0.6$. For section (2) in the diverging part of the nozzle, determine A_2, p_2, and T_2 if $\text{Ma}_2 = 3.0$ and the gas is air.

11.43 Upstream of the throat of an isentropic converging–diverging nozzle at section (1), $V_1 = 150$ m/s, $p_1 = 100$ kPa(abs), and $T_1 = 20$ °C. If the discharge flow is supersonic and the throat area is 0.1 m^2, determine the mass flowrate in kg/s for the flow of air.

11.44 The flow blockage associated with the use of an intrusive probe can be important. Determine the percentage increase in section velocity corresponding to a 0.5% reduction in flow area due to probe blockage for airflow if the section area is 1.0 m^2, $T_0 = 20$ °C, and the unblocked flow Mach numbers are **(a)** Ma = 0.2, **(b)** Ma = 0.8, **(c)** Ma = 1.5, **(d)** Ma = 30.

11.45 (See Fluids in the News article titled "Rocket Nozzles," Section 11.4.2.) Comment on the practical limits of area ratio for the diverging portion of a converging–diverging nozzle designed to achieve supersonic exit flow.

Section 11.5.1 Adiabatic Constant Area Duct Flow with Friction (Fanno Flow)

11.46 An ideal gas enters [section (1)] an insulated, constant cross-sectional area duct with the following properties:

$$T_0 = 293 \text{ K}$$
$$p_0 = 101 \text{ kPa(abs)}$$
$$\text{Ma}_1 = 0.2$$

For Fanno flow, determine corresponding values of fluid temperature and entropy change for various levels of pressure and plot the Fanno line if the gas is helium.

11.47 For Fanno flow, prove that

$$\frac{dV}{V} = \frac{fk(\text{Ma}^2/2)(dx/D)}{1 - \text{Ma}^2}$$

and in so doing show that when the flow is subsonic, friction accelerates the fluid, and when the flow is supersonic, friction decelerates the fluid.

11.48 GO Standard atmospheric air ($T_0 = 15$ °C, $p_0 = 101.3$ kPa) is drawn steadily through a frictionless and adiabatic converging nozzle into an adiabatic, constant cross-sectional area duct. The duct is 3 m long and has an inside diameter of 0.15 m. The average friction factor for the duct may be estimated as being equal to 0.03. What is the maximum mass flowrate in kg/s through the duct? For this maximum flowrate, determine the values of static temperature, static pressure, stagnation temperature, stagnation pressure, and velocity at the inlet [section (1)] and exit [section (2)] of the constant area duct. Sketch a temperature–entropy diagram for this flow.

11.49 The duct in Problem 11.48 is shortened by 50%. The duct discharge pressure is maintained at the choked flow value determined in Problem 11.48. Determine the change in mass flowrate through the duct associated with the 50% reduction in length. The average friction factor remains constant at a value of 0.03.

11.50 If the same mass flowrate of air obtained in Problem 11.48 is desired through the shortened duct of Problem 11.49, determine the back pressure, p_2, required. Assume f remains constant at a value of 0.03.

11.51 If the average friction factor of the duct of Example 11.12 is changed to **(a)** 0.01 or **(b)** 0.03, determine the maximum mass flowrate of air through the duct associated with each new friction factor; compare with the maximum mass flowrate value of Example 11.12.

11.52 If the length of the constant area duct of Example 11.12 is changed to **(a)** 1 m or **(b)** 3 m, and all other specifications in the problem statement remain the same, determine the maximum mass flowrate of air through the duct associated with each new length; compare with the maximum mass flowrate of Example 11.12.

11.53 The duct of Example 11.12 is lengthened by 50%. If the duct discharge pressure is set at a value of $p_d = 46.2$ kPa(abs), determine the mass flowrate of air through the lengthened duct. The average friction factor for the duct remains constant at a value 0.02.

11.54 Air flows adiabatically between two sections in a constant area pipe. At upstream section (1), $p_{0,1} = 689$ kPa, $T_{0,1} = 333$ K, and $\text{Ma}_1 = 0.5$. At downstream section (2), the flow is choked. Estimate the magnitude of the force per unit cross-sectional area exerted by the inside wall of the pipe on the fluid between sections (1) and (2).

Section 11.5.2 Frictionless Constant Area Duct Flow with Heat Transfer (Rayleigh Flow)

11.55 Cite an example of an actual subsonic flow of practical importance that may be approximated with a Rayleigh flow.

11.56 Standard atmospheric air [$T_0 = 288$ K, $p_0 = 101$ kPa(abs)] is drawn steadily through an isentropic converging nozzle into a frictionless diabatic ($q = 500$ kJ/kg) constant area duct. For maximum flow, determine the values of static temperature, static pressure, stagnation temperature, stagnation pressure, and flow velocity at the inlet [section (1)] and exit [section (2)] of the constant area duct. Sketch a temperature–entropy diagram for this flow.

11.57 Air enters a 0.15 m inside diameter duct with $p_1 = 138$ kPa, $T_1 = 27$ °C, and $V_1 = 60$ m/s. What frictionless heat addition rate in J/s is necessary for an exit gas temperature $T_2 = 815$ °C? Determine p_2, V_2, and Ma_2 also.

11.58 Air enters a length of constant area pipe with $p_1 = 200$ kPa(abs), $T_1 = 500$ K, and $V_1 = 400$ m/s. If 500 kJ/kg of energy is removed from the air by frictionless heat transfer between sections (1) and (2), determine p_2, T_2, and V_2. Sketch a temperature–entropy diagram for the flow between sections (1) and (2).

11.59 An ideal gas enters [section (1)] a frictionless, constant area duct with the following properties:

$$T_0 = 293 \text{ K}$$
$$p_0 = 101 \text{ kPa(abs)}$$
$$\text{Ma}_1 = 0.2$$

For Rayleigh flow, determine corresponding values of fluid temperature and entropy change for various levels of pressure and plot the Rayleigh line if the gas is helium.

11.60 Air flows through a constant area pipe. At an upstream section (1), $p_1 = 101$ kPa, $T_1 = 294$ K, and $V_1 = 60$ m/s. Downstream at section (2), $p_2 = 68$ kPa and $T_2 = 977$ K. For this flow, determine the stagnation temperature and pressure ratios, $T_{0,2}/T_{0,1}$ and $p_{0,2}/p_{0,1}$, and the heat transfer per unit mass of air flowing between sections (1) and (2). Is the flow between sections (1) and (2) frictionless? Explain.

11.61 Describe what happens to Fanno flow when heat transfer is allowed to occur. Is this the same as a Rayleigh flow with friction considered?

Section 11.5.3 Normal Shock Waves

11.62 The Mach number and stagnation pressure of air are 2.0 and 200 kPa(abs) just upstream of a normal shock. Estimate the stagnation pressure loss across the shock.

11.63 The stagnation pressure ratio across a normal shock in an airflow is 0.6. Estimate the Mach number of the flow entering the shock.

11.64 Just upstream of a normal shock in an airflow, Ma = 3.0, T = 333 K, and p = 206 kPa. Estimate values of Ma, T_0, T, p_0, p, and V downstream of the shock.

11.65 A total pressure probe like the one shown in **Video V3.8** is inserted into a supersonic airflow. A shock wave forms just upstream of the impact hole. The probe measures a total pressure of 500 kPa(abs). The stagnation temperature at the probe head is 500 K. The static pressure upstream of the shock is measured with a wall tap to be 100 kPa(abs). From these data, estimate the Mach number and velocity of the flow.

11.66 The Pitot tube on a supersonic aircraft (see **Video V3.8**) cruising at an altitude of 9144 m senses a stagnation pressure of 83 kPa. If the atmosphere is considered standard, determine the airspeed and Mach number of the aircraft. A shock wave is present just upstream of the probe impact hole.

11.67 An aircraft cruises at a Mach number of 2.0 at an altitude of 15 km. Inlet air is decelerated to a Mach number of 0.4 at the engine compressor inlet. A normal shock occurs in the inlet diffuser upstream of the compressor inlet at a section where the Mach number is 1.2. For isentropic diffusion, except across the shock, and for standard atmosphere, determine the stagnation temperature and pressure of the air entering the engine compressor.

11.68 Determine, for the airflow through the frictionless and adiabatic converging–diverging duct of Example 11.8, the ratio of duct exit pressure to duct inlet stagnation pressure that will result in a standing normal shock at: **(a)** $x = +0.1$ m, **(b)** $x = +0.2$ m, **(c)** $x = +0.4$ m. How large is the stagnation pressure loss in each case?

11.69 A normal shock is positioned in the diverging portion of a frictionless, adiabatic, converging–diverging airflow duct where the cross-sectional area is 0.009 m^2 and the local Mach number is 2.0. Upstream of the shock, p_0 = 1378 kPa and T_0 = 667 K. If the duct exit area is 0.014 m^2, determine the exit area temperature and pressure and the duct mass flowrate.

11.70 GO Supersonic airflow enters an adiabatic, constant area (inside diameter = 0.3 m) 9 m long pipe with Ma_1 = 3.0. The pipe friction factor is estimated to be 0.02. What ratio of pipe exit pressure to pipe inlet stagnation pressure would result in a normal shock wave standing at **(a)** x = 1.5 m, or **(b)** x = 3 m, where x is the distance downstream from the pipe entrance? Determine also the duct exit Mach number and sketch the temperature–entropy diagram for each situation.

11.71 Supersonic airflow enters an adiabatic, constant area pipe (inside diameter = 0.1 m) with Ma_1 = 2.0. The pipe friction factor is 0.02. If a standing normal shock is located right at the pipe exit, and the Mach number just upstream of the shock is 1.2, determine the length of the pipe.

11.72 Air enters a frictionless, constant area duct with Ma_1 = 2.0, $T_{0,1}$ = 15 °C, and $p_{0,1}$ = 101.3 kPa. The air is decelerated by heating until a normal shock wave occurs where the local Mach number is 1.5. Downstream of the normal shock, the subsonic flow is accelerated with heating until it chokes at the duct exit. Determine the static temperature and pressure, the stagnation temperature and pressure, and the fluid velocity at the duct entrance, just upstream and downstream of the normal shock, and at the duct exit. Sketch the temperature–entropy diagram for this flow.

11.73 Air enters a frictionless, constant area duct with Ma = 2.5, T_0 = 20 °C, and p_0 = 101 kPa(abs). The gas is decelerated by heating until a normal shock occurs where the local Mach number is 1.3. Downstream of the shock, the subsonic flow is accelerated with heating until it exits with a Mach number of 0.9. Determine the static temperature and pressure, the stagnation temperature and pressure, and the fluid velocity at the duct entrance, just upstream and downstream of the normal shock, and at the duct exit. Sketch the temperature–entropy diagram for this flow.

■ Lifelong Learning Problems

11.1LL Is there a limit to how fast an object can move through the atmosphere? Explain.

11.2LL Discuss the similarities between hydraulic jumps in open-channel flow and shock waves in compressible flow. Explain how this knowledge can be useful.

11.3LL Estimate the surface temperature associated with the reentry of the Space Shuttle into the Earth's atmosphere. Why is knowing this important?

11.4LL [See Fluids in the News article titled "Hilsch Tube (Ranque Vortex Tube)," Section 11.1.] Explain why a Hilsch tube works and cite some high and low gas temperatures actually achieved. What is the most important limitation of a Hilsch tube, and how can it be overcome?

11.5LL [See Fluids in the News article titled "Supersonic and Compressible Flows in Gas Turbines," Section 11.3.] Using typical physical dimensions and rotation speeds of manufactured gas turbine rotors, consider the possibility that supersonic fluid velocities relative to blade surfaces are possible. How do designers use this knowledge?

11.6LL Develop useful equations describing the constant temperature (isothermal) flow of an ideal gas through a constant cross-sectional area pipe. What important practical flow situations would these equations be useful for? How are real gas effects estimated?

■ FE Exam Problems

Sample FE (Fundamentals of Engineering) exam questions for fluid mechanics are provided in *WileyPLUS* or on the book's website, www.wiley.com/college/munson.